INFORMATION TO USERS

This reproduction was made from a copy of a document sent to us for microfilming. While the most advanced technology has been used to photograph and reproduce this document, the quality of the reproduction is heavily dependent upon the quality of the material submitted.

The following explanation of techniques is provided to help clarify markings or notations which may appear on this reproduction.

1. The sign or "target" for pages apparently lacking from the document photographed is "Missing Page(s)". If it was possible to obtain the missing page(s) or section, they are spliced into the film along with adjacent pages. This may have necessitated cutting through an image and duplicating adjacent pages to assure complete continuity.

2. When an image on the film is obliterated with a round black mark, it is an indication of either blurred copy because of movement during exposure, duplicate copy, or copyrighted materials that should not have been filmed. For blurred pages, a good image of the page can be found in the adjacent frame. If copyrighted materials were deleted, a target note will appear listing the pages in the adjacent frame.

3. When a map, drawing or chart, etc., is part of the material being photographed, a definite method of "sectioning" the material has been followed. It is customary to begin filming at the upper left hand corner of a large sheet and to continue from left to right in equal sections with small overlaps. If necessary, sectioning is continued again—beginning below the first row and continuing on until complete.

4. For illustrations that cannot be satisfactorily reproduced by xerographic means, photographic prints can be purchased at additional cost and inserted into your xerographic copy. These prints are available upon request from the Dissertations Customer Services Department.

5. Some pages in any document may have indistinct print. In all cases the best available copy has been filmed.

University
Microfilms
International

300 N. Zeeb Road
Ann Arbor, MI 48106

Sausa, Rosario C.

CARBON DIOXIDE LASER INDUCED CHEMISTRY OF VANADIUM OXYTRICHLORIDE AND DICHLOROSILANE

City University of New York PH.D. 1983

PLEASE NOTE:

In all cases this material has been filmed in the best possible way from the available copy. Problems encountered with this document have been identified here with a check mark __✓__.

1. Glossy photographs or pages _____
2. Colored illustrations, paper or print _____
3. Photographs with dark background __✓__
4. Illustrations are poor copy _____
5. Pages with black marks, not original copy _____
6. Print shows through as there is text on both sides of page _____
7. Indistinct, broken or small print on several pages __✓__
8. Print exceeds margin requirements _____
9. Tightly bound copy with print lost in spine _____
10. Computer printout pages with indistinct print _____
11. Page(s) _____ lacking when material received, and not available from school or author.
12. Page(s) _____ seem to be missing in numbering only as text follows.
13. Two pages numbered _____. Text follows.
14. Curling and wrinkled pages _____
15. Other _____

CO_2 Laser Induced Chemistry of Vanadium Oxytrichloride and Dichlorosilane

by

Rosario C. Sausa

A dissertation submitted to the Graduate Faculty in Chemistry in partial fulfillment of the requirements for the degree of Doctor of Philosophy, The City University of New York.

1983

This manuscript has been read and accepted for the Graduate Faculty in Chemistry in satisfaction of the dissertation requirement for the degree of Doctor of Philosophy.

9/23/83
date

A. M. [signature]
Chairman of Examining Committee

9/28/83
date

David C. Locke
Executive Officer

Seymour Aronson

P. Gary Mennitt

L. Massa
Supervisory Committee

The City University of New York

Abstract

Infrared CO_2 laser induced chemistry of vanadium oxytrichloride ($VOCl_3$) and dichlorosilane (SiH_2Cl_2) was studied both on and off resonance and the results, along with the unique characteristics of each method, discussed.

Multiphoton excitation of $VOCl_3$, under collisional and collision-free conditions, resulted in dissociation via its ground electronic state and in a visible fluorescence. The photodissociative pathways leading to product formation were found to be both pressure and laser fluence dependent. Low pressure and laser fluence led to the formation of $VOCl_2$ while high pressure and laser fluence favored VO. The prompt fluorescence was also studied as a function of pressure and laser fluence, and was shown to arise from a spontaneous one-photon radiative decay from an electronic state belonging to the $VOCl_2$ fragment.

A similar study conducted on SiH_2Cl_2 revealed that $SiCl_2 + H_2$ were its photodissociative products under collisionless conditions. The observed ultraviolet luminescence was attributed to the electronically excited $SiCl_2$ fragment.

The reaction mechanisms leading to product formation as well as models for populating a fragment's electronic state were proposed and discussed in conjunction with present multiphoton excitation and dissociation theory.

Dielectric breakdown and laser combustion methods were used to produce various vanadium oxides and silicon containing films from $VOCl_3$ and SiH_2Cl_2. The products, which were finely divided particles of very large surface area and high purity, may be used in numerous industrial applications.

To my parents and Lydia.

Acknowledgement

It gives me great pleasure to express my utmost graditude to Professor Vic Ronn for giving me the opportunity to become a member of his group as an undergraduate and introducing me to scientific research. Only then did science become lively, exciting, and stimulating. His scientific guidance and valued friendship are most treasured.

To the members of Vic's group, Myron, Shiann, Shu, and Yedidyah, I am thankful for their friendship and enlightening conversations. In particular, I am deeply grateful to Alan for his scientific help while Vic was on sabbatical and Jaime for his constant help, advice, and invaluable friendship. Special thanks go to Visiting Professor José Riveros. His stay at our laboratory enriched all of us.

I am also grateful to the professional, administrative, technical, and secretarial staff of the Chemistry Department of the City University of New York and, in particular, the Chemistry Department of Brooklyn College. Their friendship, cooperation, and assistance made my stay a most pleasant one. Special thanks go to Terry Rudd for the expert typing of this manuscript and Ottmar Safferling, our esteemed glassblower, for performing the most difficult jobs in the shortest period of times and for teaching me what little glassblowing I know. Their patience and friendship will never be forgotten.

I would also like to convey my thanks to the members of my committee, Professors Seymour Aronson, Louis Massa, and P. Gary Mennitt, for their advice, stimulating conversations, and interest in my research. Thanks are also due to Professor Derrick Lindsey and his group at City College for allowing me to conduct a few experiments in their laboratory. Their hospitality, assistance, and friendship made my short stay a pleasant one.

Last, but not least, I'd like to thank the members of my family for their love, support, and constant encouragement.

TABLE OF CONTENTS

LIST OF TABLES

LIST OF FIGURES

LIST OF FIGURES (continued)

LIST OF FIGURES (continued)

CHAPTER 1 - A BRIEF OVERVIEW

The laser, an acronym for light amplification by stimulated emission of radiation, provides the most coherent, manifested in both monochromaticity (temporal coherence) and uniphase wavefront (spatial coherence), directional, and controllable radiation source available. Laser radiation, ranging from the infrared to the ultraviolet region of the electromagnetic spectrum, may be used for studying new methods of molecular excitation that are not possible with "classical" light sources. These new methods, which include single, double, and multiple photon absorptions, are indispensible for studying the nature of chemical bonds, perhaps the most central question in all of chemistry, as well as photophysical and photochemical processes.

The Russian announcement of successful CO_2 laser isotope separation of SF_6 species in 1973 [1,2], verified by American scientists within a few months [3], spawned the belief that an era of mode selective chemistry had arrived. Chemists, and physicists alike, envisioned that high powered lasers, tuned to specific vibrations occuring in molecules, could violate the laws of statistical thermodynamics by breaking particular selected bonds which were not necessarily the weakest. This, coupled with the projected synthesis of novel

compounds and more efficiently produced industrial chemicals, triggered a growth in the past ten years of laser induced chemistry in which infrared lasers and, in particular, pulsed CO_2 lasers have played a major role.

The widespread use of the CO_2 pulsed laser in inducing many chemical reactions is attributed to its large output power of high intensity in short duration. In addition, its lasing action at wavelengths between 9.6 - 10.6 μ, a region where many molecules absorb, and high efficiency, up to 20% conversion of pumping to radiant power, make it, undoubtedly, the most important gas laser from both an industrial and scientific point of view [4,5].

There are two basic mechanisms by which an infrared laser can induce a chemical reaction. The first, multiple photon absorption (MPA), requires a resonance between the laser radiation and an absorption band of the molecule. Once this resonant condition is satisfied, the molecule may then absorb sufficient infrared photons within its ground state manifold to reach the continuum and thus dissociate.

The multiple photon absorption process is presented in Chapter Two and is applied in the "collisionless" and collisional dissociation of vanadium oxytrichloride ($VOCl_3$) and dichlorosilane (SiH_2Cl_2). The collisionless photodissociation is accompanied by an observable

electronic luminescence which is attributed to electronically excited $SiCl_2$ and $VOCl_2$ radicals. The electronic luminescence induced by multiple photon excitation is not addressed by statistical theories, such as R.R.K.M. (Rice, Ramsberger, Kassel, and Marcus)[6], nor predicted a priori by currently accepted models of infrared multiphoton chemistry [7,8]. According to these theories, photodissociation from the ground state potential energy surface typically accompanies the formation of ground state products and is not generally expected to yield electronically excited fragments. Nevertheless, electronic fragment luminescence, under collisionless conditions, has been observed and is presented along with proposed mechanisms in Chapter Two.

The second mechanism, laser induced dielectric breakdown [9-11], requires no resonant condition and is most effective at high pressures since it proceeds by an avalanche of electrons resulting from the large A.C. electric field of the laser's radiation. A comparison of the molecular dissociation of $VOCl_3$ and SiH_2Cl_2 with resonant and nonresonant radiation was thus studied and the results, along with the unique characteristics of each method, discussed in Chapter Three.

Both $VOCl_3$ and SiH_2Cl_2 are prime candidates for gas phase studies in infrared laser induced chemistry. First, SiH_2Cl_2 is a gas at room temperature and $VOCl_3$, although

a liquid at room temperature, has a high vapor pressure. Second, the strong absorption by their $\nu_1(V = 0)$ and $\nu_2(SiH_2)$ stretching vibrational modes make them suitable for CO_2 laser excitation. Third, the use of vanadium oxides as catalysts in many organic and inorganic reactions, and the use of silicon in the construction of semiconductors and solar power conversion cells make both $VOCl_3$ and SiH_2Cl_2 important industrial chemicals since they can be used as starting material for novel synthetic routes.

REFERENCES

1. V. S. Letokhov, Science 180, 451 (1973).

2. R. V. Ambartzumian, V. S. Letokhov, E. A. Ryabov, and N. V. Chekolin, Pis'ma Zh. Eksp. Teor. Fiz. (Russian) 20, 597 (1974). [Sov. Phys., JETP Lett. 20, 273 (1974)].

3. J. L. Lyman, R. J. Jensen, J. P. Rink, C. P. Robinson, and S. D. Rockwood, Appl. Phys. Lett., 27, 87 (1975).

4. C. K. N. Patel, Phys. Rev. Lett. 12, 588 (1964).

5. A. L. Robinson, Science 193, 1230 (1976).

6. P. J. Robinson, K. A. Holbrook, Unimolecular Reactions, (Wiley-Interscience, New York 1972).

7. J. G. Black, E. Yablonovitch, N. Bloembergen, and S. Mukamel, Phys. Rev. Lett. 38, 1131 (1977).

8. R. V. Ambartzumian, Yu. A. Gorokhov, V. S. Letokhov, G. N. Makarov, and A. A. Puretzkii, Pis'ma Zh. Eksp. Teor. Fiz (Russian) 71, 440 (1976).

9. J. P. Wright, Proc. Phys. Soc., 84, 41 (1964).

10. A. M. Ronn, Chem. Phys. Letts., 42, 202 (1976).

11. C. G. Morgan, Laser Induced Electrical Breakdown of Gases, edited by J. M. Meek and J. D. Graggs (Wiley-Interscience: New York, 1978) Chap. 9.

CHAPTER 2

ELECTRONIC LUMINESCENCE RESULTING FROM MULTIPLE PHOTON EXCITATION OF $VOCl_3$ and SiH_2Cl_2

2.1 INTRODUCTION

The first reports of infrared multiple photon dissociation of molecules also stated that this process is accompanied by electronic emission [1-5]. Since then, there has been much interest in and speculation about the origin of this molecular luminescence. Early infrared experiments using continuous wave (CW) CO_2 laser excitation were thought to produce luminescence by simple heating of the sample [1,2]. This mechanism, however, cannot explain the visible or ultraviolet luminescence observed from a pulsed CO_2 laser at moderate power levels. Much of this molecular emission has been attributed to radical recombination or, in cases where the pressure and laser energy were too high, to dielectric breakdown. From recent investigations, the electronic luminescence has been assigned to either electronically excited fragments [6-9] or electronically excited parent molecules [10-12]. Whereas the latter, coined inverse electronic relaxation, has been observed in a collisionless regime, fragment luminescence has for most cases been observed under conditions where the pressures were too high to be collisionless.

We assign the luminescence to the electronically excited $VOCl_2$ and $SiCl_2$ fragments formed from the collisionless multiphoton excitation of $VOCl_3$ and SiH_2Cl_2. This is not predicted, a priori, by currently accepted models of infrared multiphoton chemistry and seems to violate the general rule that the ground state of a molecule correlates adiabatically with ground state products.

The results, along with a discussion of a systematic study conducted to determine the photodissociative products of $VOCl_3$ and SiH_2Cl_2, and the origin of the luminescence under collisionless and collisional conditions, follows this introductory section. Some novel, as well as existing mechanisms for the above processes are proposed and discussed in conjunction with present multiphoton excitation and dissociation theory. In particular, the following questions are addressed:

- Why should a molecule dissociate with the absorption of infrared radiation? After all, the strength of a typical chemical bond is $\simeq$ 100 kcal/mole while the energy of a CO_2 laser photon is $\simeq$ 2.3 kcal/mole?
- Is the multiphoton process coherent all the way up the vibrational ladder of the molecule's ground state potential energy surface?

- Was the bond which was excited broken?
- Is mode selective chemistry possible?

and
- How is a fragment formed in its electronic state by the absorption of infrared photons?

2.2 THEORY

Ordinarily, there exists a one-to-one correspondence between the number of photons absorbed and the number of molecules making a transition to an excited state. This is known as the Stark-Einstein law of photochemistry. However, in exceptional circumstances, this law is violated. A high-powered CO_2 laser provides a very high density of photons, greater than 10^3 photons per molecule*, thus allowing some probability that a molecule will absorb more than one photon. Indeed, it has been shown experimentally that, under collisionless conditions, SF_6 absorbs more than 30 photons while remaining translationally cold, dissociates, and

---

* For a CO_2 laser with an output of 1 J of energy at a wavelength of 10.6 μ, there are, using the equation $E = nhc/\lambda$, approximately 5×10^{19} photons. The volume of interaction of the laser beam whose radius is .5 cm and is focused by a 5-inch lens is obtained from the equation, $v_t = 2/3\ \pi r^2 h$, and yields ~ 7 cm^3. Since the total number of molecules at a pressure of 100 mtorr and a cell volume of .25 ℓ is $\sim 8 \times 10^{17}$ (calculated by using PV = nRT relationship, Avagadro's number, and using room temperature) and the fraction of molecules which interact with the laser radiation is 7/250 (8×10^{17}) or ~ 2×10^{16}, it follows then that there are ~ 10^3 photons per molecule.

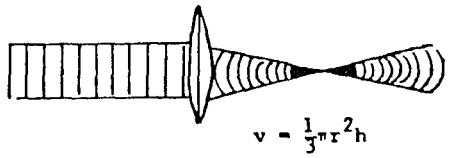

maintains its isotopic selectivity [13,14].

Using SF_6 as an example, a model used to describe the process of multiple photon absorption and subsequent dissociation is shown in Fig. (1) and (2). It is evident from Fig. (1) that the ground state potential energy surface of a polyatomic molecule can be divided into three regions. Region (I) is characterized by discrete levels which have a small density of vibrational states. Region (II), the quasicontinuum, is characterized by a high density of vibrational-rotational states and Region (III), the true continuum, is where dissociation occurs.

In the first region, vibrational anharmonicity in the quantum gaps is a obstacle that a molecule must overcome for successful excitation. This anharmonicity may be compensated by either rotational transitions or vibrational-rotational broadening, a mechanism unique to strong laser fields.

The rotational compensation model, termed PQR [16], is based on the absorption of laser photons in the sequence P branch ($v = 0, J \rightarrow v = 1, J-1$), Q branch ($v = 1, J-1 \rightarrow v = 2, J-1$), and R branch ($v = 2, J-1 \rightarrow v = 3, J$). Thus, it is rotational compensation of the anharmonicity that, according to this model, guarantees the resonance condition for the first three steps of the vibrational ladder $\{|v>\}$, even at modest power levels.

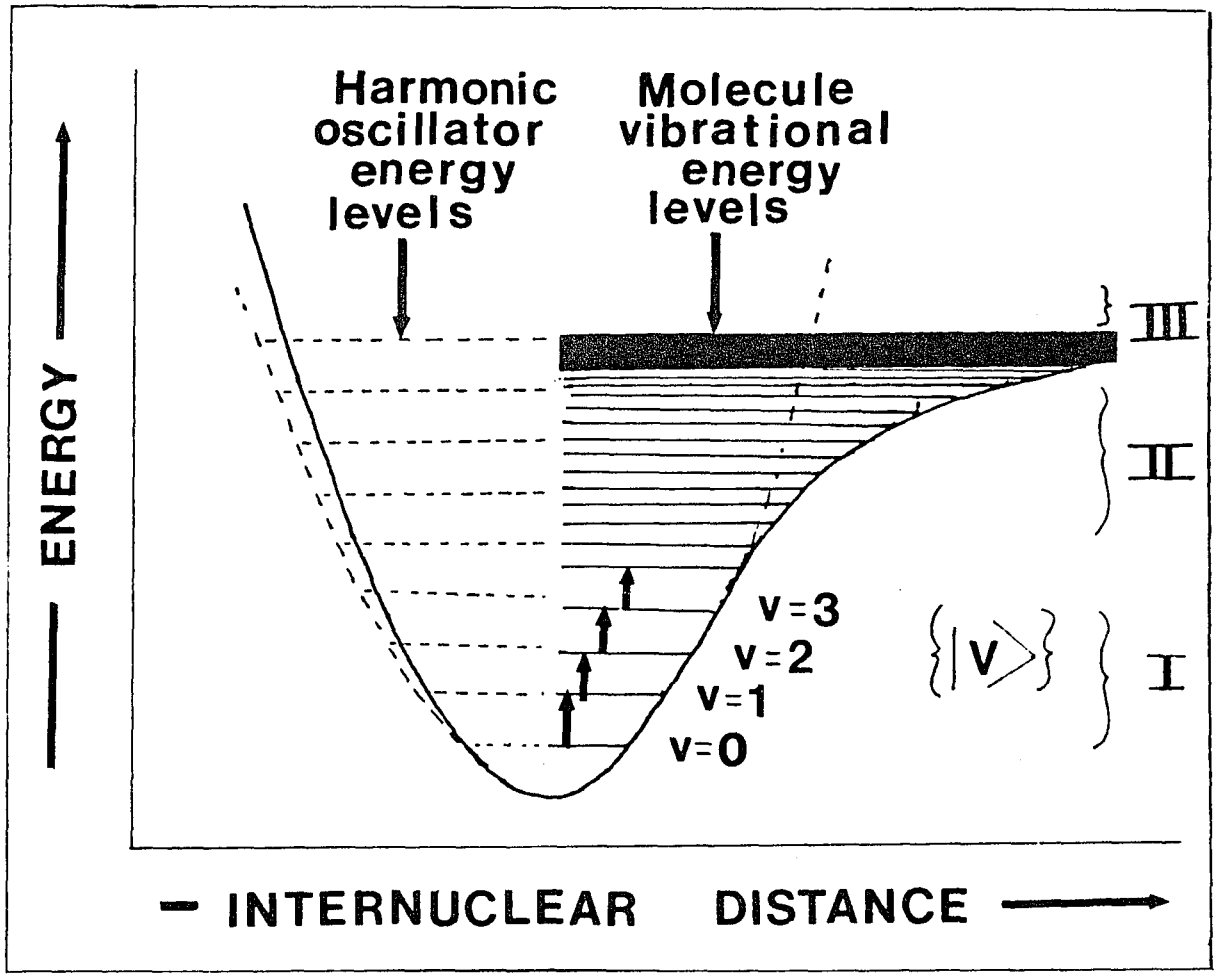

Figure (1) - Potential energy diagram: Region I, II, and III refer to the discrete, quasicontinuum, and dissociative continuum regions.

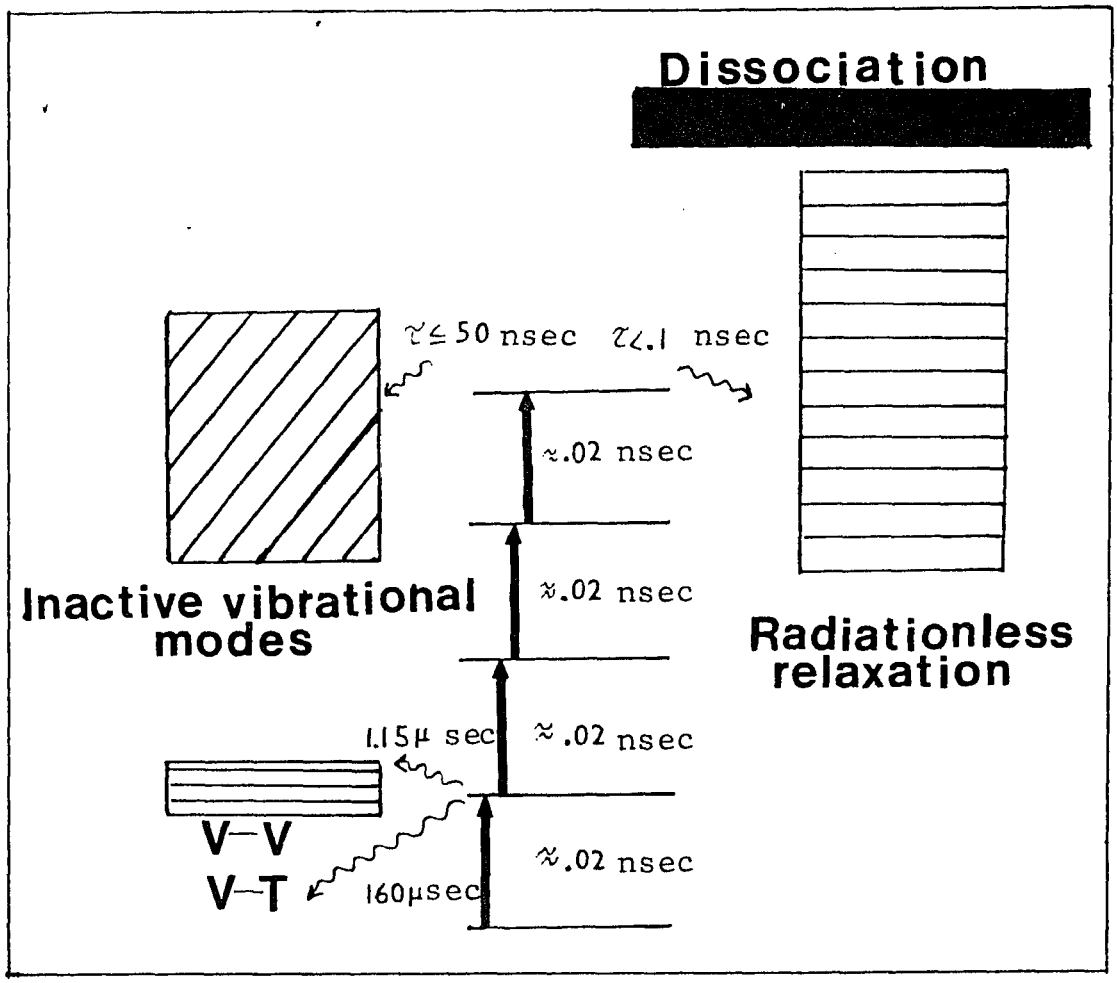

Figure (2) - A schematic diagram similar to Fig. (1). The numerical values shown are for SF_6 at a laser power of 1 GW/cm^2 and a pressure of 1 torr [15].

The vibrational-rotational broadening mechanism focuses on the splitting of the molecule's vibrational-rotational energy levels by the oscillating electric field of the laser radiation. This broadening is a result of both the D.C. and A.C. Stark shift. The latter is sometimes referred to as power broadening.

For a diatomic molecule (rigid rotor approximation) the magnitude of the D.C. Stark shift is given by the following expression [15].

$$\overline{\Delta\nu} = \left(\frac{B_e}{2}\right)\left(\frac{\mu E_o}{h\nu}\right)^2 \qquad (2.1)$$

where B_e is the rotational constant, μ the transition dipole moment, E_o the electric field strength, ν the laser frequency, and h Planck's constant.

The multilevel power broadening, A.C. Stark shift, arises because a transition between oscillator levels occurs in a time which is short compared to the time in which the laser field gets out of phase with the oscillator. A normal Boltzmann distribution between the levels cannot be obtained; the result is a decreased extinction coefficient and a broadening of the absorption line. This effect is determined by the Rabi frequency and the detuning of $\nu-\nu_o$ where ν is the laser frequency and ν_o the oscillator frequency. The Rabi frequency is

defined as [15]

$$\bar{\nu}_R = \frac{\mu E_o}{h} \tag{2.2}$$

where the symbols have been previously defined in equation (2.1). Since the probability of excitation of an oscillator is given by the following expression [15],

$$P_{ex} \sim \left(\frac{\nu_R}{\nu-\nu_o}\right)^2 \sin^2 \left[\frac{(\nu-\nu_o)}{2}t\right] \tag{2.3}$$

it is apparent, then, that significant excitation will take place if the Rabi frequency is large compared to the anharmonicity of the pumped modes.

Anharmonic splittings inherent in degenerate overtones and Fermi resonance between overtones or combination bands are other factors which can, to different degrees in different molecules, contribute to the compensation of the anharmonicity in Region (I).

Region (II), dubbed the quasicontinuum, is arbitrarily defined at a critical energy of say, 4000 cm^{-1} (ν = 3-4) above the ground vibrational state. At ν = 3-4 or thereabouts, the vibrational density of states becomes very large, resulting in a quasicontinuum of states. In the quasicontinuum, the high density of vibrational and rotational states provide all the "fine tuning" necessary to match the photon frequency with the

quantum gap between vibrational levels. Now, further absorption by a sequence of one photon processes coupled with rapid (subpicosecond timescale) intramode energy transfer can promote the molecule to still higher vibrational levels until it reaches the true continuum, Region (III), and dissociates [17,18].

An elegant experiment performed by Letokhov et al. [19] corroborated the mechanism of multiphoton absorption. They dissociated SF_6 using two CO_2 lasers. Low power radiation from the first laser pulse excited SF_6 three steps up the anharmonic ladder. A second pulse, completely detuned from an SF_6 absorption band, was then capable of dissociating the molecule at a much smaller threshold power than would be required in a simple frequency MPD experiment. Thus, this experiment, which has been repeated on other molecules, supports the notion of a quasicontinuum in which resonance between the laser radiation and a molecular absorption feature is not required. Moreover, they obtained optimal isotopic separation yields with the first laser detuned 10 cm^{-1} to the red from the resonance line. This, they concluded, corroborated the PQR mechanism previously described.

From the presented model, several points regarding isotope separation (intermolecular selectivity), bond selective chemistry (intramolecular selectivity), laser pulse requirements, and the role of collisions on the

multiple photon process can be made.

Isotope separation, as implied in Fig. (1), is possible for molecules whose isotopic shift is larger than the spectral width, $\overline{\Delta\nu}$, caused by power broadening.

Perhaps the most pressing question in multiple photon dissociation is that of bond selective chemistry. In the case of SF_6, uncertainty arises since the molecule contains six chemically equivalent fluorine atoms. However, in a MPD experiment in which SF_5Cl was used, it was demonstrated that the weaker S-Cl bond preferentially ruptured to the stronger S-F stretching mode which was excited. Similar conclusions have been reached from most, if not all, experiments done to date. That is, multiple photon dissociation follows the expected fragmentation pattern along a dissociation coordinate that is weaker than the rest. This fact is readily explained by the statistical thermodynamic RRKM theory which predicts that the laser energy, initially deposited in one particular vibrational mode of the molecule, radomizes to other modes of vibrations once a sufficient level of excitation is achieved in the quasicontinuum in a time of 30 picoseconds [20]. Thus, multiple photon dissociation is not bond specific. However, if the excitation can be delivered in a very short time, less than picoseconds, with sufficient intensity to cause bond breakage, there is insufficient time for thermal

excess energy sharing within the molecule and the excited bond would rupture. Such times are indeed short, yet well within experimental ability. The potential payoff will be tremendous, since bond selective dissociation will then become a reality.

On the laser pulse requirement, it is evident from the presented model that the leading part of the pulse must be intense enough to excite the molecule over the discrete states into the quasicontinuum, and the remaining portion of the pulse must contain enough fluence (J/cm^2) to excite the molecule beyond the dissociation limit.

Pressure effects which lead to molecular collisons complicate the "ideal image" of collisionless dissociation and must also be addressed. Although it depends upon the molecule involved and the level of exciation, for relatively large molecules such as SF_6, it appears that intermolecular V-V and V-(T/R) relaxation occurs in roughly 10^{-6} and 10^{-4} sec respectively at a pressure of 1 torr. Therefore, it is necessary to work at relatively low pressure to avoid scrambling of the vibrational excitation and thus maintaining unique, non "Bunsen burner" chemistry. Ronn et al. [21] have found that the isotope separation efficiency of $^{34}SF_6$ and $^{32}SF_6$ is progressively lost as the pressure is increased from .1 to 1 torr due to scrambling collisions.

A simple calculation shows that SF_6 experiences

approximately 10^{-1}* collisions per μsec at 10^{-1} torr. This collisional frequency is small relative to the span of a CO_2 laser pulse (typically .1 - 1 μsec) and thus collisions play only a minor role [21].

The scope of the work presented in this chapter is divided into two parts. The first involves an investigation of the multiple photon dissociation of $VOCl_3$ and SiH_2Cl_2 under collisional and collisionless conditions. The products formed, together with the reaction mechanisms involved, will be shown to be pressure and fluence dependent.

---

* The collisional frequency for SF_6, as well as $VOCl_3$ and SiH_2Cl_2, was obtained by using the following kinetic expression [22]: $z_{AA} = \sqrt{2}\pi(d_A)^2 < v_A > (N_A/V)$ collisions/sec. The term d_A represents the diameter of the molecules (cm) and $< v_A >$, which is equal to $(8\ RT/\pi M)^{\frac{1}{2}}$, the average speed of the molecules. The symbols R, T, and M stand for the gas constant (8.314×10^7 erg/mole·K), temperature (K), and M the molecular weight of the gas (g/mole) respectively. The average velocity will have units of cm/sec if the equality 1 erg = 1 g·cm^2/sec^2 is used. The term (N_A/V), which represents the number of molecules per unit volume (cm^3), is given by $(P_A N_o/RT)$, where the relationship PV = nRT = $(N/N_o)RT$ is used. The symbol P_A represents the pressure (atm), N_o Avagadro's number (6.02×10^{23} mole^{-1}), T the temperature, and R the gas constant (82.06 cm^{3}atm/mole·K). The diameters used for SF_6, $VOCl_3$, and SiH_2Cl_2, calculated by taking twice the largest bond length, are 3.12×10^{-8} cm [23], 4.24×10^{-8} cm [Table (I), page 28] and 4.06×10^{-8} cm [Table (III), page 72] respectively.

The second part involves the spectroscopic investigation of fragmént electronic luminescence arising from the collisionless multiphoton excitation of $VOCl_3$ and SiH_2Cl_2. This, as was pointed out before, is not predicted a priori by currently accepted models of infrared multiphoton chemistry and thus various mechanisms allowing for populating the fragments electronic states are proposed.

2.3 EXPERIMENTAL

A schematic diagram of the experimental apparatus is shown in Fig. (3). A number of lasers were employed as excitation sources. For multiple photon absorption and dissociation experiments, a home built Rogowski-type [Fig. (4) and (5)] pulsed CO_2-N_2-He TEA laser was used [24]. Pulsing of this laser was accomplished with a trigger generator (model 050C, Tachisto, Inc.) in conjunction with a pulse transformer (U.S. Scientific Instruments) and a pressurized spark gap (0-30 PSIG, 12-50 kv SG501, Tachisto, Inc.). This laser is capable of an energy output of ~ 2.5 Joules per pulse at repetition rates of 1-5 pps and can be tuned to the rotational lines of the P and R branches of both the 9.6 and 10.6 μ region, allowing some 60 discrete wavelengths. The pulse shapes, measured by a photon drag

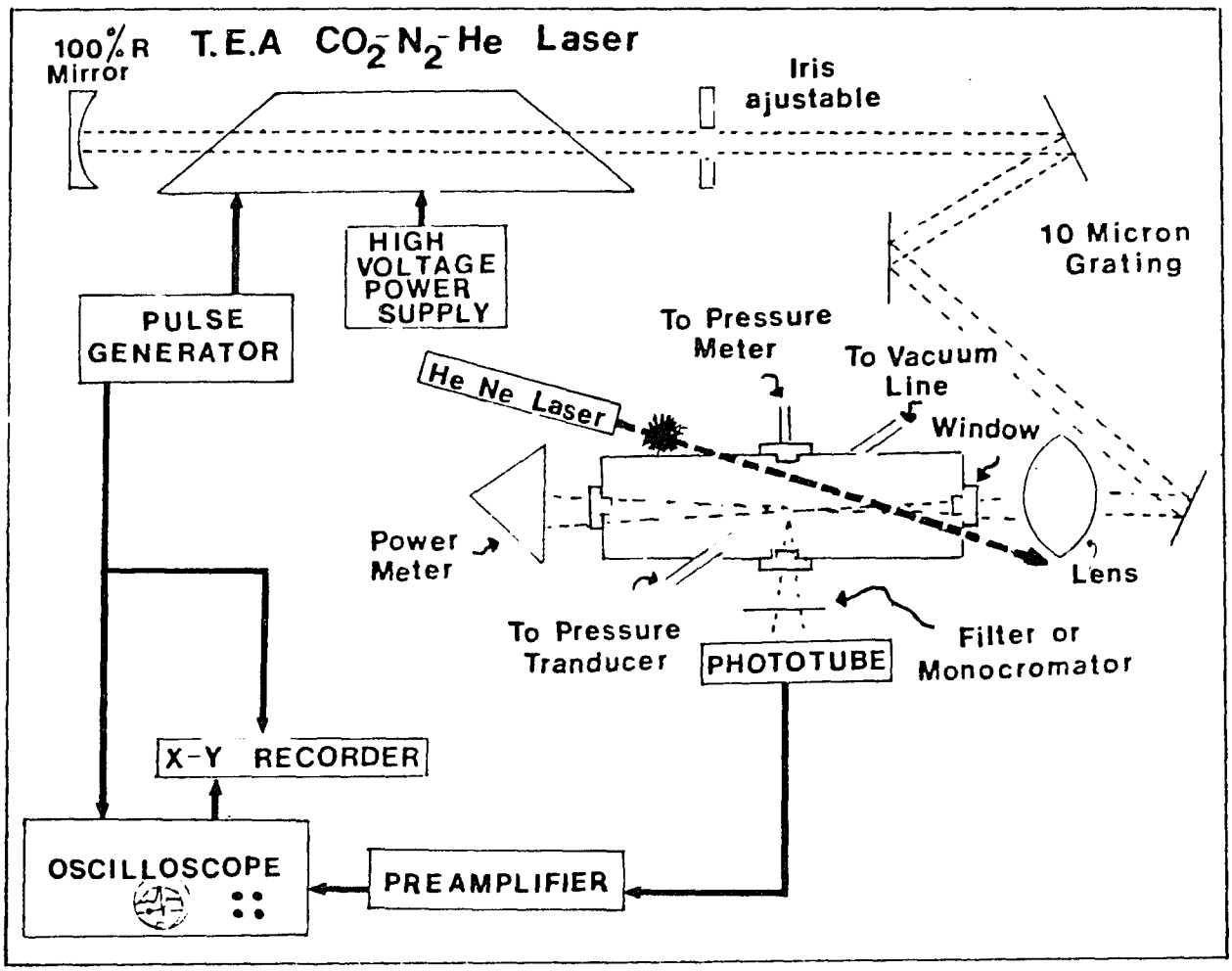

Figure (3) - A schematic diagram of the experimental apparatus used for laser induced fluorescene studies.

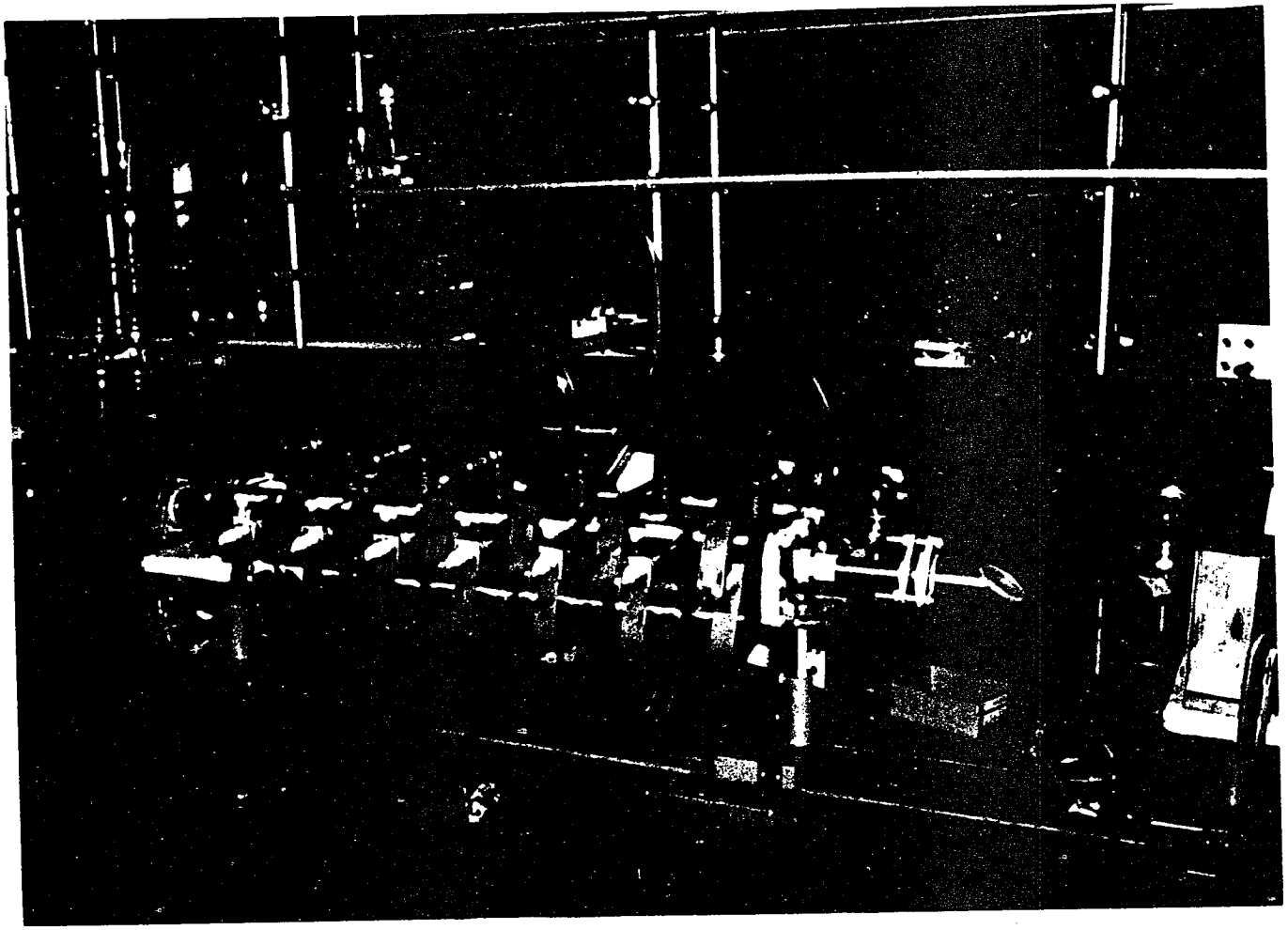

Figure (4) - A photograph of a home-built Rogowski-type CO_2-TEA laser.

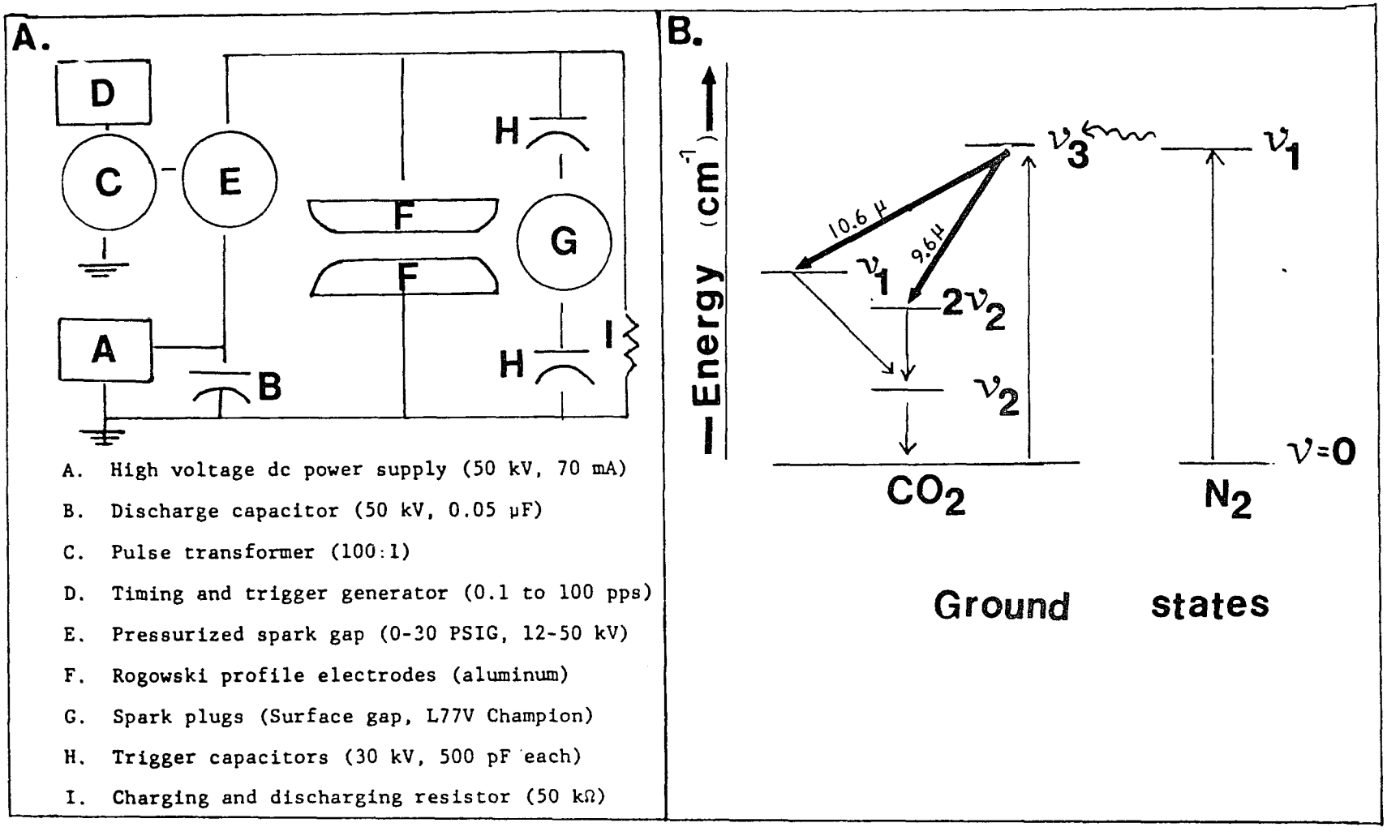

A. High voltage dc power supply (50 kV, 70 mA)

B. Discharge capacitor (50 kV, 0.05 μF)

C. Pulse transformer (100:1)

D. Timing and trigger generator (0.1 to 100 pps)

E. Pressurized spark gap (0-30 PSIG, 12-50 kV)

F. Rogowski profile electrodes (aluminum)

G. Spark plugs (Surface gap, L77V Champion)

H. Trigger capacitors (30 kV, 500 pF each)

I. Charging and discharging resistor (50 kΩ)

Figure (5) - A schematic diagram of the CO_2 TEA laser (A) with an energy level diagram showing its stimulated emission (B).

(Rofin 02591) were varied by the amount of N_2 present and are shown in Fig. (6). In N_2-rich mixtures, the pulse duration was ~ 600 nsec at FWHM with a tail extending to 1.5 μsec while, in lean mixtures, it was ~ 300 nsec at FWHM with a 800 nsec tail. For one photon absorption experiments, both N_2 and KrF lasers were employed. The N_2 laser (NRC model .5-5-150/B) has an output of 150 mwatts at 337.1 nm with a repetition rate of 60 Hz. The pulse duration was 5 nsec at FWHM. The KrF laser (Tachisto TAC system 250) has an output of 100 mJ at 248 nm, a repetition rate of 1-10 pps, and a pulse duration of 10 nsec at FWHM.

Vanadium oxytrichloride ($VOCl_3$), obtained as a yellow liquid (purity > 99.95%) underwent a very careful three-stage bulb-to-bulb vacuum distillation and freeze-thaw cleanout before each set of experiments. To prevent photodecomposition from the flourescent lights, $VOCl_3$ was always kept in either a dark bottle or in a glass container which was wrapped with aluminum foil. In addition, all experiments were performed with no room lights on. VO, obtained from Cerac Corporation with > 99.5% purity, together with V_2O_3, V_2O_4, and V_2O_5, obtained from Alpha/Inorganic Corp. (> 99% purity), were used for comparative purposes as commercially supplied. $VOCl_2$ was obtained from Varlacoid Chemical Corp. (> 99.5% purity) and was used for fluorescence experiments. VOCl was prepared by heating $VOCl_2$ to approximately 350°C in vacuum while

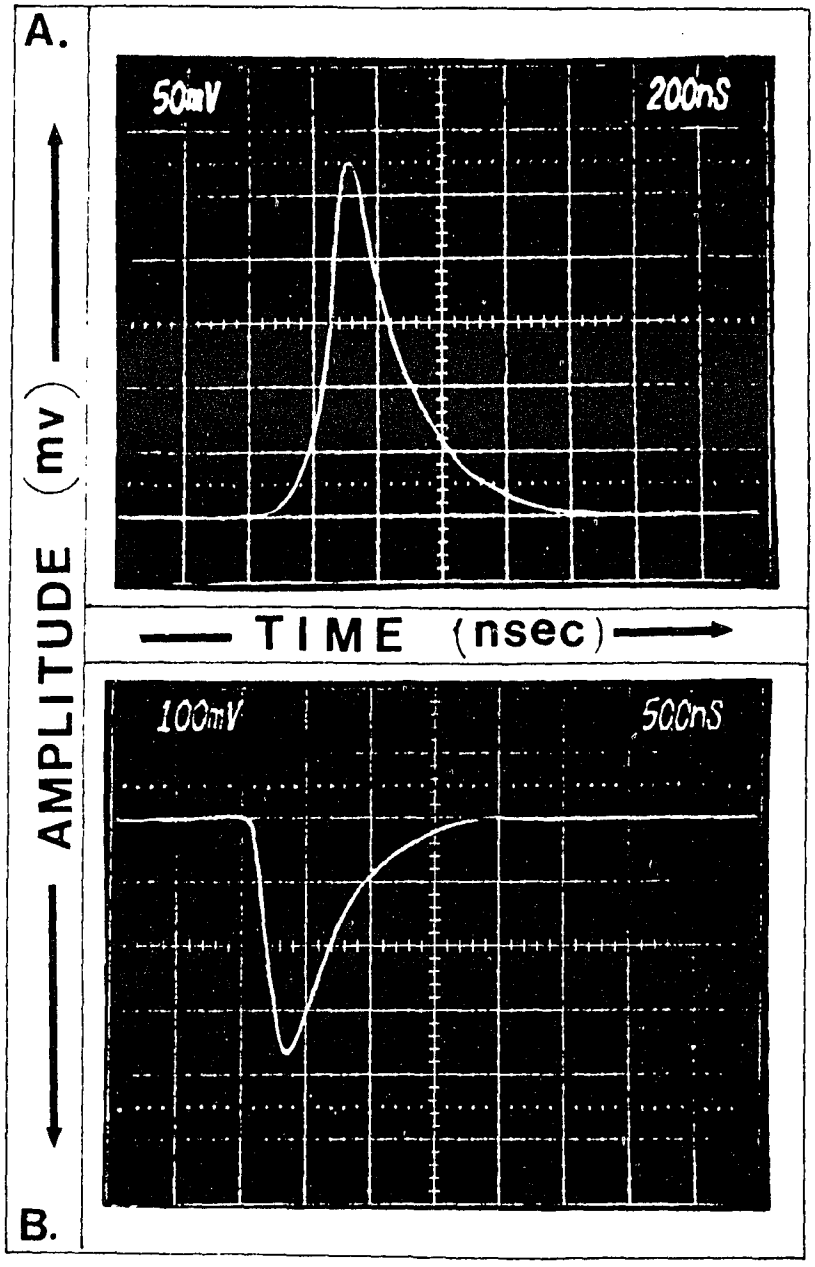

Figure (6) - Oscillograms of typical short (A) and long (B) CO_2 laser pulses.

pumping out the chlorine, a by-product. SiH_2Cl_2 was obtained from Airgenics Corp. with a stated purity of > 99.9%. The diluent gases Ar, H_2, O_2, and Cl_2 were Matheson research grade and were used without further purification.

Dimethyl sulfide (DMS), which was A.C.S. certified and spectroanalyzed, was obtained from Fisher Scientific Co. and used as a solvent for $VOCl_3$, $VOCl_2$, and VOCl.

Experiments were conducted under both static and flow conditions. The cells utilized varied in size and shape (4 cm^3 - 500 cm^3) but were either pyrex or brass body with NaCl or quartz windows connected via "O" ring joints. In experiments where $VOCl_3$ was used, contamination was avoided by constructing the cells with teflon valves instead of greased taps. CO_2 laser focusing was achieved by a number of lenses. Both antireflection (AR) coated germanium of 10" and 15" focal length and ZnSe 5" focal length were used. At the focal point, the intensity of the laser radiation was in the 10^9 W/cm^2 range* with a corresponding field strength of 10^6 V/cm.**

---

* The spot radius of a laser beam which has wavelength of 10.6 um, radius of .5 cm, and focused by a 5" lens is obtained from the relationship S.R. = $\lambda f/\pi r$ and yields a value of ~ 8×10^{-3} cm with a corresponding area of ~ 2×10^{-4} cm^2. The power associated with the laser energy, 10^6 Watts for 1 J of energy in 1 μsec, together with the area of the laser beam yields a power density, I, of ~ 10^9 W/cm^2.

** Using Poynting's equation, $I = \varepsilon cE^2$ [where ε, the space permitivity, is equal to 8.55×10^{-12} $coul^2/nt \cdot m^2$ or 8.55×10^{-12} $coul/V \cdot m$ (1 N/coul = 1 V/m) and c, the speed of light (3.0×10^8 m/sec)] and the equality 1 W = coul·V/sec, one obtains the relationship $I = 2.57 \times 10^{-3} E^2$, where I is in units of W/cm^2 and E in units of V/cm. Hence, by using this relationship and an intensity of ~ 10^9 V/cm^2, one obtains a field strength, E, of ~ 10^6 V/cm.

Pressure measurements, which were made with a MKS baratron and/or ionization guage, ranged from 10^{-4} - 10^{2} torr. With a MKS baratron, pressure readings could be obtained to the nearest 10^{-3} torr while with an ionization guage an uncertainty of ±.1 unit could be extracted from various scales ranging from 10^{-10} - 10^{-3} torr. Low pressures were achieved by using an oil diffusion vacuum system (~ 10^{-6} torr).

The laser energy, up to 2.5 Joules, was measured by a coherent 201 power meter. For comparative purposes, it was sometimes necessary to convert the laser energy to fluence (J/cm^2) or intensity (W/cm^2) units. This was accomplished by measuring the burn pattern of the focused pulse and its duration.

The luminescence experiments were conducted in a 65 cm-long cell in order to avoid any possible "window fluorescence" and under flow conditions using (~ 10^{2} cm^3/sec) which insured continuously replenished fresh sample. To prevent detection of stray light, all luminescence experiments were performed at night and the cell used was wrapped with black tape, leaving only an entrance window, exit window, and viewing area for the phototube uncovered.

The luminescence was viewed perpendicularly through narrow band filters (O.C.L.I. ~ 10 nm at FWHM) or a monochromator (¼ meter Jarrel Ash or Spex model 1215) with a resolution of 5 nm. Photo detection was achieved with a Hammamatsu R955, EMI-9816K13, or RCA 341034

phototube. The signal was amplified and displayed on a Tektronix 7704 oscilloscope. The signal was averaged for a minimum of 10 shots and then photographed for analysis. The response time for the detector and associated electronics was less than .1 μsec.

At a given pressure, the rate of rise or fall of the fluorescence signal was obtained as $1/\tau$ from a plot of emission intensity versus time displayed on an oscillogram. From an examination of the formula of an exponential curve,

$$y = Ae^{-kt} \tag{2.4}$$

where y is the amplitude at any time t, A the maximum amplitude, and $k = 1/\tau$ the decay constant, it's apparent that τ is the relaxation time, defined as the $t = \tau$ required for the signal to decay to 1/e of its initial value.

Product analysis was carried out by infrared absorption (Beckman IR 10 or Perkin-Elmer 267) and/or mass spectrometry (Varian CH-7 or AEI-902S). Product and reactant peaks were compared prior to and subsequent to laser excitation of reactants for a present number of shots at predetermined pressures, frequencies, and power levels. In addition, a He-Ne laser with an output of ~ .5 mW at 6328 Å was used as a probe in the detection of particulates as a result of their scattering.

UV-VIS absorption and emission spectra were taken with a Cary 17 and Cary Fluorolog respectively.

2.4 RESULTS AND DISCUSSION

A. Vanadium Oxytrichloride

1. UV and IR absorption spectra of $VOCl_3$

Vanadium oxytrichloride ($VOCl_3$) is a prime candidate for studies in laser induced chemistry. $VOCl_3$ is a pale yellow liquid which freezes at -79.5°C and boils at 127°C. Its high vapor pressure, 12.4 torr at 25°C, and strong absorption at 1040 cm^{-1}, $\nu_1(a_1)$ fundamental mode, make it suitable for CO_2 laser excitation.

It is hydrolyzed with extraordinary rapidity in moist air and, when it is exposed to the atmosphere, a dense yellowish-red cloud of vapor forms in accordance with the following equation:

$$2VOCl_3 + 3H_2O \rightarrow V_2O_5 + 6HCl \qquad (2.5)$$

The physical properties of $VOCl_3$ are consistent with its being a covalently unsaturated monomer. Electron diffraction data on the vapor indicate that the four bonds to the vanadium are directed almost tetrahedrally [Table (I)].

The UV-VIS absorption spectrum of $VOCl_3$ in the gas phase at approximately 200 mtorr is shown in

Table I. (A) Published bond lengths and angles of $VOCl_3$ [25].
(B) Published rotational constants of $VOCl_3$ [26].

$VOCl_3$ (C_{3v})	
A. BOND LENGTHS & ANGLES	
r(V–Cl) A° = 2.12 ±.03	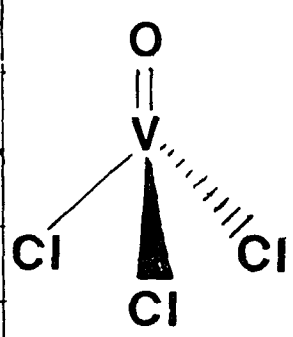
r(V–O) A° = 1.56±.04	
r(Cl–Cl) A° = 3.50±.03	
r(O–Cl) A° = 3.00±.04	
∢ Cl–V–Cl = 111 ± 2°	
∢ Cl–V–O = 108± 2°	
B. ROTATIONAL CONSTANTS	
A (cm^{-1}) = .038	
B (cm^{-1}) = .058	
C (cm^{-1}) = .058	

Fig. (7b). This spectrum exactly coincides with the one taken by Miller and White, Fig. (7a), and reveals two absorption bands whose peaks are centered at 244 nm and 333 nm of about equal intensity. As was pointed out, the $VOCl_3$ molecule can be considered to have a tetrahedral shape with a trigonal distortion (C_{3v}). As a consequence, the three-fold degenerate levels corresponding to the irreducible representations of the tetrahedral molecule will split. The t_1 level gives rise to an a_2 and e representation. Since the a_2 representation corresponds to a non-bonding molecular orbital, its energy will be higher than that of the e level. The t_2 level gives rise to an a_1 and e representation. This can be seen in Fig. (8), a simplified molecular orbital energy diagram of $TiCl_4(T_d)$ and $VOCl_3$ (C_{3v})[28]. From Fig. (8), it is evident that the 333 nm band, which is of lower energy, corresponds to a $(1a_2)(\pi) \rightarrow (1a_2)^1(5e)^1(\pi^*)$ trasition while the 244 nm band corresponds to a $(1a_2)^2(\pi) \rightarrow (1a_2)^1(6e)^1(\sigma^*,\pi^*)$ transition.

The infrared spectra of $VOCl_3$ has been completely determined in the vapor state. The molecule has C_{3v} symmetry and, on this basis, there are three totally symmetric vibrations (species a_1) and three doubly degenerate vibrations (species e). All six fundamentals are both infrared and Raman active. The fundamental modes are given in Table (II).

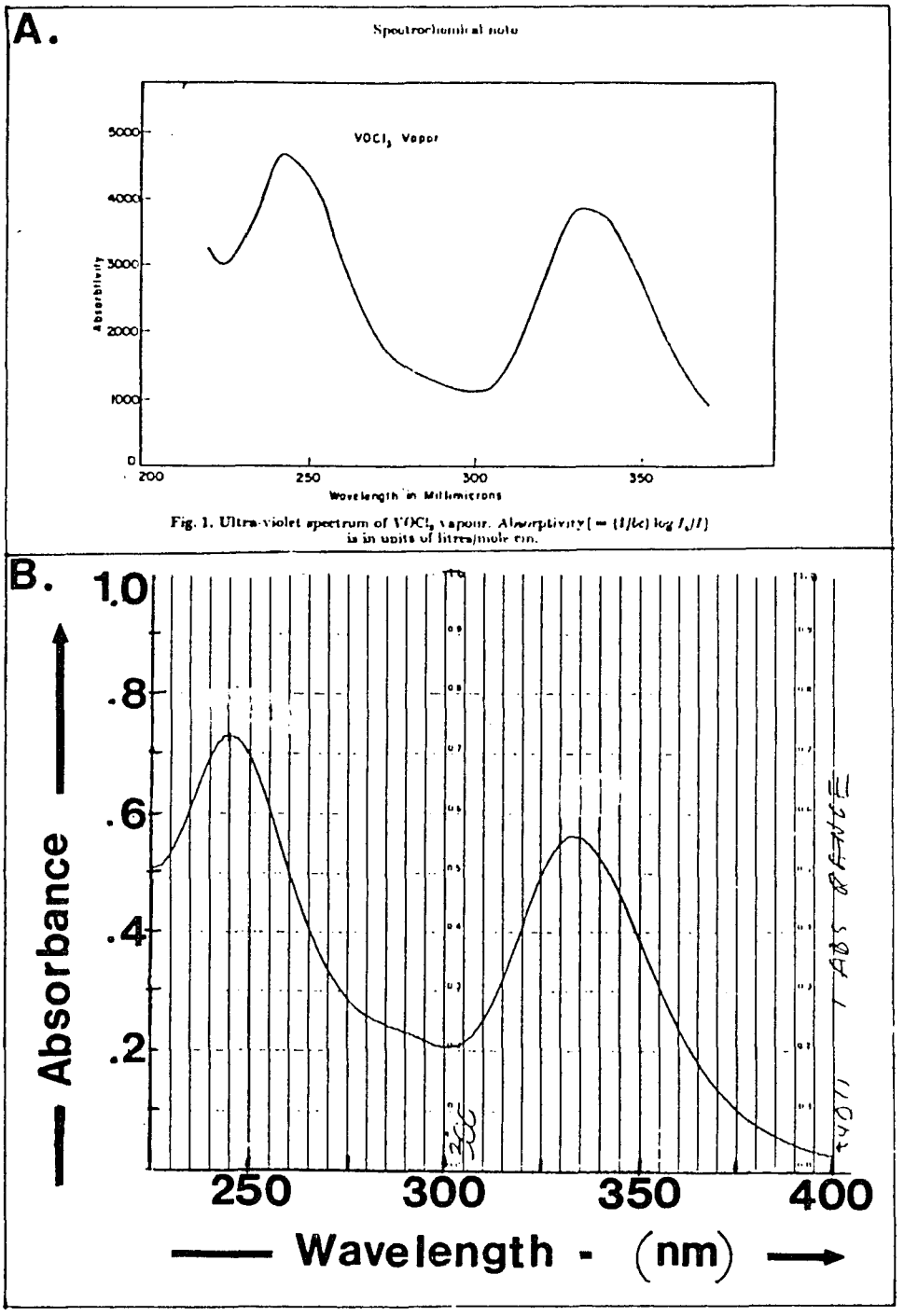

Fig. 1. Ultra-violet spectrum of $VOCl_3$ vapour. Absorptivity [$= (1/lc) \log I_0/I$] is in units of litres/mole cm.

Figure (7) - A comparison between published (A) [27] and recorded (B) UV absorption spectrum of $VOCl_3$ in the gas phase.

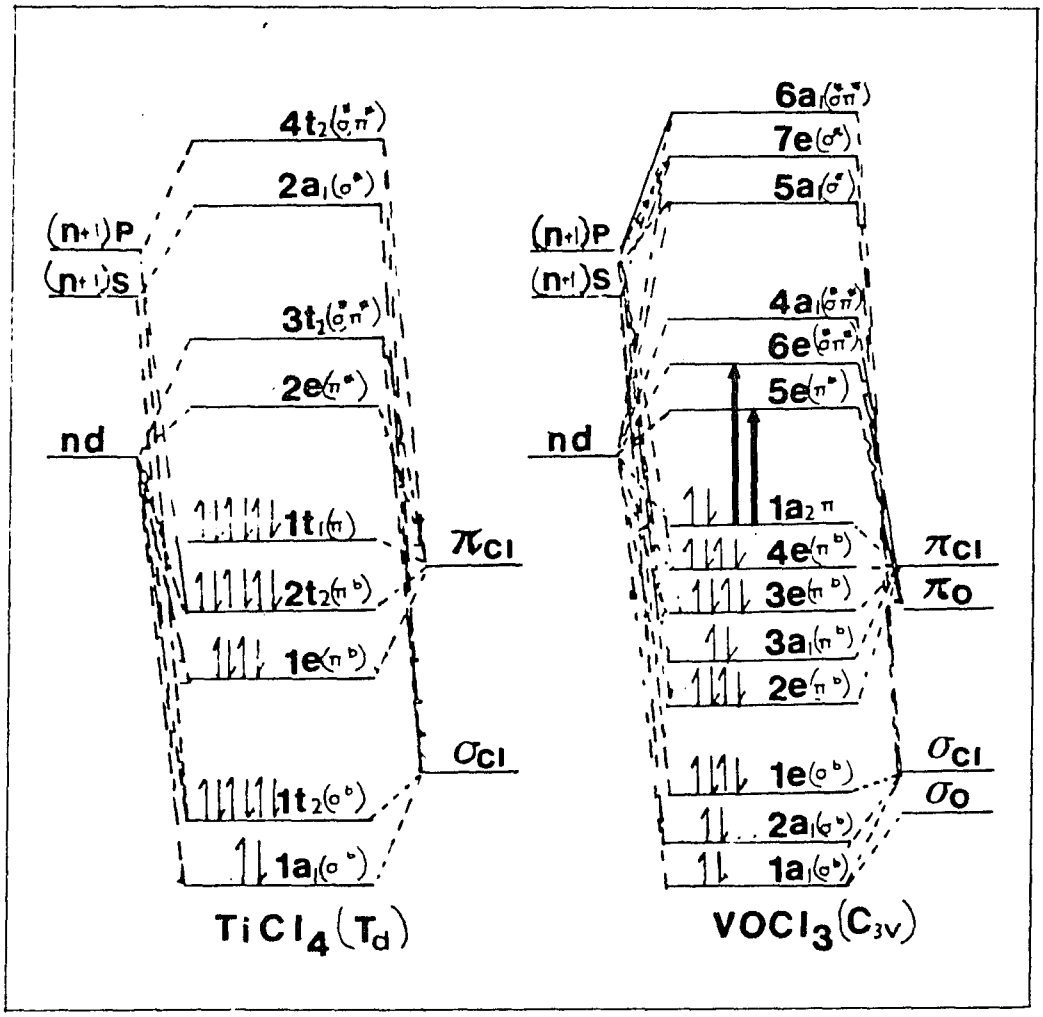

Figure (8) - A simplified molecular orbital energy level diagram of $TiCl_4$ and $VOCl_3$.

Table II. Published vibrational frequencies of $VOCl_3$ in the gas phase [29].

MODE	DESCRIPTION	ν (cm^{-1})
$\nu_1(a_1)$	V=O stretch	1042.5
$\nu_2(a_1)$	VCl_3 sym stretch	409.5
$\nu_3(a_1)$	VCl_3 sym bend	163
$\nu_4(e)$	VCl_3 asym stretch	503
$\nu_5(e)$	Cl_3-V-O rock	248
$\nu_6(e)$	VCl_3 asym bend	124.5

The infrared absorption spectrum of the $\nu_1(a_1)$ fundamental mode of $VOCl_3$ at approximately 5 torr of pressure is shown in Fig. (9). Upon higher resolution, it is seen [Fig. (10)] that, the $\nu_1(a_1)$ fundamental band occuring at 1040 cm^{-1}, consists of P($\Delta J = -1$), Q($\Delta J = 0$), and R($\Delta J = 1$) branches. This absorption spectrum shows a fairly wide potentially absorbing region for a tunable CO_2 laser. A mapping of such absorptions was carried out and is shown in Fig. (11). It can be seen that the strongest laser absorption line is the P(26) of the 9.6 μ band corresponding to the Q branch of the $VOCl_3$ molecule at 1041.28 cm^{-1}. The absorption coefficient was obtained from the absorbance vs. pressure plot in Fig. (12) and yielded $\varepsilon_{p(26)9.6\mu} = 5.3 \times 10^{-3}$ $cm^{-1}torr^{-1}$. No measurable absorption was detected when the laser was tuned to the Q or R branch transitions of the 9.6 μ branch.

Once the strongest absorption laser line for $VOCl_3$ was determined, studies in terms of both dissociation and luminescence were investigated and are presented in the following sections.

2. Multiphoton Dissociation of $VOCl_3$

As in all multiphoton experiments, one is faced with the primary question of the mechanism responsible for the reactions observed. Anticipating such, our experimental logic was designed to test and

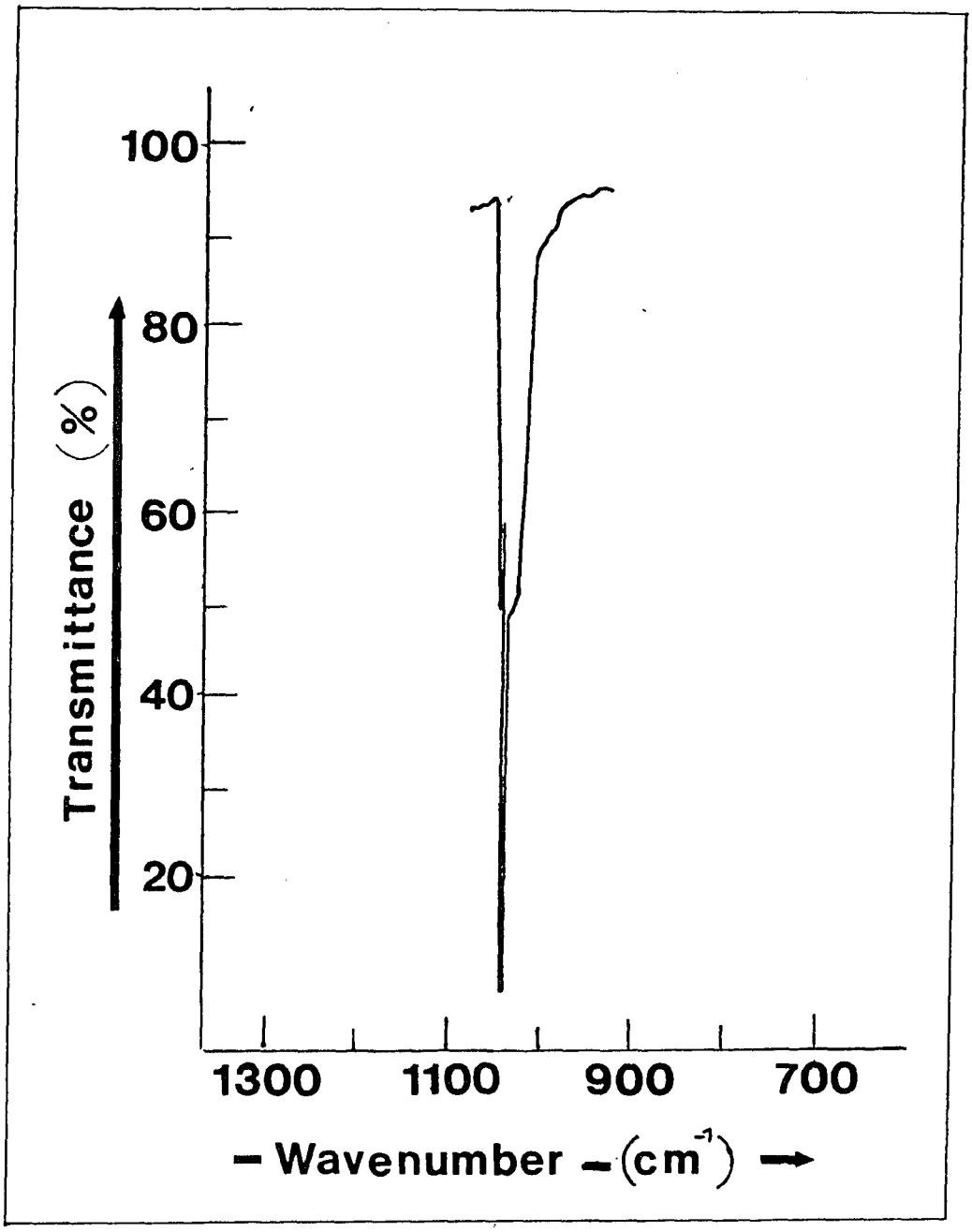

Figure (9) - The infrared spectrum of $VOCl_3$ (~ 5 torr).

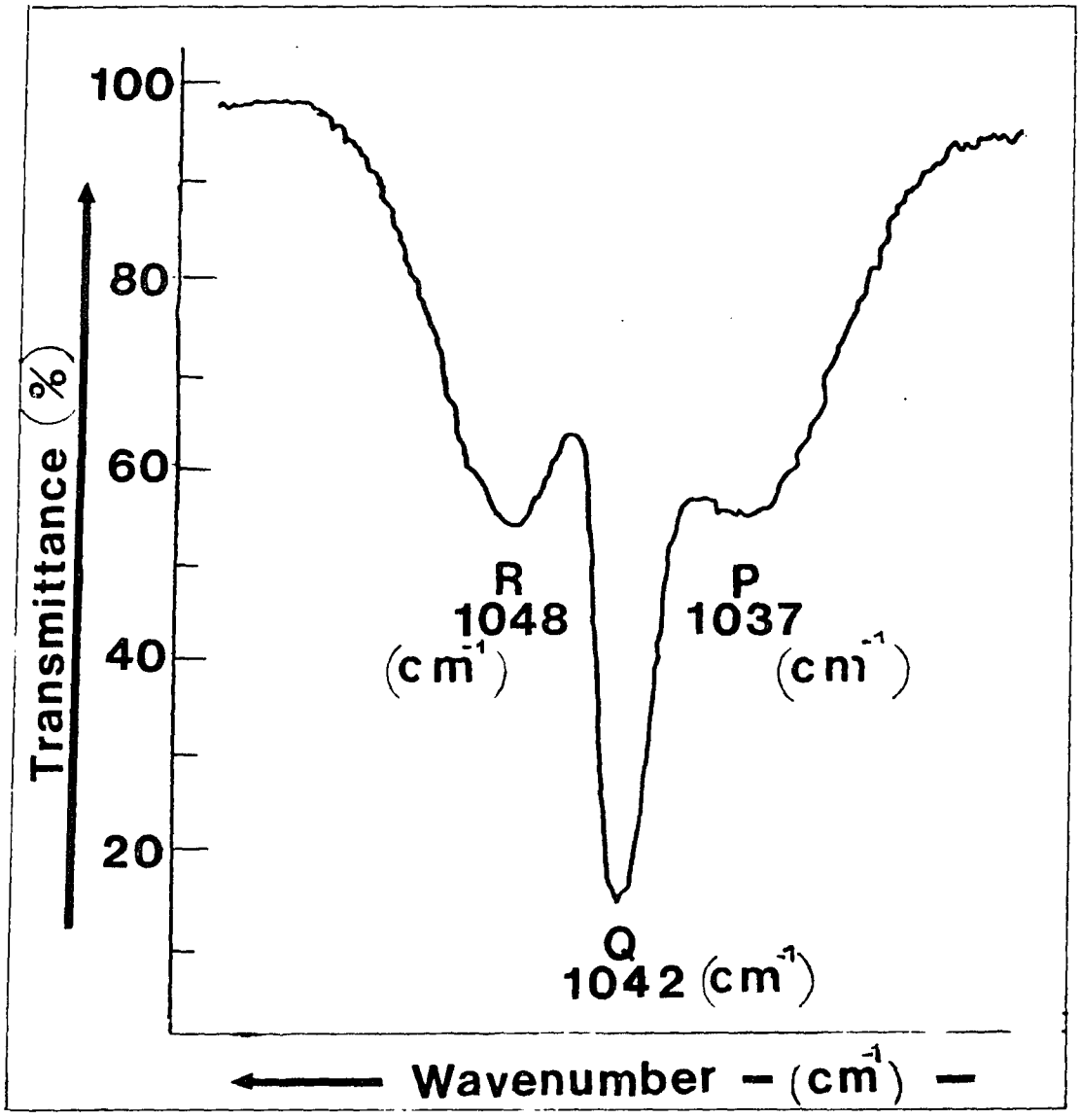

Figure (10) - A ten-fold expansion of Fig. (9) revealing the P, Q, and R branches of the $\nu_1(a_1)$ fundamental mode.

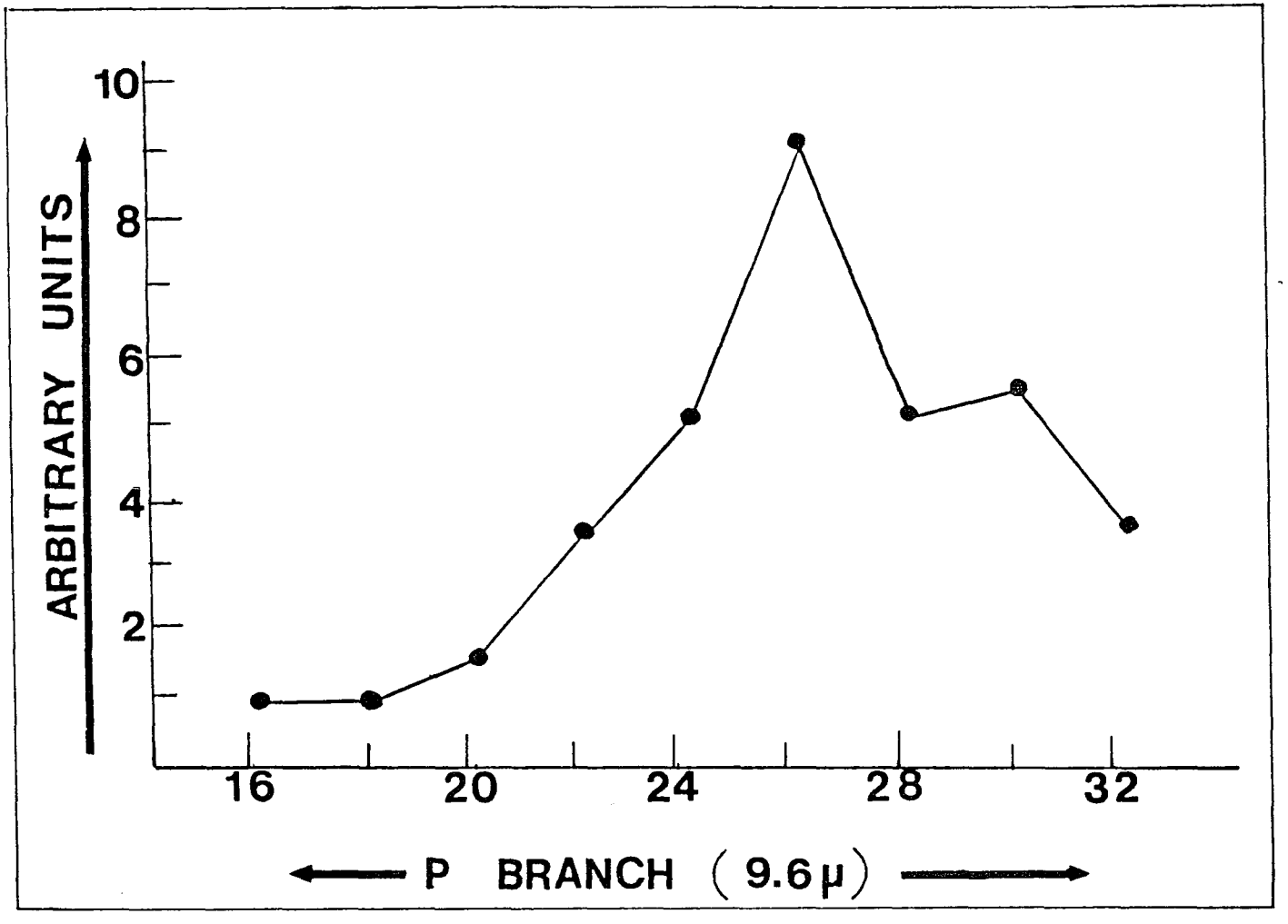

Figure (11) - The absorption spectrum of $VOCl_3$ when excited with rotational transitions within the P branch of the CO_2 laser's 9.6 μ region (unfocused geometry).

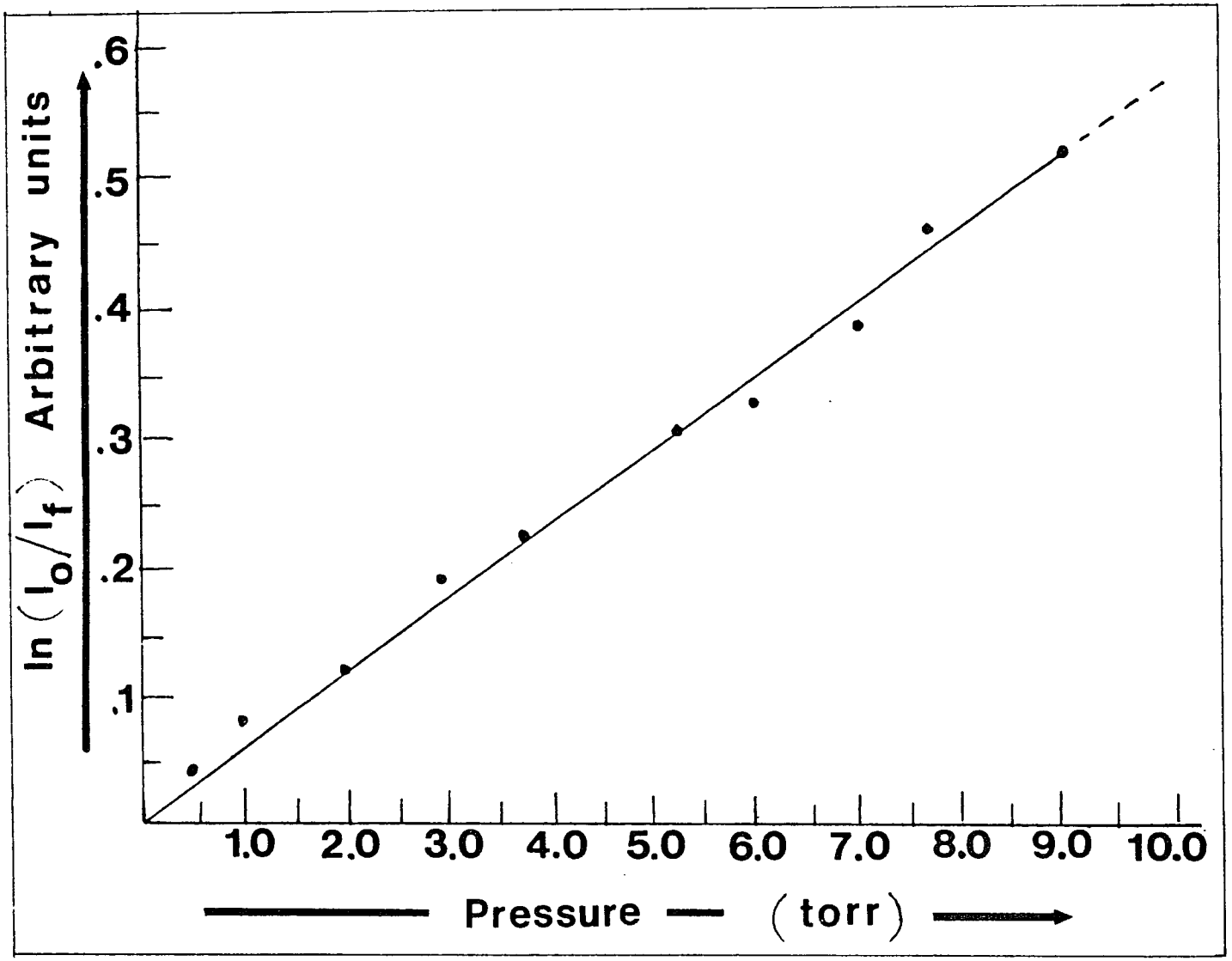

Figure (12) - A Beer-Lambert plot of $VOCl_3$ using the P(26) and the 9.6 μ band transition and a cell whose length was 10 cm.

establish the validity of a particular operating mechanism from the particular products formed and the luminescence observed as a function of pressure, fluence (J/cm^2), and scavenger gas, i.e., Cl_2, Ar, or H_2.

Prior to presenting our results, it is noteworthy to mention the results on the photodissociation of $VOCl_3$ by J. E. Eberhard et al. as well as H. G. Briggs et al. Eberhard and co-workers used a CO_2 laser to estimate the energy of activation of $VOCl_3$ to be ~ 65 kJ/mole [30]. They propose that the initial multiphoton dissociation event is the detachment of one Cl atom and that recombination would occur unless some scavenger is present. Thus, they rule out the possibility of using $VOCl_3$ as a means of enriching the vanadium isotope. It must be pointed out, however, that the fluence levels used were very low (~ 1.6 J/cm^2). Briggs and co-workers conducted a flash photolysis study of the $VOCl_3$ vapor at a pressure of 146 N/m^2 (~ 1.1 torr) with a photoflash energy and duration of 1350 J and 35 μsec respectively. Their results yielded an absorption spectrum of VO which was formed, they speculate, by a stepwise pyrolytic decomposition of $VOCl_3$ via $VOCl_2$ and VOCl [31]. In their work, there was no mention of any existing recombination.

Our results on the infrared multiphoton dissociation of $VOCl_3$ show that, when the molecule was

irradiated with unfocused pulsed CO_2 laser radiation tuned to $\nu_1(a_1)$ vibrational mode, no measurable dissociation occured. In addition, no measurable dissociation was detected when the laser radiation was focused and tuned to an off-resonant line. However, when the laser was tuned to the P(26) of 9.6 μ region, a resonant line, and focused, dissociation occured. The results are summarized as follows:

a) Pressure > 5 torr and laser energy $\geq$ .2 J.

Under such pressure and laser energy conditions, $VOCl_3$ initially dissociates to VO and Cl_2 but, then, any further dissociation cannot be achieved because VO recombines with Cl_2 to yield $VOCl_3$. The above statement is supported and deduced from the following experiments.

i) He-Ne laser scattering.

Initially, when a fresh sample of $VOCl_3$ vapor is introduced in a clean cell and irradiated with a .5 mW He-Ne laser, no scattering of particulates is visually apparent. The $VOCl_3$ sample was then irradiated with one CO_2 laser pulse. Again, using the He-Ne laser, some reflected points were observed due to the scattering of the He-Ne beam by the produced particulates After some time, ~ 20 minutes (~ 1000 pulses), the sample

again showed no particle scattering with the He-Ne laser [Fig. (13)]. From this experiment, one might instead conclude, but wrongly, that $VOCl_3$ completely dissociated. Pressure, IR, and mass spectrometric measurements showed that $VOCl_3$ was still present.

ii) Mass Spectrometry

The decrease of the major $VOCl_3$ peaks and increase in Cl_2 peaks in the mass spectrograms clearly shows that $VOCl_3$ does indeed dissociate. Also, by irradiating numerous cells containing the same number of $VOCl_3$ molecules (same volume, pressure, and temperature), it was found that no further dissociation occured after 1000 shots.

iii) Addition of Cl_2 and Ar.

Addition of Cl_2 inhibits the dissociation of $VOCl_3$ while the addition of Argon inhibits the recombination of $VO + Cl_2$.

iv) Addition of H_2.

Addition of H_2 to $VOCl_3$ drives the reaction to completion with the formation of HCl and VO. The reaction can be written as follows:

$$2VOCl_{3(g)} + 3H_{2(g)} \overset{nh\nu}{\rightarrow} 2VO_{(s)} + 6HCl_{(g)} \qquad (2.6)$$

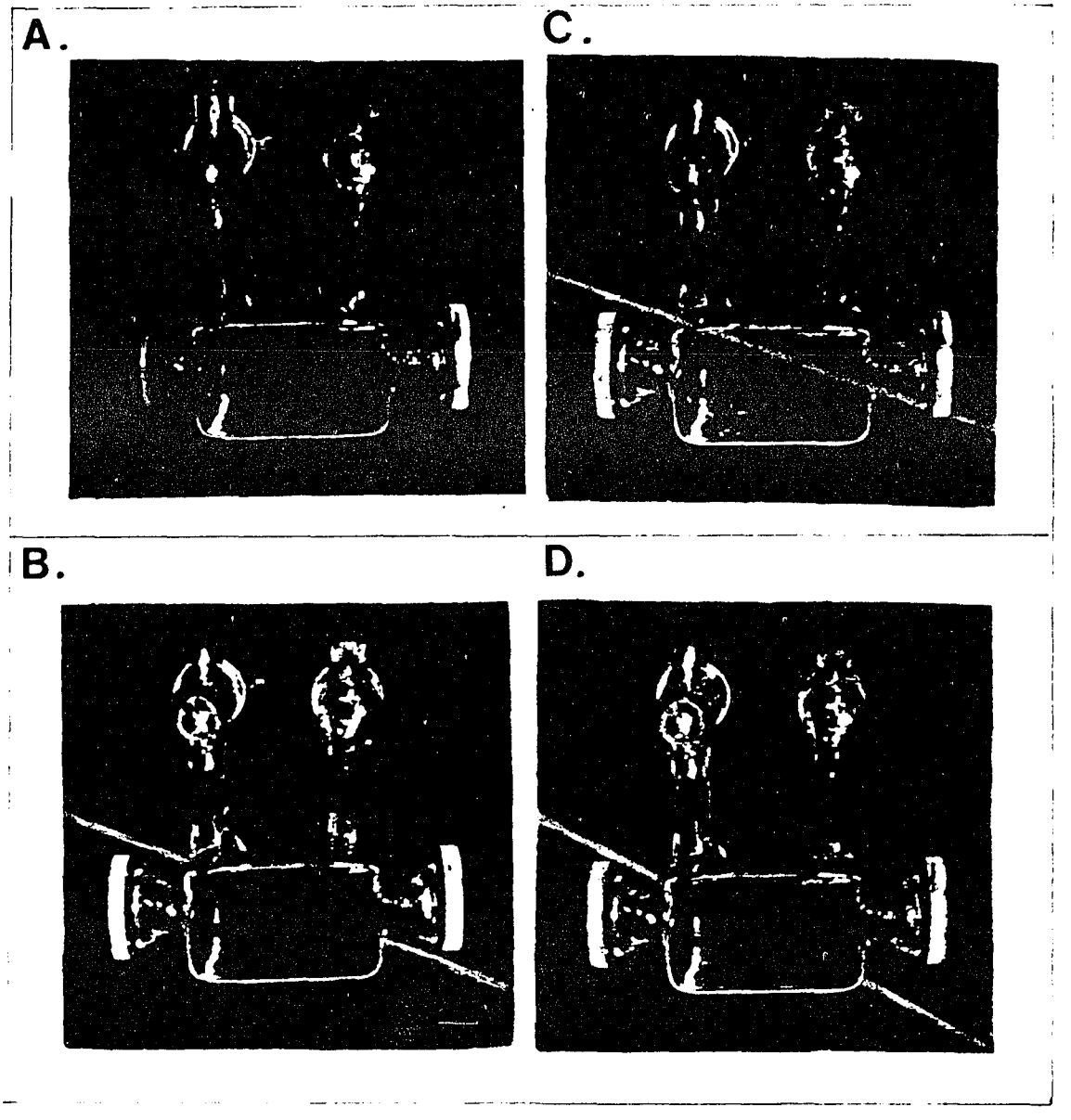

Figure (13) - Photographs showing a sequence of events. Fig. (A) is a photograph of a cell containing $VOCl_3$. Fig. (B), (C), and (D) are photographs of the same cell with a Helium-Neon laser directed through the cell before CO_2 laser excitation, after one laser pulse, and after 1000 laser pulses respectively.

The disappearance of major $VOCl_3$ bands and the appearance of HCl bands in the infrared absorption spectrum shows the dissociation of $VOCl_3$ and the formation of HCl. VO was shown to be the other dissociative product from the following facts. First, the particulates obtained from the multiphoton dissociation of $VOCl_3$ and H_2 were grey in color as should be. Other possible dissociative products, $VOCl_2$, VOCl, V_2O_3, V_2O_4, or V_2O_5, are green, brown, dark black, blue, and orange respectively. Second, addition of hydrochloric acid to the particulates gave a blue/violet solution characteristic of a hypovanadians salt. Third, the infrared spectra of the collected particles and of a VO standard in KBr pellets were identical.

v) Pressure of the cell.

Monitoring the pressure of the cell as a function of pulses shows an increase in slope, Fig. (14), which is consistent and indicative of $VOCl_3$ dissociating to VO and Cl_2 by the following equation

$$2VOCl_{3(g)} \xrightarrow{nh\nu} 2VO_{(s)} + 3Cl_{2(g)} \qquad (2.7)$$

since, for every two moles of $VOCl_3$ molecules that dissociate, three moles of Cl_2 molecules are formed. The leveling of the graph is indicative that no further dissociation is allowed after ~ 1000 shots and

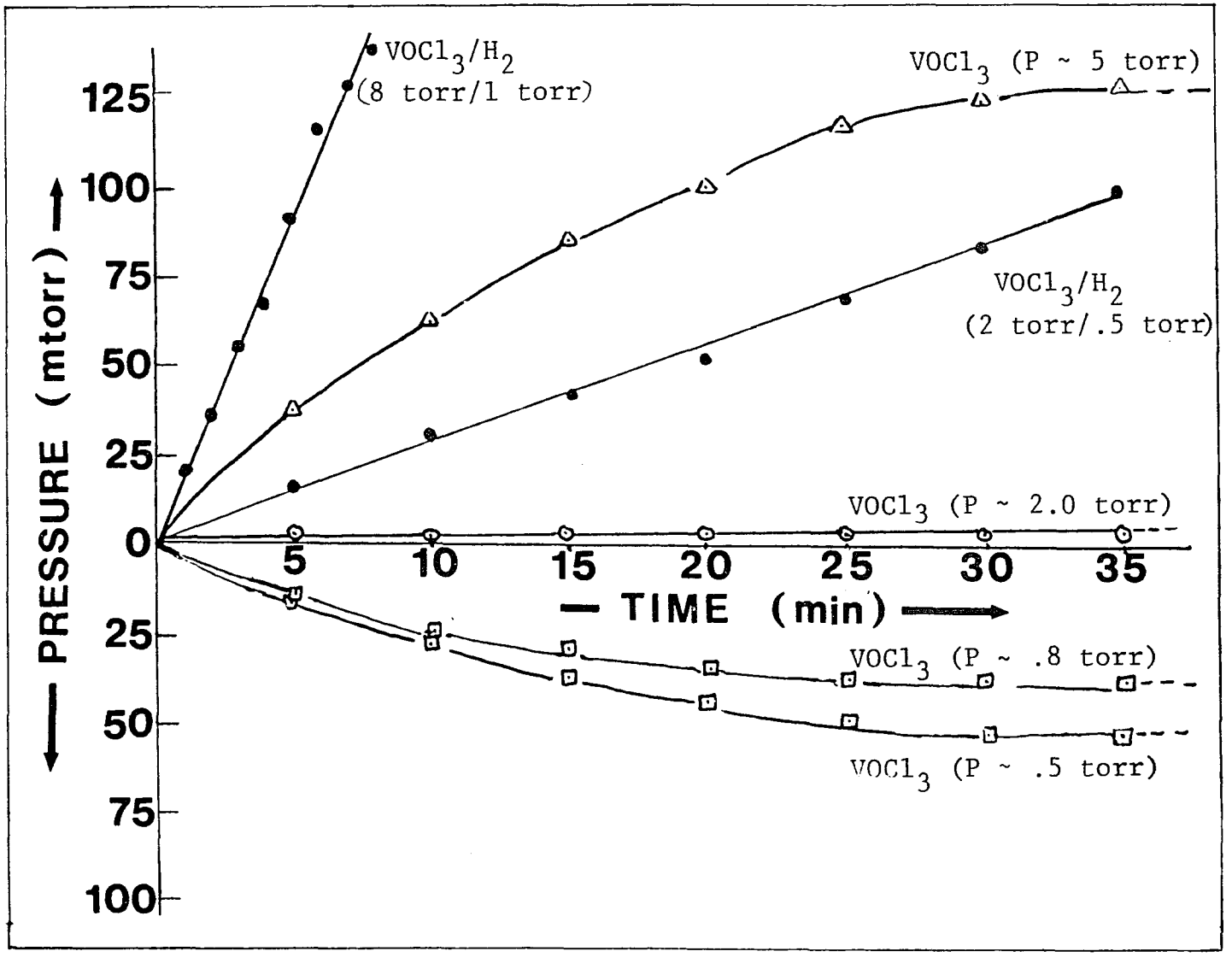

Figure (14) - A plot of a pressure change as a function of laser pulses (1 pulse = 1 sec). The laser energy which was .2 J corresponds to a fluence of ~ 8 J/cm^2.

recombination predominates.

b) Pressures < 1 torr and fluence ≤ .2 J.

At this point, it's appropriate to summarize various channels of multiphoton dissociation with the following equations

$$2VOCl_{3(g)} \rightleftharpoons \begin{cases} 2VOCl_{2(s)} + Cl_{2(g)} & (2.8) \\ 2VOCl_{(s)} + 2Cl_{2(g)} & (2.9) \\ 2VO_{(s)} + 3Cl_{2(g)} & (2.10) \end{cases}$$

From the above equations, it is seen that monitoring the pressure change of a cell containing $VOCl_3$ as function of number of pulses can be used to show the dissociative products of $VOCl_3$. The pressure change is dependent on the stoichiometric relationship of $VOCl_3$ to Cl_2. Since $VOCl_2$, VOCl, and VO are particulates, they do not contribute to the pressure change. The pressure change is also a function of the number of laser pulses, sample pressure, laser fluence, line intensity, irradiated volume, cell volume, and the presence of other gases.

The ratio of irradiated volume to cell volume would yield a large pressure differential if the cell volume is small, assuming that the irradiative volume is constant. Thus, in this experiment, a small

cell (~ 4 cm^3) was specially constructed to achieve maximum pressure change. The cell was directly connected to a baratron to read any pressure changes and irradiated with a laser frequency of P(26) of 9.6 μ. Fig. (14) shows a plot of pressure change as a function of number of laser pulses for various pressures at constant fluence (.2 J). At pressures greater than 5 torr, $VOCl_3$ dissociates to VO and Cl_2 as was discussed in the beginning of this section. However, at pressures less than 1 torr, $VOCl_3$ dissociates to $VOCl_2$ and Cl_2. At pressures greater than 1 torr and less than 5 torr, it's inconclusive. Either $VOCl_3$ dissociates to VOCl and Cl_2 or there exists a canceling out effect by the dissociative products, namely $VOCl_2$ and VO. In either case, the result is a zero pressure change. Keeping the pressure constant in this range and decreasing the fluence yielded a decrease in pressure, indicating that $VOCl_3$ is indeed dissociating to $VOCl_2$, while increasing the fluence yielded an increase in pressure, indicative of the production of VO. Again, this experiment is inconclusive in terms of whether $VOCl_2$ is produced. One can still argue that a zero pressure change is due to a cancelling out effect of $VOCl_2$ and VO while an increase or decrease of pressure, resulting from an increase or decrease of fluence respectively, is due to the production of either $VOCl_2$ or VO more so than the other.

In addition, from Fig. (14), it is seen that the addition of H_2 to $VOCl_3$ gives rise to a positive linear dependence of pressure change on the number of laser pulses. From the following reactions,

$$2VOCl_{3(g)} + H_{2(g)} \rightarrow 2VOCl_{2(s)} + 2HCl_{(g)} \quad (2.11)$$

$$VOCl_{3(g)} + H_{2(g)} \rightarrow VOCl_{(s)} + 2HCl_{(g)} \quad (2.12)$$

$$2VOCl_{3(g)} + 3H_{2(g)} \rightarrow 2VO_{(s)} + 6HCl_{(g)} \quad (2.13)$$

it can be seen that the only equation supportive of an increase in pressure, as evident from the stoichiometry, is equation (2.13). This is consistent with other experiments described earlier. We also note that the curve doesn't level off as does $VOCl_3$ in the neat. This is consistent with the complete dissociation of $VOCl_3$ with H_2 to VO and HCl. The other curves indicate that the dissociation of $VOCl_3$ comes to a stop even though $VOCl_3$ is not completely dissociated and is consistent with the recombination proposed in the previous section.

At this point, one can only speculate about the photodissociative pathways in which the products were formed. Although the energy is deposited in the V = 0 bond, the lowest dissociation channel is the preferred route and thus $VOCl_2$ is formed. $VOCl_2$ is

formed by a one-step detachment of a Cl atom from $VOCl_3$. VOCl can either be formed by a one-step elimination of a Cl_2 molecule from $VOCl_3$ or by the dissociation of $VOCl_3$ to $VOCl_2$ followed by the dissociation of $VOCl_2$ to VOCl. The formation of VO poses the same question. That is, do the Cl atoms detach simultaneously from $VOCl_3$ to form VO, or is VO formed by a stepwise fragmentation of $VOCl_3$ via $VOCl_2$ and VOCl? With these thoughts in mind, experiments concerning the origin of the luminescence arising from CO_2 laser excitation of $VOCl_3$ were undertaken and are presented below.

3. Origin of luminescence

Upon focusing the CO_2 laser with radiation tuned to the resonant P(26) line of the 9.6 μ region into a cell containing $VOCl_3$, a visible emission can be observed across the cell [Fig. (15)]. A spectrum of the luminescence at a pressure of 5 torr and a laser energy of .3 J is presented in Fig. (16). When the laser output was either tuned to an off-resonant line or was unfocused, no emission was detected.

The basic phenomena of visible emission induced via CO_2 laser excitation of a molecule can be explained by a number of mechanisms. First, if the fluence level of the laser is large enough to initiate optical breakdown, such electronic luminescence is expected. Second, such emission can be caused by radical recombina-

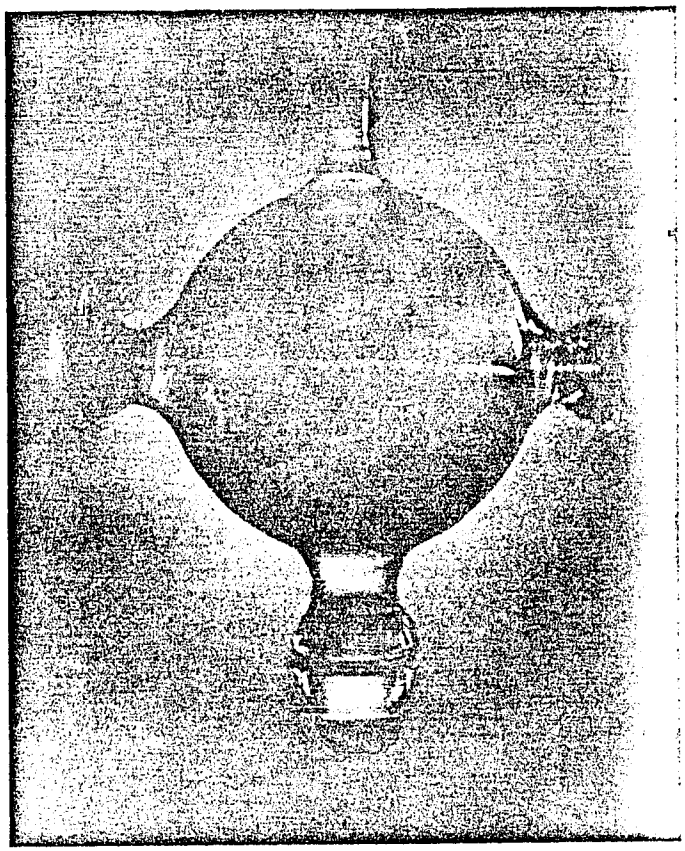

Figure (15) - A photograph of the molecular emission induced by a CO_2 laser. [32]

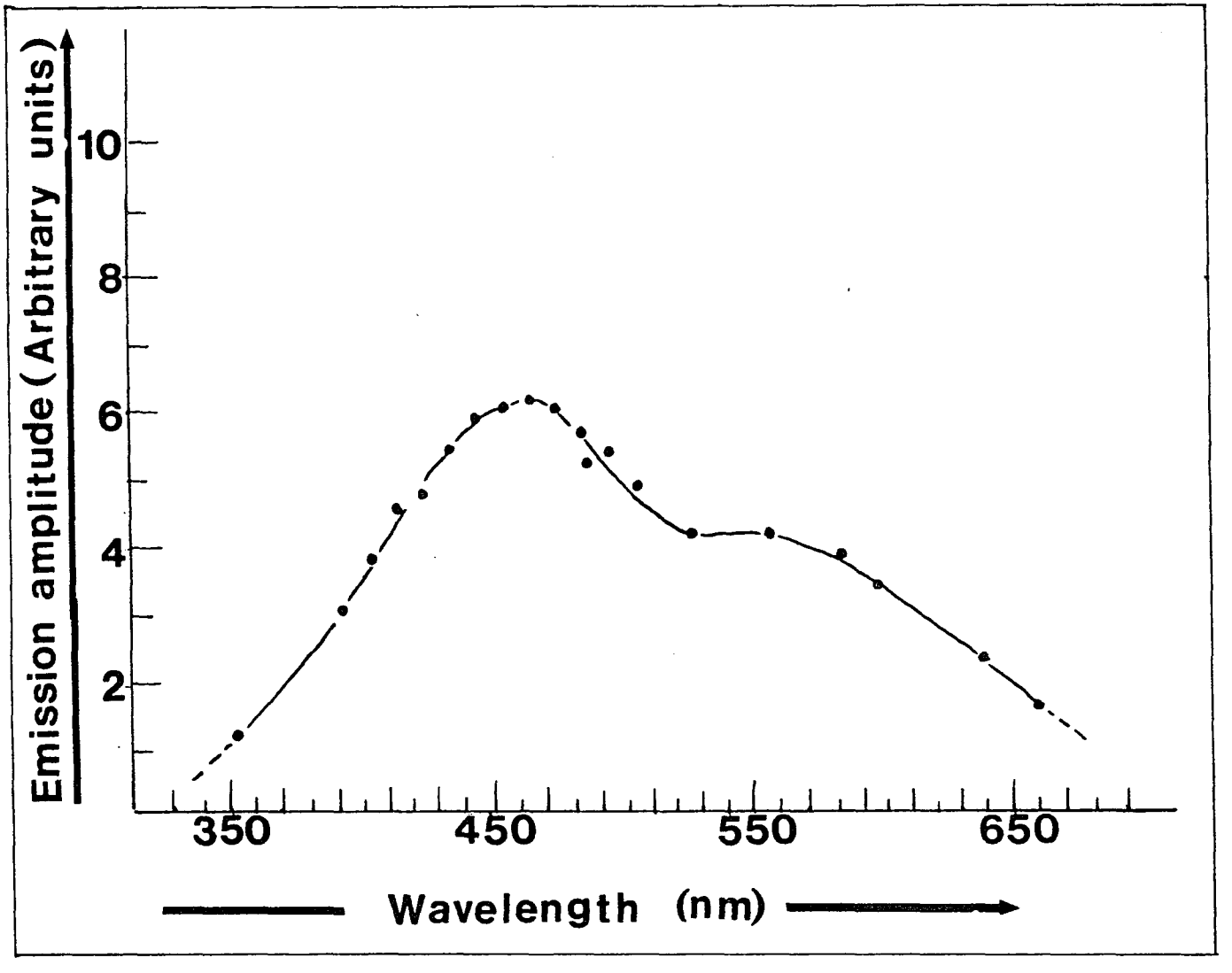

Figure (16) - An emission spectrum following irradiation of $VOCl_3$ by CO_2 laser radiation. The pressure was 5 torr and the laser energy .3 J.

tion. Third, such emission can be due to the production of electronically excited fragments. Fourth, such fluorescence can arise from the production of the electronically excited parent species.

Avoiding the rather obvious regime of high fluence and high pressure conditions insures the absence of optical breakdown with its associated plasma-like emissions. Measurements of the emission wavelengths and their dependence on laser fluence, molecular pressure, and the presence of scavenger gas should allow for some obvious and some not so obvious distinctions between the above mechanisms.

a) Multiple photon absorption leading to inverse electronic relaxation.

In certain molecules, i.e., CrO_2Cl_2 and OsO_4, mulitple photon absorption leads to emission in the visible region due to the process of inverse electronic relaxation (IER) [10,11]. A mechanism used to explain IER is shown in Fig. (17). In Fig. (17), it is seen that, once the molecule has absorbed enough photons to reach the excited electronic state whose minimum is located below the ground state dissociation limit, mixing of highly excited vibrational levels in the ground electronic state with low-lying vibronic levels of the excited electronic state can result in crossover and the excited molecule may fluoresce to its ground

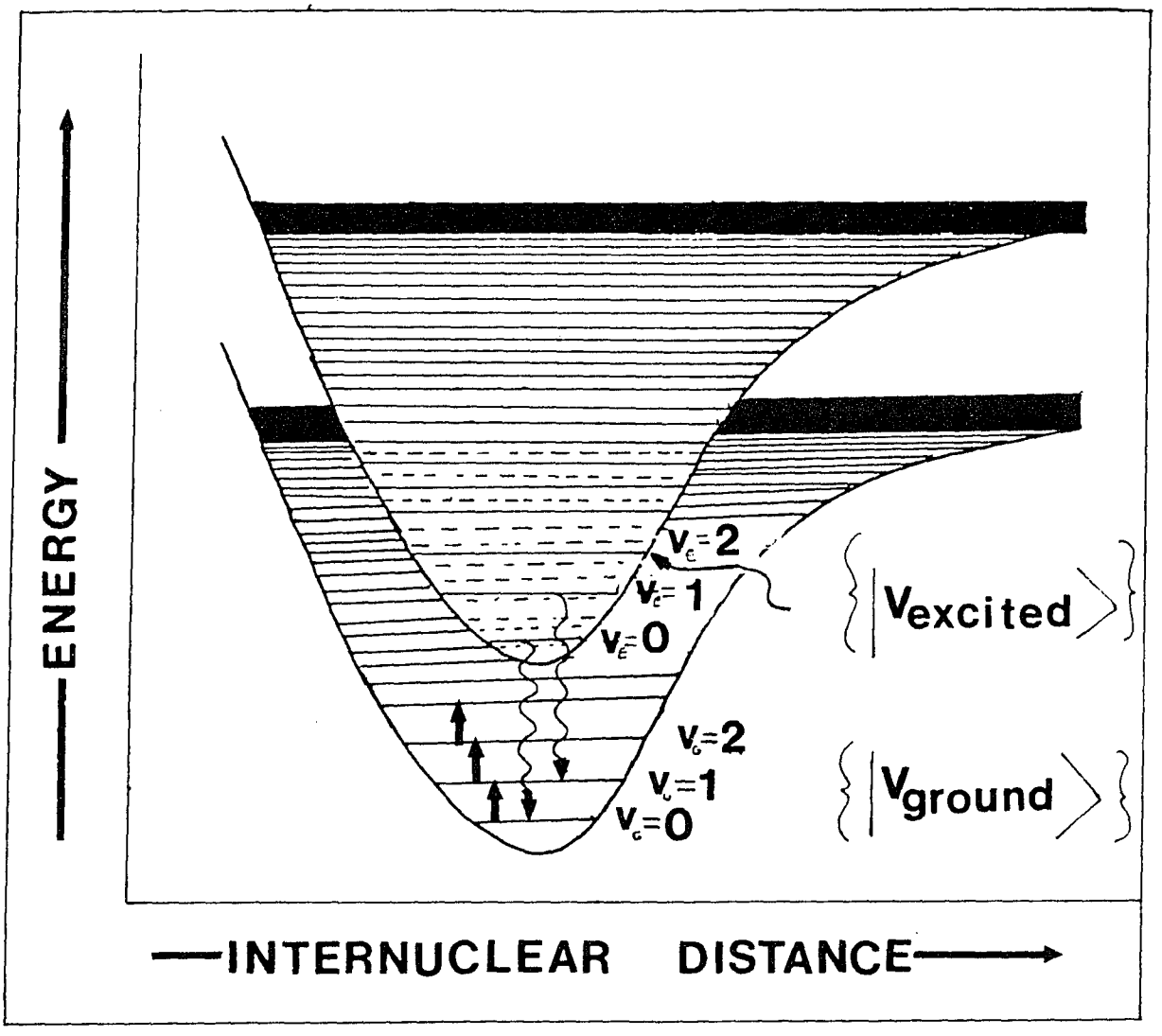

Figure (17) - A potential energy diagram of a molecule capable of IER.

electronic state.

The arguements and experimental evidence presented below are not supportive of emission from an electronically excited parent specie.

i) Energetics.

In order for IER to occur, the existence of a low-lying excited electronic state whose energy is below that of the dissociation limit is a necessary condition. When this study began, it was believed that the energy required to rupture the $VOCl_2$-Cl bond was ~ 120 ±10 kcal/mole, estimated by G. Flesh et al. from mass spectrometric studies [33]. Hence, the 333 nm bond corresponding to an energy of approximately 83 kcal/mole was at first thought to correspond to a low-lying excited electronic state whose energy was below that of the dissociation limit. Later work, done by J. P. Sung and D. W. Setser [34], estimated the dissociation energy to be ~ 86 kcal/mole. From our own work, we have estimated this energy as $\leq$ 83 kcal/mole, making the energy of the first electronic state at best equal but not smaller than the dissociation limit of the ground state. This value was deduced from the fact that irradiating a sample of $VOCl_3$ with a nitrogen laser (337.1 nm) lead to dissociation. Therefore, the dissociation energy of $VOCl_3$ is $\leq \lambda$ = 337 m or 83 kcal/mole.

ii) Nitrogen laser excitation.

This arguement, perhaps most supportive, comes from the experiments in which samples of $VOCl_3$ (pressure 500 mtorr - 5 torr) were irradiated with a N_2 laser. The argument is as follows. The dissipation of energy, in the form of IER, in a molecule in its excited state must be the same whether it was obtained via multiple photon excitation (CO_2 laser) or single photon excitation (N_2 laser). The energy to reach the first excited state of $VOCl_3$ (333 nm) corresponds approximately to the energy of a photon emitted by a N_2 laser (~ 337 nm). Since $VOCl_3$ did not emitt any light which would correspond to a transition from its excited state to its ground state, the visible emission observed from MPA cannot be a result of IER.

b) Multiple photon absorption leading to recombination.

Addition of Ar or H_2 to a sample of $VOCl_3$ should diminish or prevent any recombination that occurs in $VOCl_3$. The fact that the emission spectrum obtained with $Ar/VOCl_3$ and $H_2/VOCl_3$ is similar in wavelength but larger in amplitude than the emission spectrum from $VOCl_3$ in the neat is strongly supportive of the arguement that the emission observed is not due to any recombination process. A spectrum of $VOCl_3/H_2$ is shown in Fig. (18).

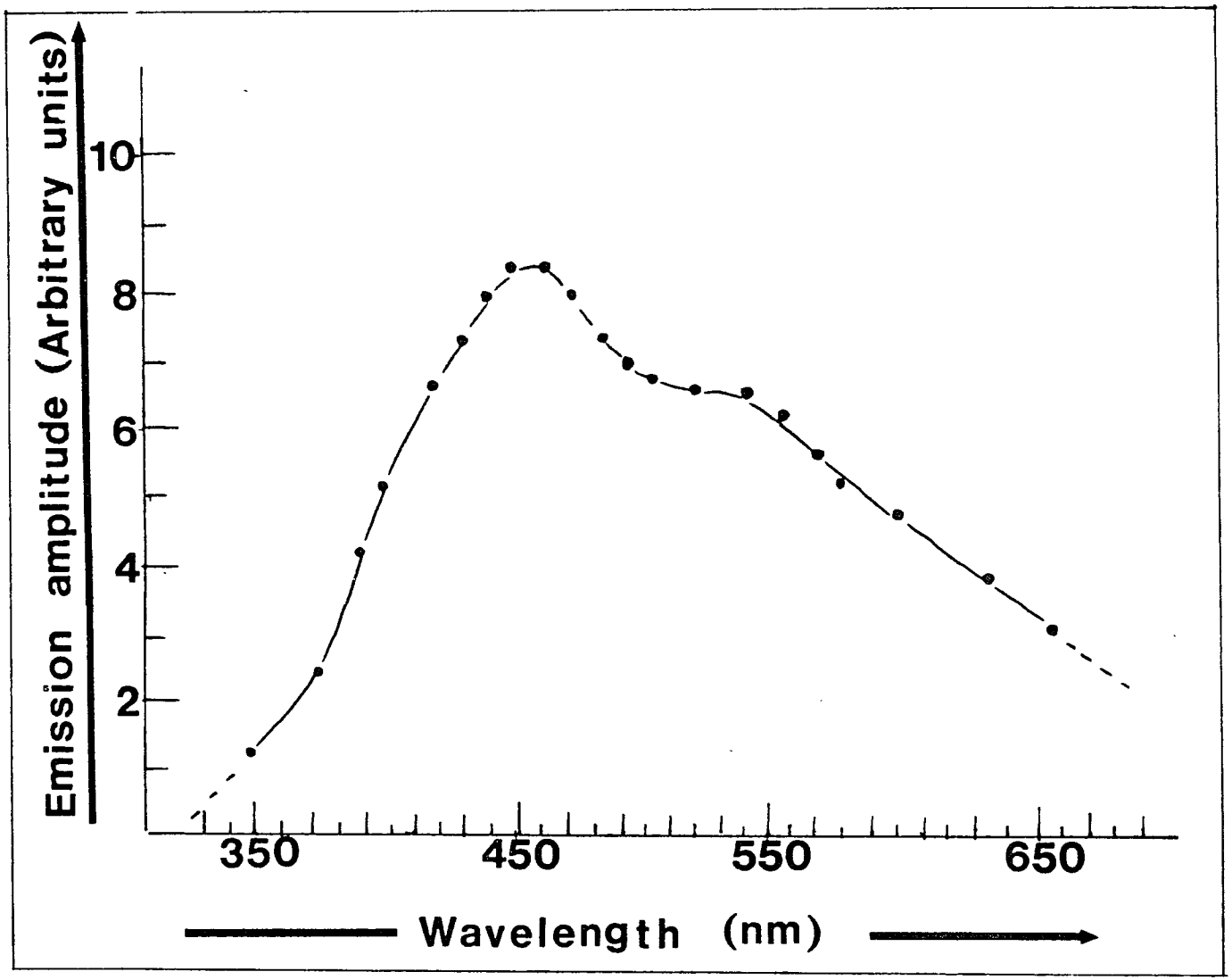

Figure (18) - An emission spectrum following irradiation of $VOCl_3$/ Hydrogen with a CO_2 laser at a pressure of 4 torr and 1 torr respectively.

c) Multiple photon absorption yielding electronically excited fragments.

One must then conclude that the emission observed is due to the production of electronically excited fragment(s). Anticipating such, studies dealing with the behavior of the fluorescence lifetime as a function of pressure, measurements of lifetimes, and the correlation of the observed emission to $VOCl_2$, VOCl, and VO emission spectra were carried out. The results can be divided either into a high pressure and fluence regime or a low pressure and fluence regime.

i) High pressure and fluence regime (> 100 mtorr and > .5 J).

Fig. (19) is a plot of VO emission intensity as a function of wavelengths obtained from a table listing the strongest intensities at various wavelengths published by Mahanti [35]. Comparing this spectrum, whose maximum is at 580, with Fig. (16) clearly reveals that the VO specie is not a major contributor to the emission obtained when $VOCl_3$ was irradiated with a CO_2 laser at high pressure.

Gas phase emission spectra of $VOCl_2$ and VOCl have unfortunately, to the best of our knowledge, never been recorded. However, since the maximum absorption bands of $VOCl_3$, taken in the gas phase, only shift by approximately 6 nm from those taken in DMS or cyclohexane

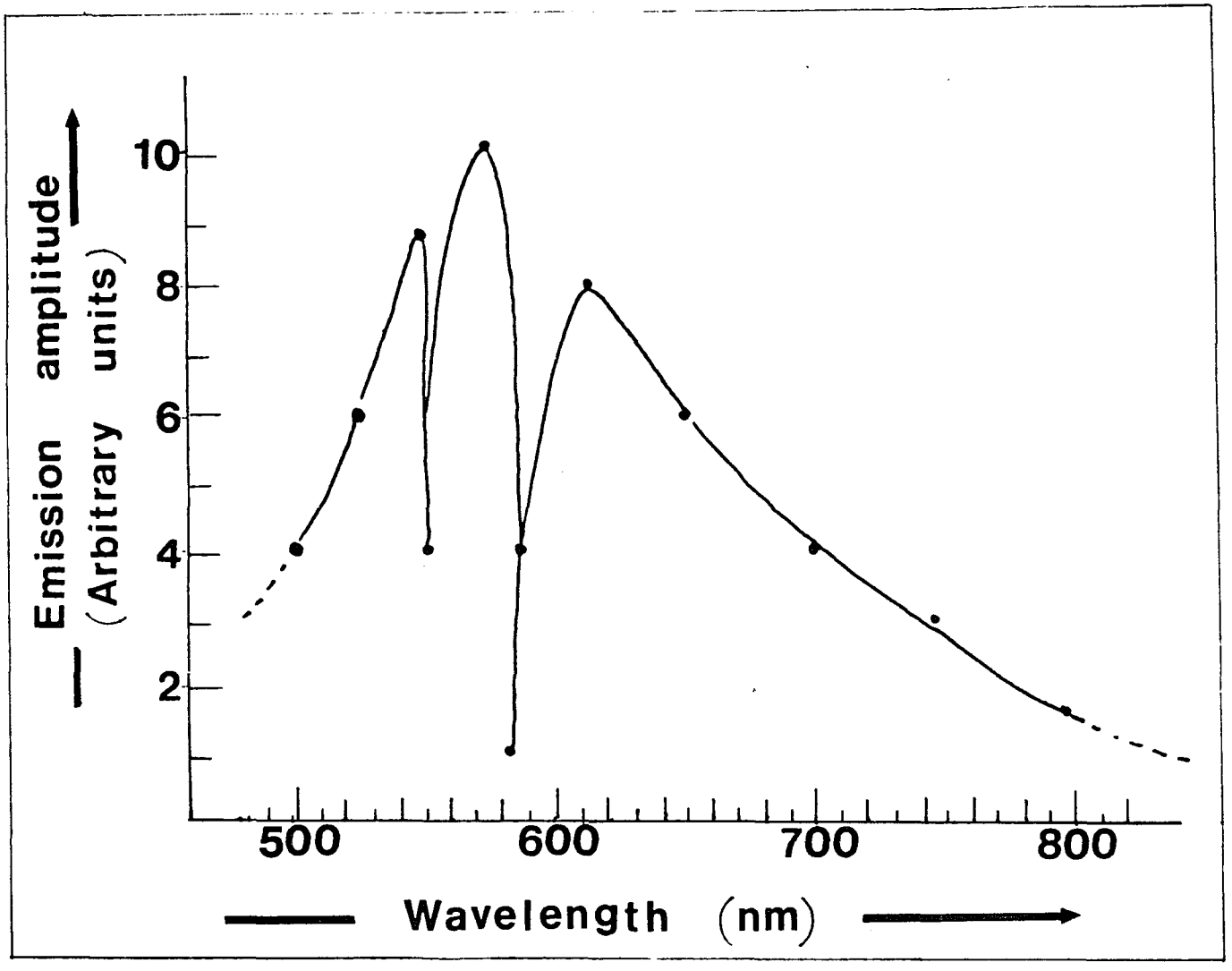

Figure (19) - The gas phase emission spectrum of VO.

solution [28], it was assumed that the gas phase emission spectra of $VOCl_3$, $VOCl_2$, and VOCl would also shift by a similar extent from those in solution. Thus, the only difference in spectra, if any, would be a slight shift in the emission maximum and a broadening due to collisions. These assumptions are verified in the results obtained. The emission spectrum of $VOCl_2$ in DMS solution (~ 10^{-6} M) when excited at 347 nm is presented in Fig. (20) while that of VOCl, under the same conditions, is shown in Fig. (21). Both graphs appear to be similar to each other, having a maximum absorption at 470 nm, and to the emission spectrum obtained by exciting $VOCl_3$ via a pulsed CO_2 laser. This strongly suggests that, at high pressure and laser energy, $VOCl_2$ and/or VOCl are the emitting species. It must also be pointed out that no emission was observed when a solution of $VOCl_3$/DMS (~ 10^{-6} M) was excited at 342 nm. This is consistent with gas phase studies of $VOCl_3$ when excited with a nitrogen laser.

ii) Low pressure and laser energy regime (< 100 mtorr and < .5 J).

Fig. (22) is a typical oscillogram taken subsequent to $VOCl_3$ excitation by a CO_2 laser tuned to P(26) 9.6 μ at a pressure of ~ 10 mtorr, laser energy of .5 J, and a wavelength of 460 nm. The amplitude and the time behavior of the emission signal as

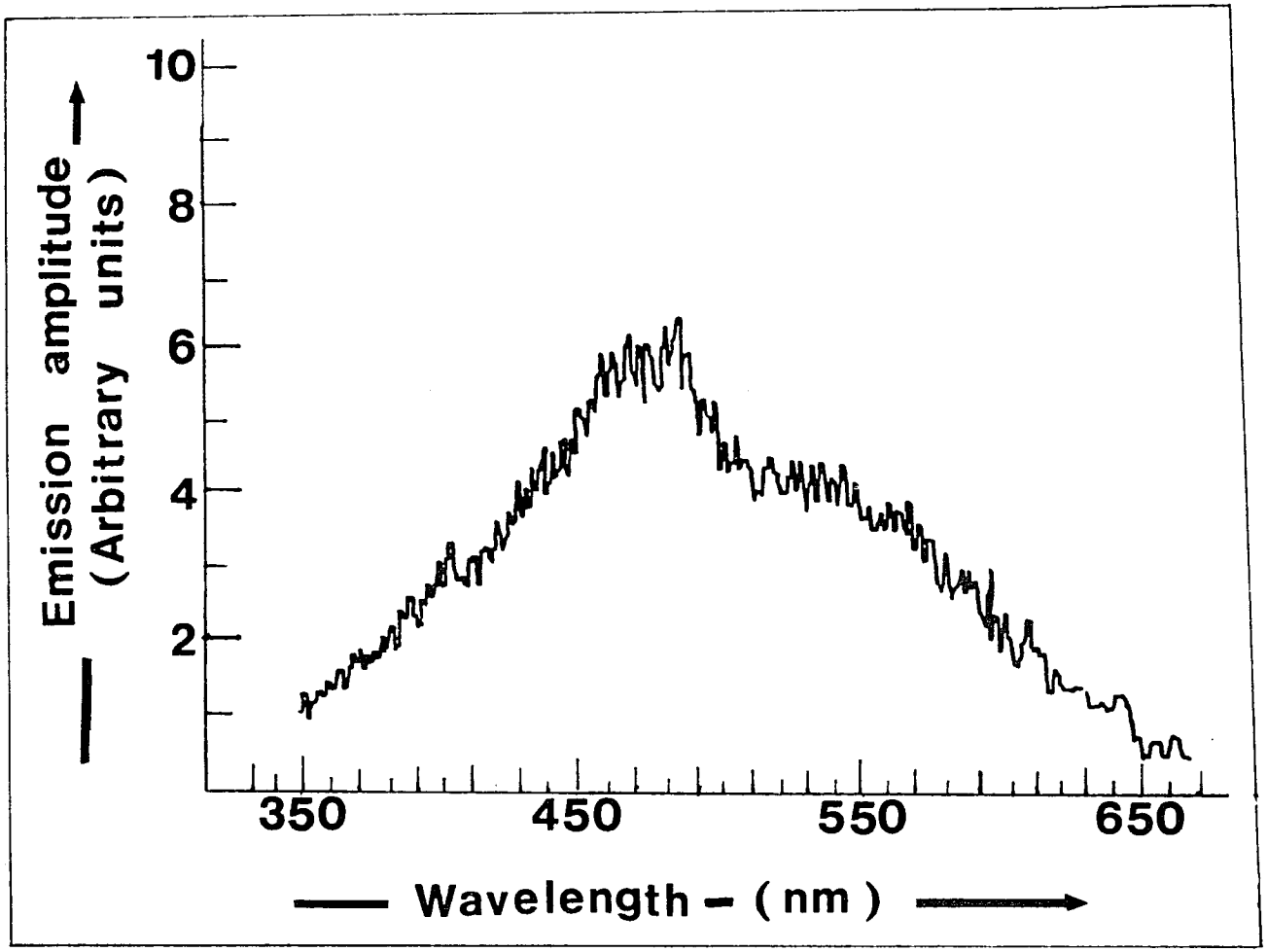

Figure (20) - An emission spectrum of $VOCl_2$/DMS (~ 10^{-6} M).

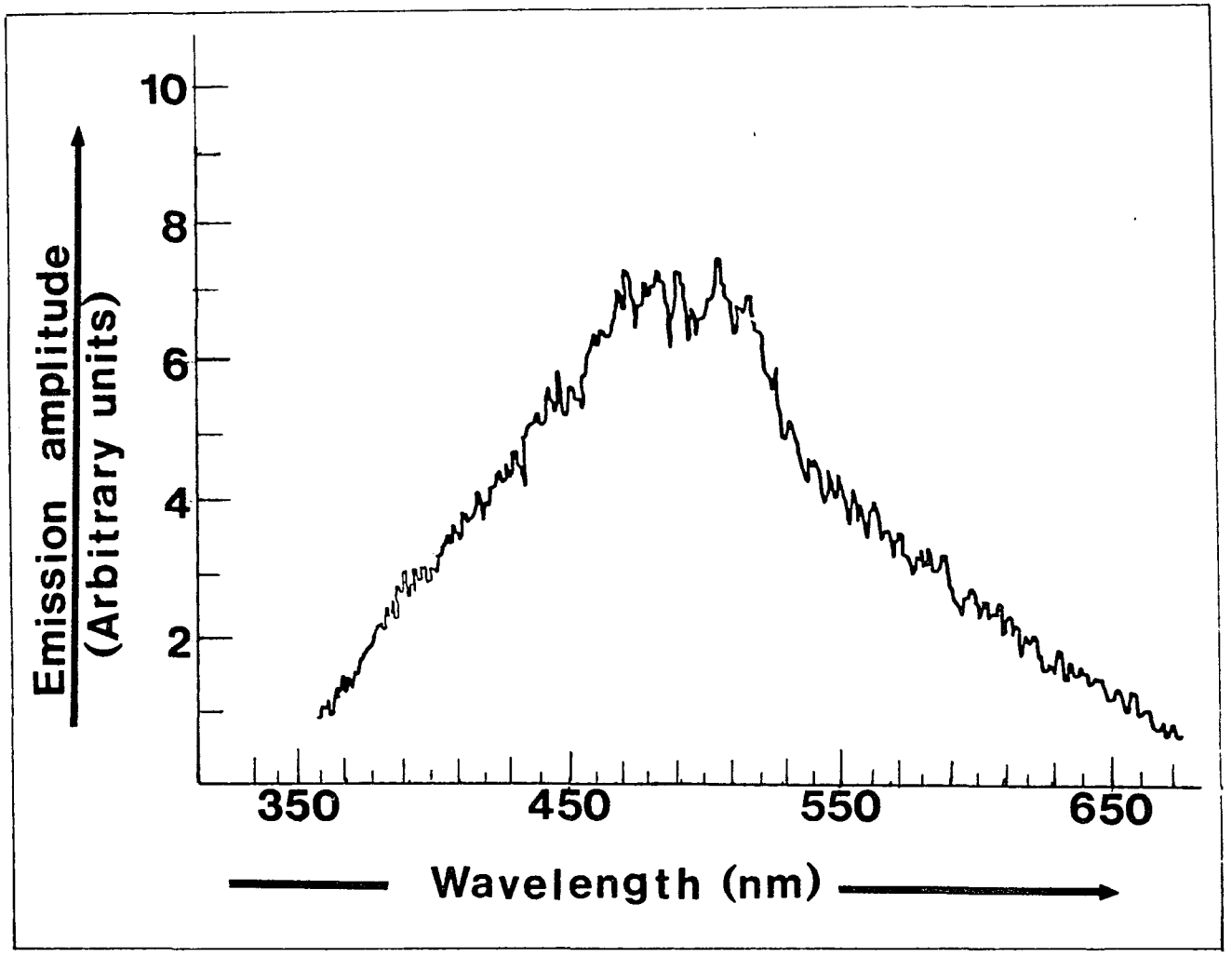

Figure (21) - An emission spectrum of VOCl/DMS (~ 10^{-6} M).

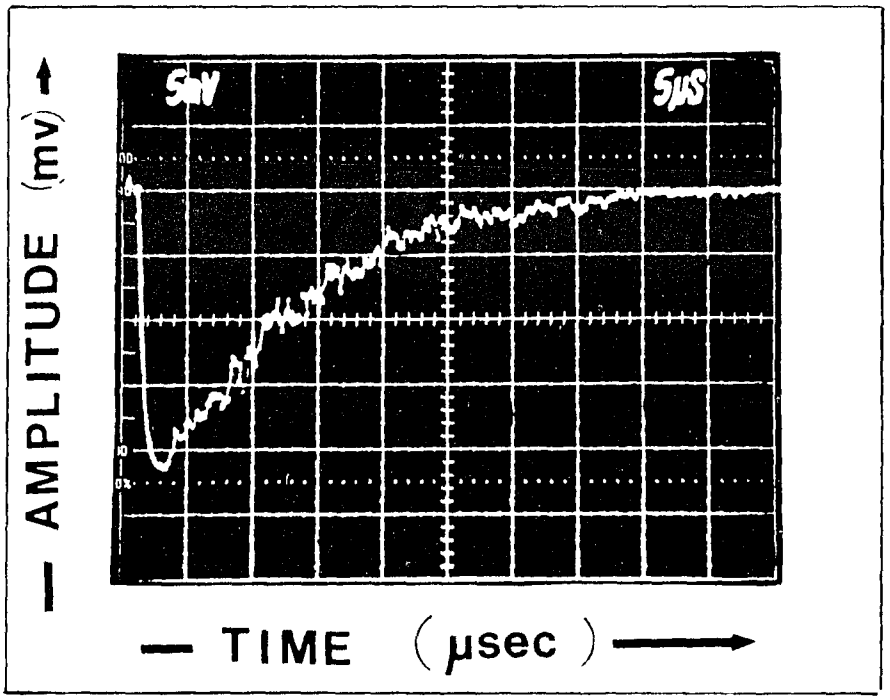

Figure (22) - An oscillogram of the 460 nm emission subsequent to CO_2 laser excitation [P(26), 9.6 μ] of $VOCl_3$ at a pressure of 10 mtorr and a fluence of .5 J.

a function of wavelength, laser energy, and pressure were investigated and are presented. Fig. (23) shows a plot of emission amplitude as a function of wavelength at 20 mtorr and .5 J while Fig. (24) presents the variation of the luminescence amplitude with laser energy at that pressure. It is evident that the spectra shown in Fig. (23), whose maximum is centered at a wavelength of 460 nm, is similar to the high pressure spectrum. The high pressure spectrum is broader as a result of collisions.

In Fig. (24), the emission amplitude in the range of .2 - 1.2 J increases with fluences, as expected, and the threshold energy for the emission can be extrapolated to .2 J. At higher laser energy, the emission signal should reach a maximum followed by a plateau, upon which further increase in laser energy causes no further increase in emission signal. This is due to the finite number of molecules that interact at the focal region with the laser radiation.

The emission risetime is essentially equal to that of the laser pulse (~ 200 nsec) and is both independent of pressure (< 1 torr) and fluence (< 1.5 J). At 20 mtorr of pressure, from kinetic theory, there are approximately $VOCl_3$-$VOCl_3$ collisions per μsec. This, together with the use of a short laser

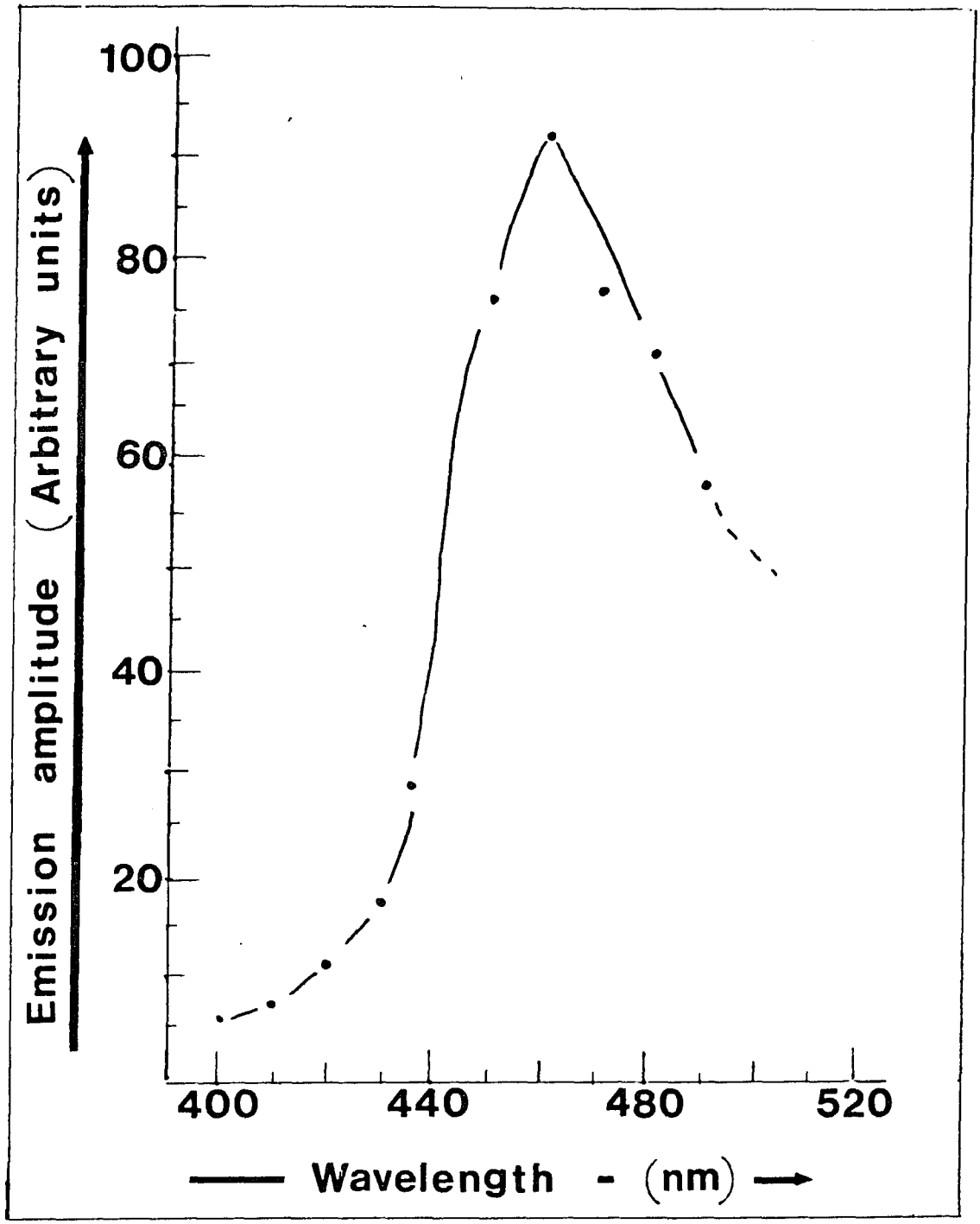

Figure (23) - An emission spectrum following the irradiation of $VOCl_3$ by a CO_2 laser tuned to the P(26) of the 9.6 μ band. The spectrum was recorded under flow conditions with a cell pressure of 20 mtorr.

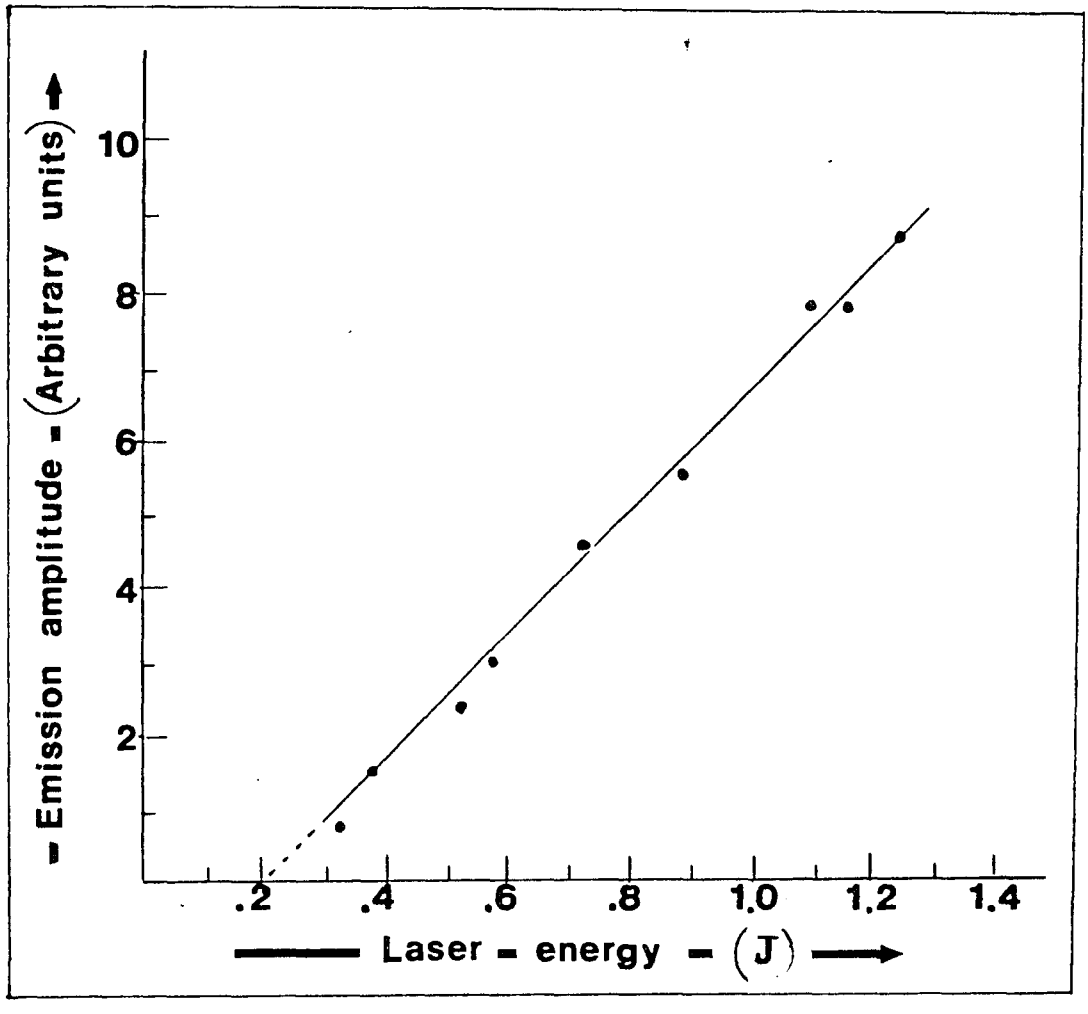

Figure (24) - A plot of emission amplitude versus laser energy at a wavelength of 460 nm and a $VOCl_3$ pressure of 20 mtorr.

pulse, ~ 300 nsec FWHM, establishes the collisionless nature of the MPA induced emission. Moreover, at high pressures, when collisions do begin to play a role, a collisional component of emission signal can be observed. No such component was observed at pressures less than $\lesssim$ 20 mtorr.

The lifetime of luminescence signal is independent of wavelength (20 mtorr) and fluence (< 1.5 J) but is pressure dependent (< 100 mtorr) as shown in Figs. (25), (26), and (27) respectively. It must be noted that the terms lifetime and decay time are often used interchangeably when the build up of the signal, as is true in the present case, is instantaneous compared to its decay.

Fig. (25) presents a graph of the lifetime as a function of wavelength taken at 20 mtorr. The lifetimes, which have a value of ~ 13.8 μsec, are independent of wavelength. This is indicative that, at a low pressure and fluence regime, there is only one existing specie contributing to the emission.

Fig. (27), a Stern-Volmer plot, shows the dependence of reciprocal lifetime (rate) to be linear with pressure under 60 mtorr. This supports the claim of collisionless production of fluorescence by MPA. However, at a pressure greater than 60 mtorrs, the dependence ceases to be linear as the slope continuously

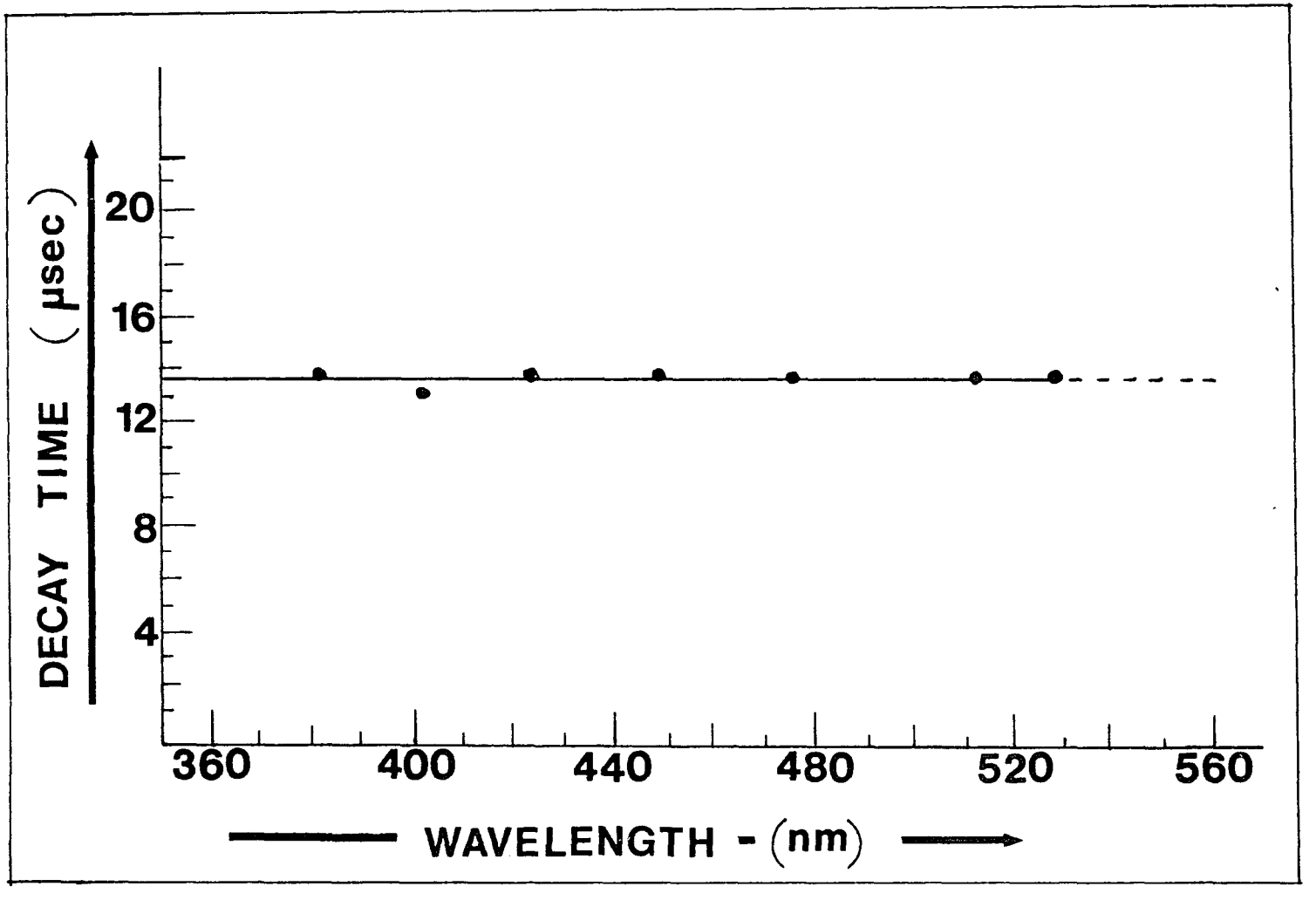

Figure (25) - A plot of emission decay time as a function of wavelength at a pressure of 20 mtorr and a laser energy of .5 J.

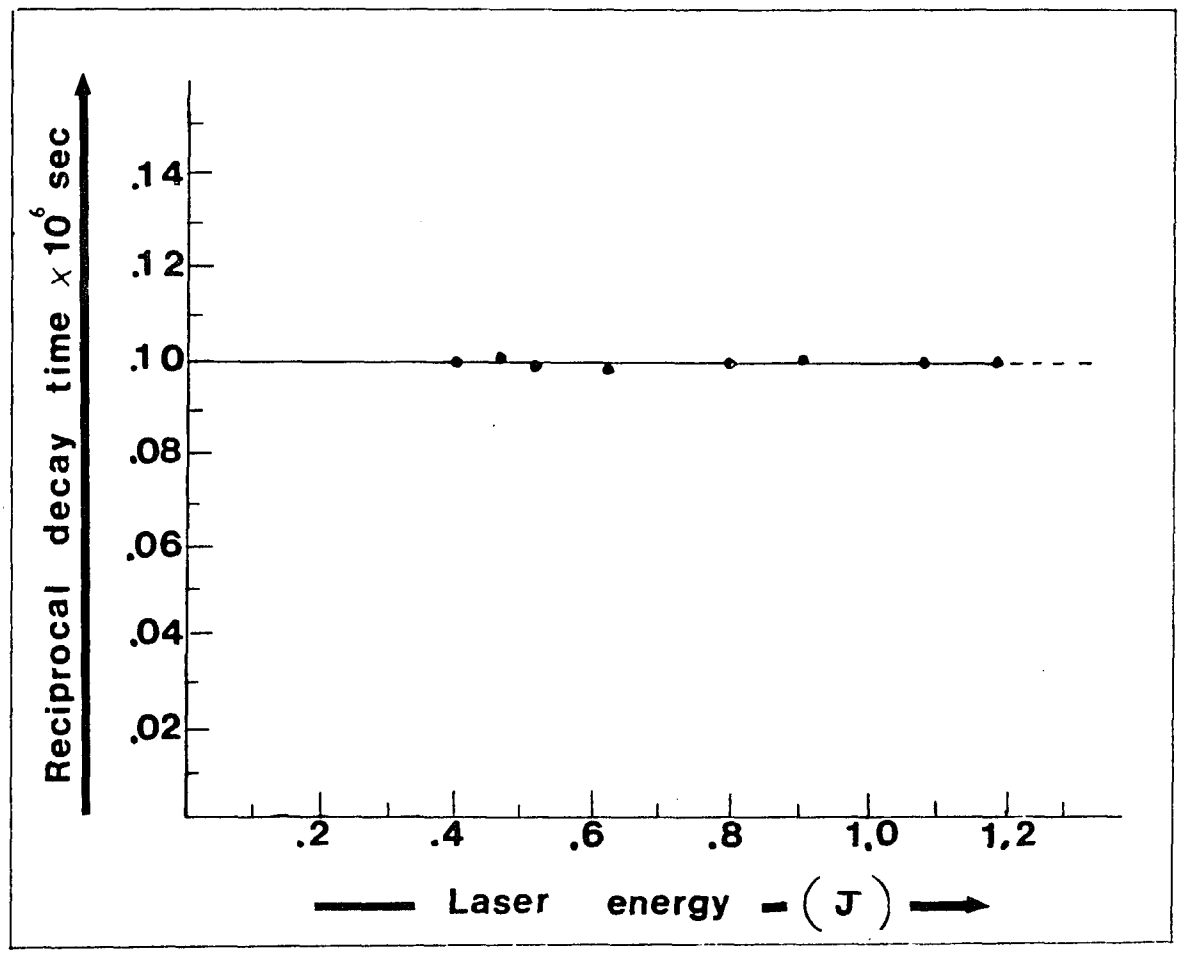

Figure (26) - A plot of reciprocal decay time as a function of laser energy at a pressure of 20 mtorr and a wavelength of 460 nm.

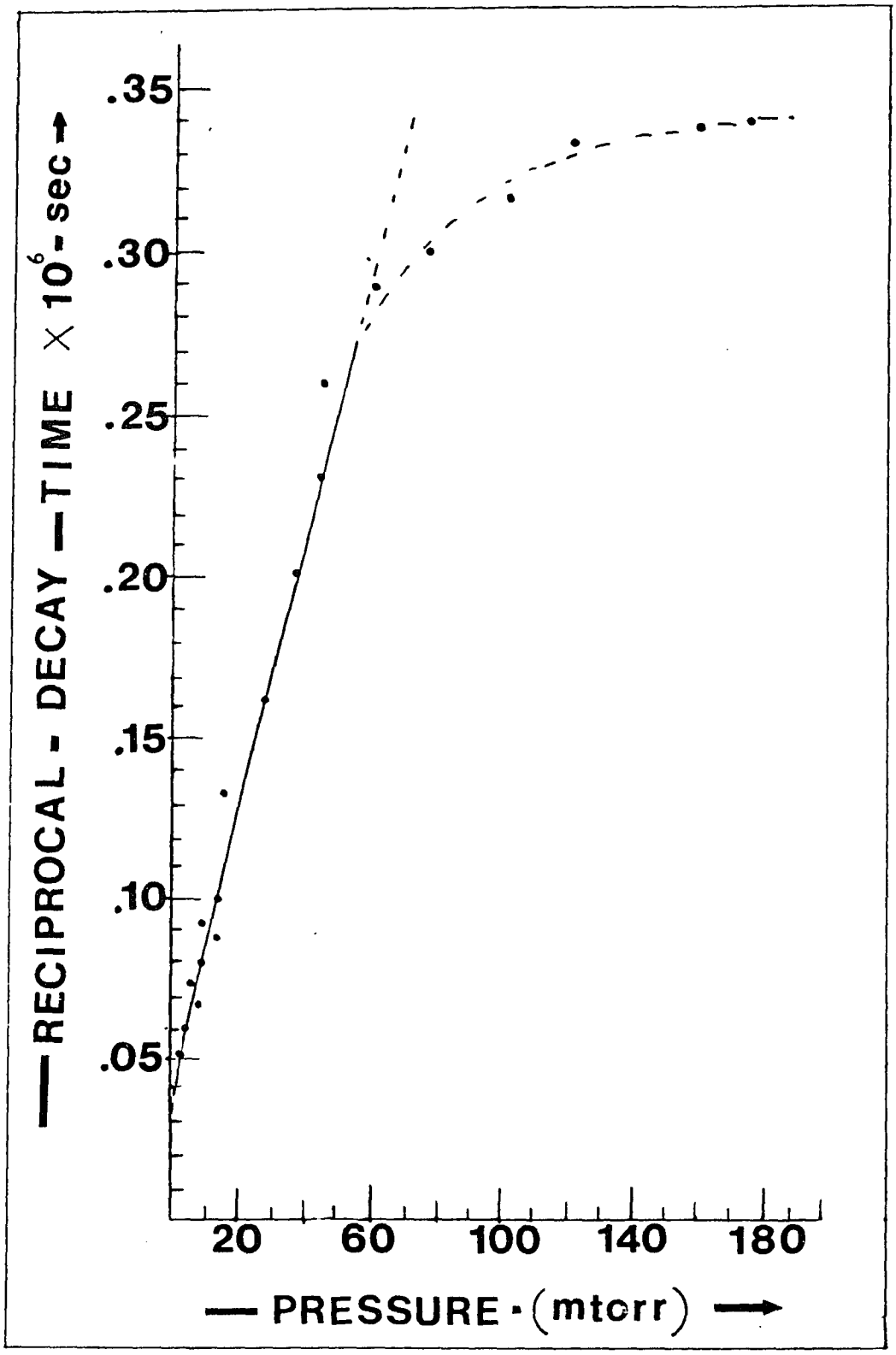

Figure (27) - A Stern-Volmer plot of the 460 nm emission.

decreases until a plateau is reached at ~ 100 mtorr. This saturation is due to collisional quenching of the electronically excited $VOCl_2$ molecules by cold $VOCl_3$ molecules.

The linear portion of the Sterm-Volmer plot obeys the relationship

$$\frac{1}{\tau} = \frac{1}{\tau_o} + \frac{P}{\tau_q} \qquad (2.14)$$

where τ is the lifetime, τ_o the collisionless (monomolecular) radiative lifetime, τ_q^{-1} the collisional quenching rate constant, and P the $VOCl_3$ pressure. From Fig. (28), an expanded version of Fig. (27), the slope yields a collisional quenching rate constant of 4.3×10^6 $sec^{-1}torr^{-1}$. The collision-free lifetime of the 460 nm signal, also obtained from Fig. (28) by extrapolating to zero pressure, was 2.9×10^1 μsec.

The experimental results presented in this subsection imply that, at pressures of 20 mtorr and .5 J, there is only one existing specie present with a spectrum similar to $VOCl_2$. This, together with the result that $VOCl_2$ is the photodissociative product at a pressure less than 1 torr and a laser energy of .2 J, strongly suggest that the luminescence is a result of only $VOCl_2$ at low pressures and laser energy. Its

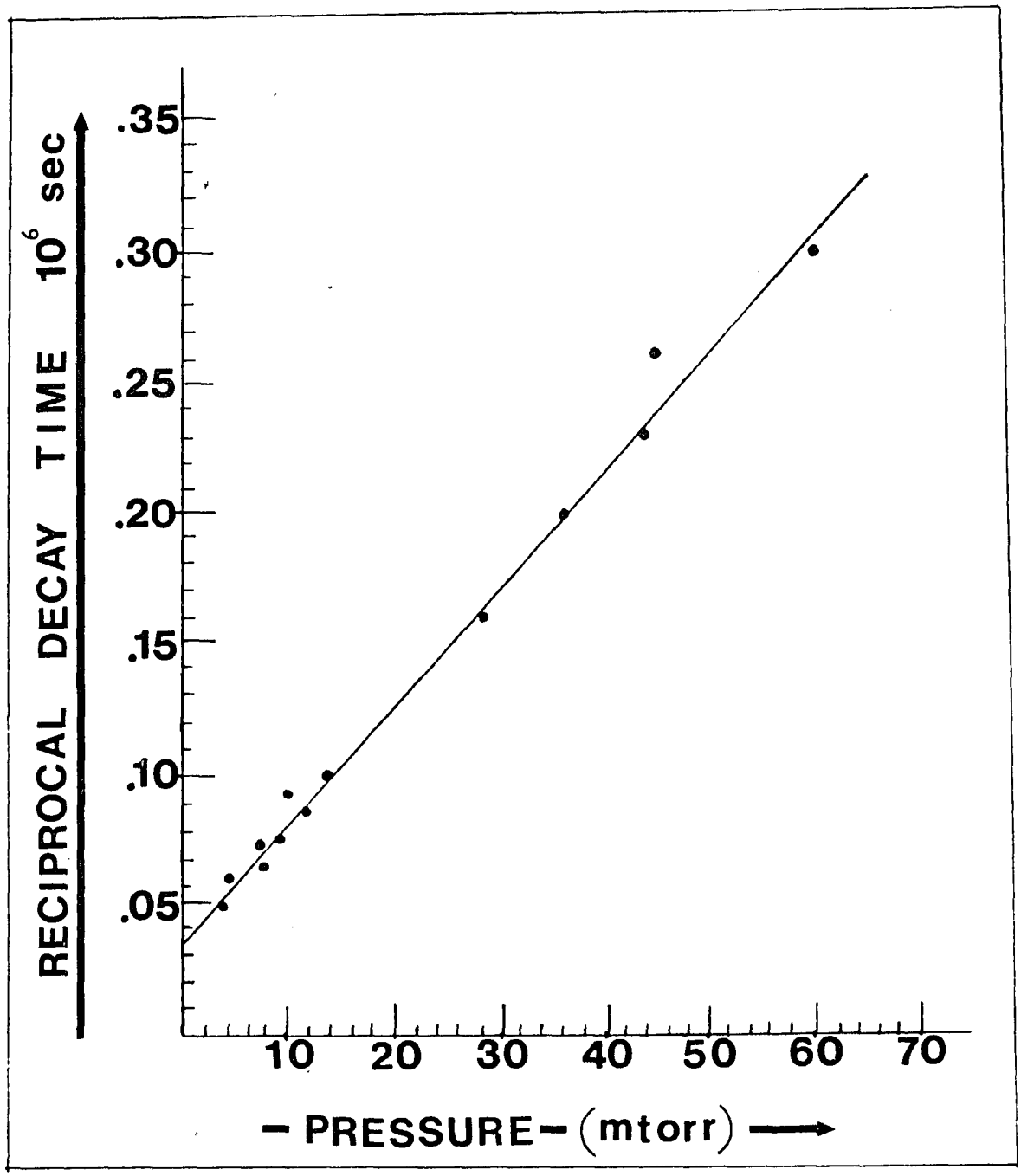

Figure (28) - A Stern-Vomer plot of the 460 nm emission (expanded scale).

radiative lifetime and quenching rate are 4.3×10^6 $sec^{-1}torr^{-1}$ and 2.9×10^1 μsec respectively.

In conclusion, then, $VOCl_2$ is the photodissociative and product of $VOCl_3$ at low pressures and laser energy. It is formed by the detachment of one chlorine atom via IR MPD and is responsible for the observed luminescence. At intermediate pressures and laser energy, there exists the possibility that, in addition to $VOCl_2$, VOCl contributes to the observed luminescence. If the VOCl specie does contribute to the luminescence, then the zero pressure change that resulted from the dissociation of $VOCl_3$ [Fig. (14)] can be attributed to the formation of $VOCl_2$ and not a cancelling-out effect between VO and $VOCl_2$ as previously mentioned. The contribution of $VOCl_2$ to the luminescence strongly suggests that VOCl, if formed, is not formed by the one-step elimination of Cl_2 from $VOCl_3$ but rather in a stepwise fragmentation via $VOCl_2$. The result that $VOCl_3$ dissociates to VO and Cl_2 at higher pressures and laser energy, and the result that the low pressure spectrum of $VOCl_2$ is similar to the high pressure spectrum recorded when $VOCl_3$ was dissociated, imply that VO cannot be formed in a one-step simultaneous detachment of the three chlorine atoms but, rather, a stepwise dissociation of $VOCl_3$ via $VOCl_2$ and possibly VOCl.

B. Dichlorosilane

1. IR and UV absorption spectra of SiH_2Cl_2.

SiH_2Cl_2 is a colorless gas which melts at -122°C and boils at 8.3°C. It autoignites in moist air and, when it is exposed to the atmosphere, a dense white cloud of vapor forms in accordance with the following equation

$$nSiH_2Cl_2 + nH_2O \rightarrow (-H_2Si\text{-}O\text{-})_n + 2nHCl \qquad (2.15)$$

The product $(H_2SiO)_n$ is known to be polymeric prosiloxine.

The molecular geometry of SiH_2Cl_2 is given in Table (III) while its fundamental modes of vibration, together with their assignment, are given in Table (IV). Inspection of Table (IV) reveals that the SiH_2 bending mode at 954 cm^{-1}, $\nu_2(a_1)$, falls within the region where the CO_2 laser emits (9-11 μ). The infrared spectrum of SiH_2Cl_2 taken at a pressure of 5 torr is shown in Fig. (29) and, upon expanding the scale, it is seen [Fig. (30)] that the $\nu_1(a_2)$ band is composed of two branches. The P branch is composed of rotational transitions of type $\Delta J = 1$ and is centered at 947 cm^{-1} while the R branch, composed of $\Delta J = +1$ rotational transitions, is centered at 960 cm^{-1}.

An inspection of Fig. (31), an infrared spectrum of SiH_2Cl_2 irradiated by various CO_2 laser lines,

Table III. (A) Published bond lengths and angles [36].
(B) Published rotational constants [37].

A. BOND LENGTHS & ANGLES	
r(Si-H) A° = 1.459	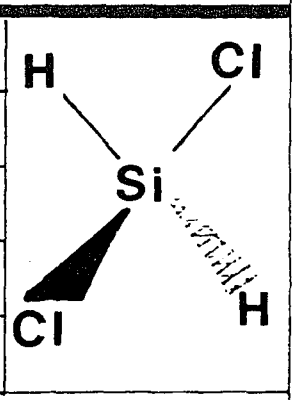
r(Si-Cl) A° = 2.034	
∠ H-Si-H = 110.05°	
∠Cl-Si-Cl = 109.76°	
∠ H-Si-Cl = 109.25°	
B. ROTATIONAL CONSTNTS	
$A(cm^{-1})$ = .471	
$B(cm^{-1})$ = .086	
$C(cm^{-1})$ = .074	

Table IV. Published vibrational frequencies of SiH_2Cl_2 [38].

MODE	DESCRIPTION	$\nu(cm^{-1})$
A_1 ν_1	SiH_2 sym stretch	2224
ν_2	SiH_2 bend	954
ν_3	$SiCl_2$ sym stretch	527
ν_4	$SiCl_2$ bend	188
A_2 ν_5	torsion	710
B_1 ν_6	SiH_2 asym stretch	2237
ν_7	rocking	602
B_2 ν_8	rocking	876
ν_9	$SiCl_2$ asym stretch	590

[a] The value represents the intensity minimum of the P & R branch.

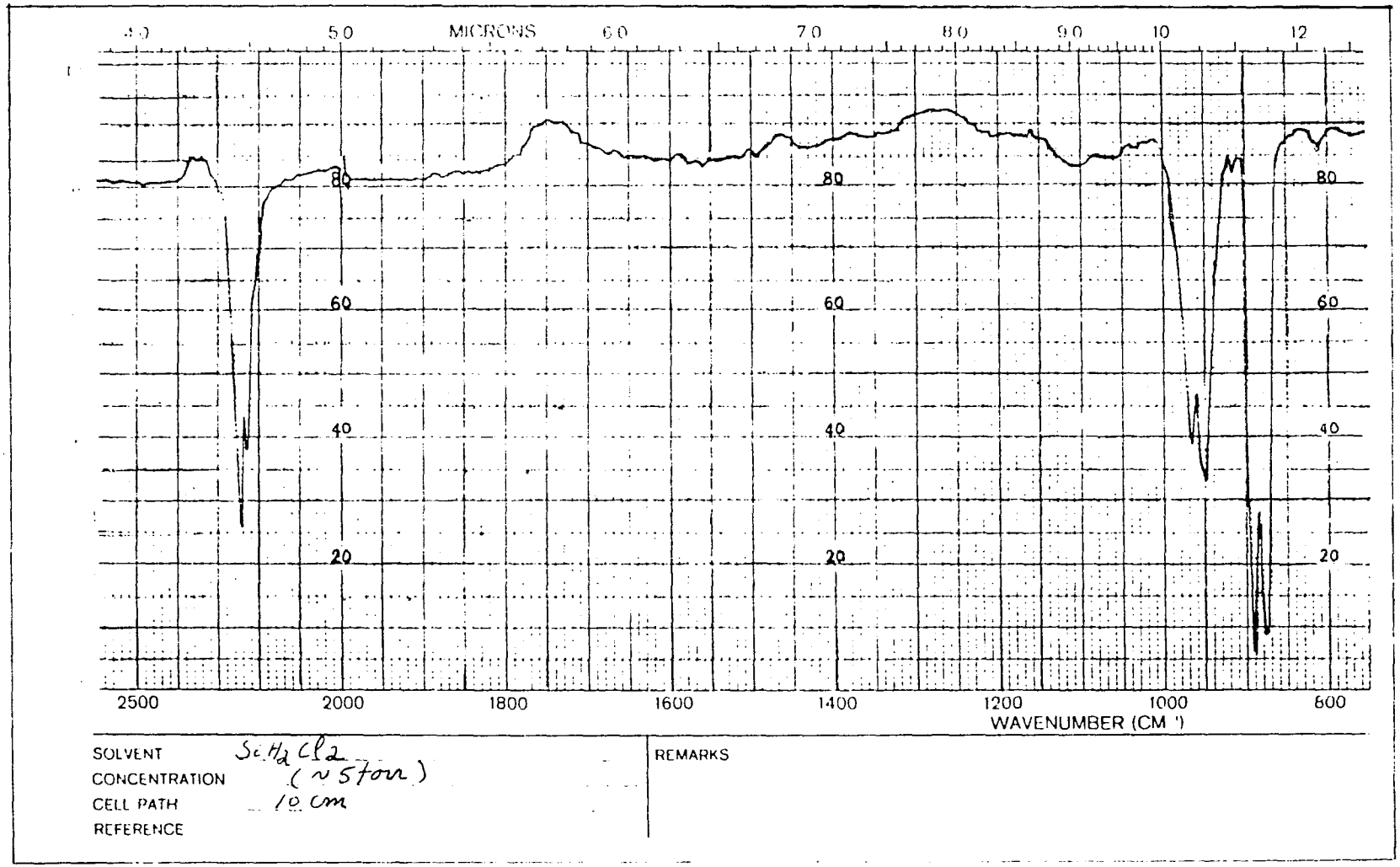

Figure (29) - The infrared spectrum of SiH_2Cl_2 (~ 5 torr).

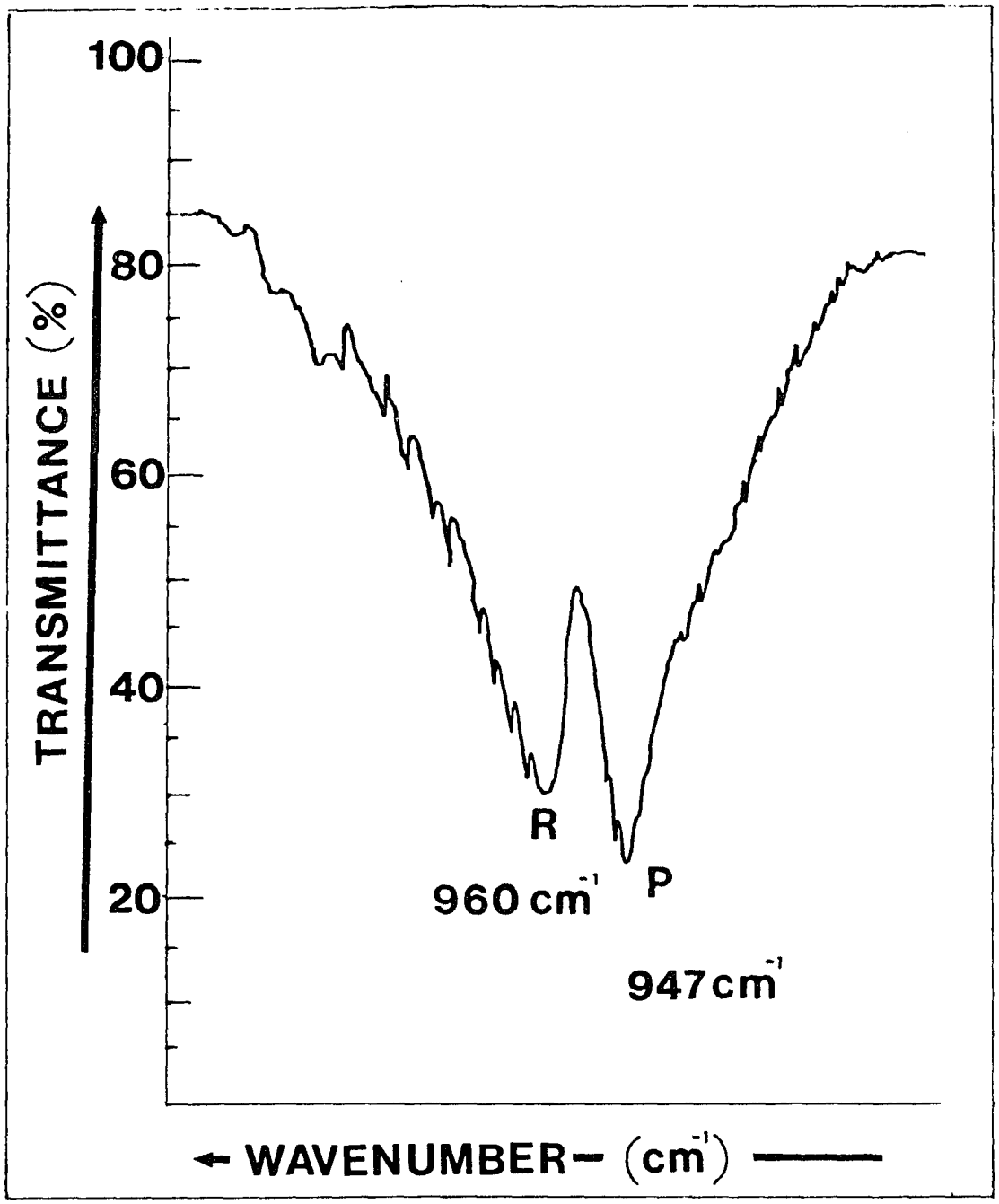

Figure (30) - A ten-fold expansion of the $\nu_2(a_1)$ vibrational mode revealing its P & R branches. The pressure of SiH_2Cl_2 was ~ 5 torr.

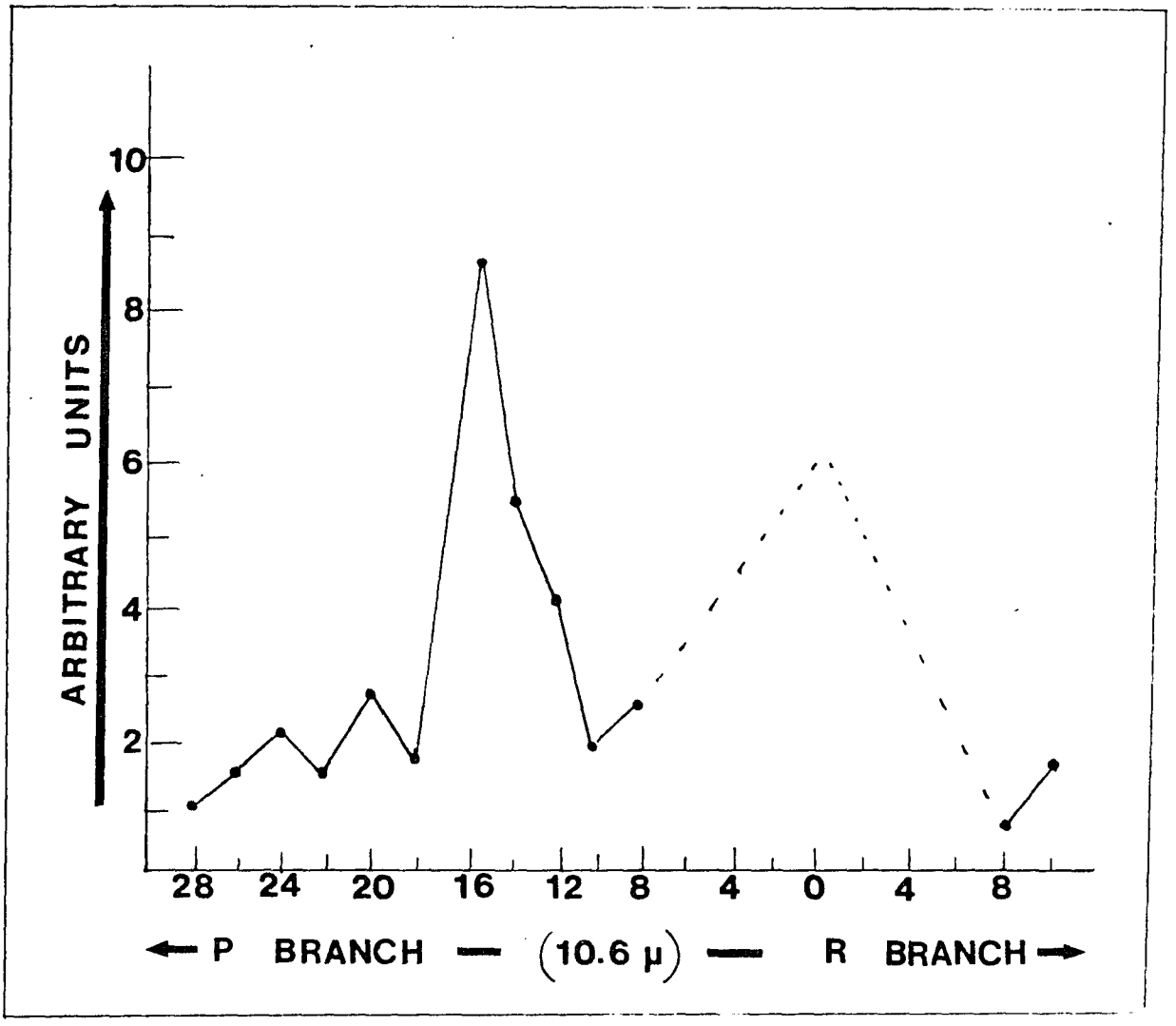

Figure (31) - The absorption spectrum of SiH_2Cl_2 when excited by both the P and R branches of the CO_2 laser's 10.6 μ transitions (unfocused geometry).

reveals that the strongest laser absorption line is the P(16) of the 10.6 μ, 947.74 cm^{-1}, corresponding to the P branch of the $\nu_2(a_1)$ band. Parts of the $\nu_2(a_1)$ R branch, along with its center, could not be mapped since they correspond to either weak or non-CO_2 laser transitions. When SiH_2Cl_2 was irradiated by the CO_2 laser's P branch transitions of the 9.6 μ band at pressures less than 1 torr, no signal could be detected.

Fig. (32) is a Beer-Lambert plot of SiH_2Cl_2 using the P(16) line. The plot is linear for pressures less than 20 torr and yields an absorption coefficient of 6.59×10^{-3} $torr^{-1}cm^{-1}$. At higher pressures, the absorbance varies exponentially with pressure with over 95% of the laser energy being absorbed at ~ 40 torr.

The UV-VIS absorption spectra of SiH_2Cl_2 taken by Causley et al. [39] revealed that, in the pressure range of 10^{-3} - 2 torr, there were no absorption bands below 400 nm except for those due to Rydberg transitions. The lowest energy absorption was at 151.0 nm and was assigned as a np(Si-Cl) → σ* transition.

In the next section, the dissociation and luminescence results obtained for SiH_2Cl_2 upon CO_2 laser excitation will be presented and discussed.

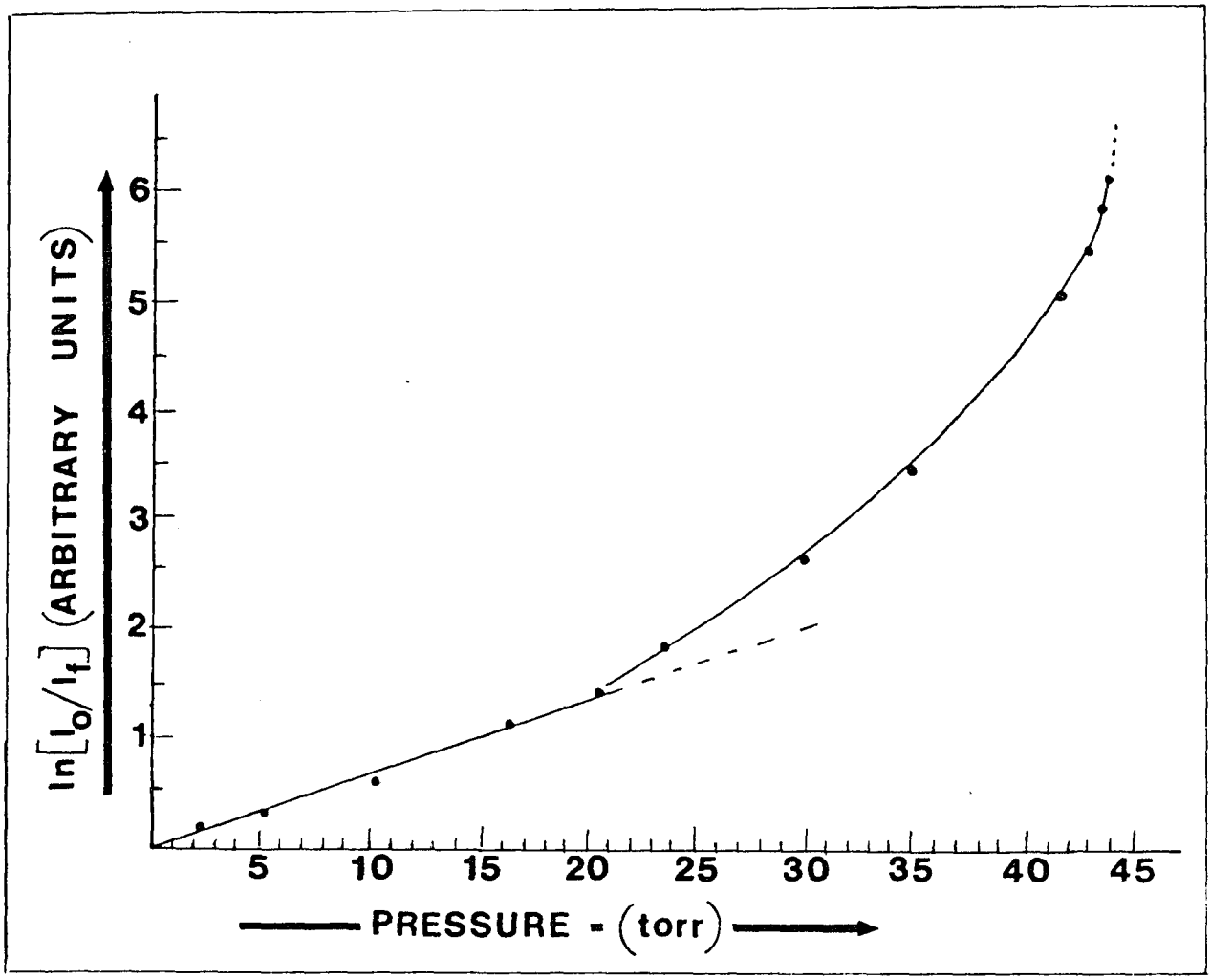

Figure (32) - A Beer-Lambert plot of SiH_2Cl_2. The laser was tuned to the P(16) of the 10.6 μ band and the cell was 10 cm long.

2. Multiple photon dissociation of SiH_2Cl_2.

Until now, no previous work on the multiphoton dissociation of SiH_2Cl_2 existed. Silane (SiH_4) and tetrachlorosilane ($SiCl_4$), on the other hand, have been investigated. Deutch et al. have reported on the collisional multiphoton dissociation of SiH_4 [40]. They claim that the dissociation, accompanied by a visible luminescence, results in the production of a thin particle film. They argue that the particles are not silicon but, rather, a solid SiH polymer because, upon irradiation of 1:1 mixtures of SiH_4:N_2O at total pressures of 1 - 15 torr, they do not observe visible emission from SiO. In contrast, such emission has been observed using the reaction of silicon atoms produced by a glow discharge in silane with N_2O. The luminescence is attributed to atomic and molecular hydrogen as well as SiH. $SiCl_4$ has only a weak absorption band, assigned to the $\nu_1 + \nu_3$ combination band, in the CO_2 lasing region and thus multiphoton dissociation experiments with moderate energy levels (~ 2 J) have proved to be fruitless. However, $SiCl_4$ has been dissociated by dielectric breakdown to yield a silicon-containing film and Cl_2 [41] (Chapter 3).

As was pointed out earlier, the products formed in infrared multiphoton dissociation are determined by those formed from the lowest energy pathway

available to the molecule as predicted by the RRKM theory of unimolecular reactions. Therefore, it is important that one carefully study the thermodynamic data of the prominent pathways for the decomposition of dichlorosilane when attempting to ascertain the products of dissociation.

The important reactions of dichlorosilane under laser excitation, along with the energy needed to drive them [42], are summarized as follows:

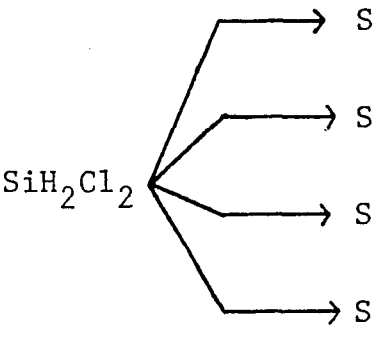

$$SiH_2Cl_2 \rightarrow SiH_2 + Cl_2 \quad \sim 112 \text{ kcal/mole} \quad (2.16)$$

$$SiH_2Cl_2 \rightarrow SiCl_2 + H_2 \quad \sim 49 \text{ kcal/mole} \quad (2.17)$$

$$SiH_2Cl_2 \rightarrow Si + 2HCl \quad \sim 14 \text{ kcal/mole} \quad (2.18)$$

$$SiH_2Cl_2 \rightarrow Si + H_2 + Cl_2 \quad \sim 58 \text{ kcal/mole} \quad (2.19)$$

From the above equations, one would expect SiH_2Cl_2 to dissociate to Si + 2HCl since it requires the least energy, ~ 14 kcal/mole. However, equation (2.18) presumes the formation of HCl and Si. A better understanding of the thermodynamics involved can be obtained from the following equations:

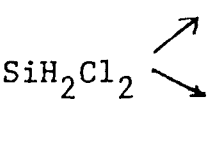

$$SiH_2Cl_2 \rightarrow SiH_2Cl + Cl \quad D(SiH_2Cl\text{-}Cl) = 110.7 \text{ kcal/mole} \quad (2.20)$$

$$SiH_2Cl_2 \rightarrow SiCl_2H + H \quad D(SiCl_2H\text{-}H) = 92.1 \text{ kcal/mole} \quad (2.21)$$

The above equations represent the initial bond breakage that SiH_2Cl_2 must undergo if any of the products in equation (2.16 - 2.19) are to be formed. It can be seen that equation (2.21) is the lower energy channel and, thus, must be thermodynamically preferred. $SiHCl_2$ may further dissociate to $SiCl_2$ or SiHCl. This is shown by the following equations.

$$SiCl_2H \nearrow SiCl_2 + H \qquad D(SiCl_2\text{-}H) = 51.7 \text{ kcal/mole} \quad (2.22)$$

$$SiCl_2H \searrow SiClH + Cl \qquad D(SiHCl\text{-}Cl) = 78.0 \text{ kcal/mole} \quad (2.23)$$

where equation (2.22) yields the lowest energy route. Hence, the reaction in which $SiCl_2$ is formed represents the thermodynamic preferred channel of dissociation. The above discussion assumes a stepwise fragmentation pattern. However, even a one-step molecular elimination favors the formation of $SiCl_2 + H_2$. This is evident from the following equations:

$$SiH_2Cl_2 \longrightarrow SiH_2 + Cl_2 \qquad \sim 124 \text{ kcal/mole} \quad (2.24)$$

$$SiH_2Cl_2 \longrightarrow SiCl_2 + H_2 \qquad \sim 39 \text{ kcal/mole} \quad (2.25)$$

$$SiH_2Cl_2 \longrightarrow SiHCl + HCl \qquad \sim 67 \text{ kcal/mole} \quad (2.26)$$

These simple calculations reveal that a stepwise fragmentation or a one-step molecular elimination of SiH_2Cl_2 thermodynamically favor the production of $SiCl_2$ and H_2. If, however, two HCl molecules could be eliminated in one step, then Si and HCl would be the preferred products. This, from previous experience, seems unlikely.

The photodissociation of SiH_2Cl_2, using either a pulsed CO_2 or KrF laser as a photolysis source, was investigated and is now presented.

When SiH_2Cl_2 was irradiated with unfocused CO_2 laser radiation, tuned to the $\nu_2(a_1)$ band, no measurable dissociation was detected. A similar conclusion was reached when SiH_2Cl_2 was irradiated with focused off-resonant CO_2 laser radiation.

Fig. (33) shows the decrease in the $\nu_2(a_1)$ absorption band as a function of number of laser pulses when ~ 1 torr of SiH_2Cl_2 was irradiated with a focused CO_2 laser radiation tuned to the P(16) of 10.6 μ band. The decrease in the absorption band and the presence of particulates, detected after 1 laser pulse with a He-Ne laser, strongly imply that SiH_2Cl_2 was photodissociated upon CO_2 laser excitation. The photodissociative products were found to be $SiCl_2$ and H_2 as predicted from thermodynamic data. Hydrogen was identified by mass spectrometry and $SiCl_2$ from its emission spectrum. $SiCl_2$ has a ground state

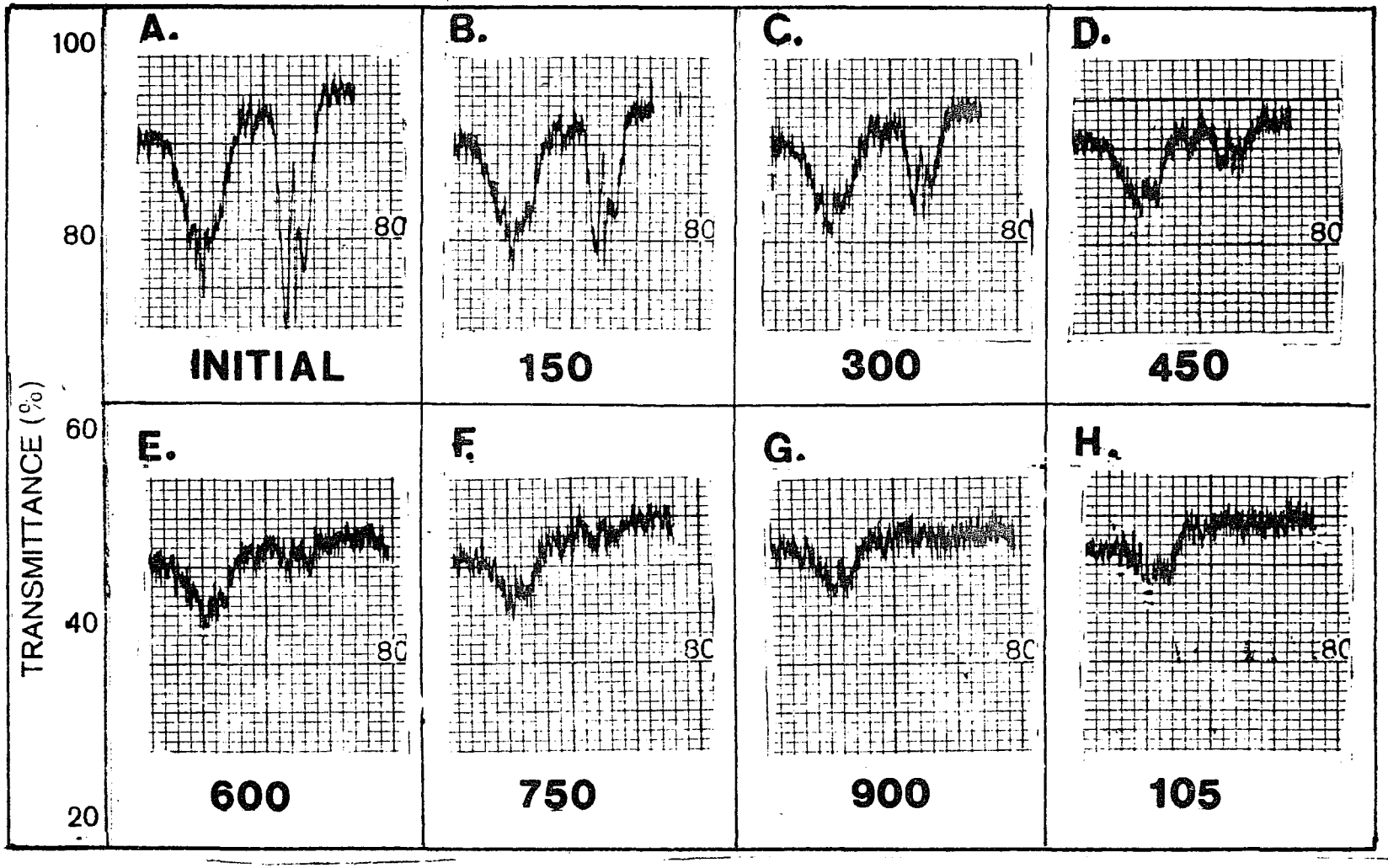

Figure (33) - The infrared spectrum of SiH_2Cl_2 (1 torr) as a function of laser pulses. The dissociation of SiH_2Cl_2 with pulses of .25 J (~ 5 J/cm^2) was monitored using the $\nu_2(a_1)$ and $\nu_8(b_2)$ vibrational transitions.

lifetime of 1 msec at 1 μ [43] and may polymerize to $(SiCl_2)_n$. In all the MPD experiments performed, the pressure was always less than 1 torr and the laser energy less than 1.5 J. Under conditions of higher pressures and/or laser energy dielectric breakdown was easily achieved and thus avoided.

Fig. (34) shows the absorption spectra of SiH_2Cl_2 before and after excitation with a KrF laser tuned to 247 nm. As is evident from the major SiH_2Cl_2 peaks, no measurable dissociation occured. This was anticipated since the above energy neither corresponds to an absorption band of SiH_2Cl_2 nor is it sufficient to drive it beyond the continuum of its electronic states. However, vacuum ultraviolet studies by D. E. Milligan and M. E. Jacox [44] showed that SiH_2Cl_2, suspended in an argon matrix at 14 K, does photodissociate and H_2 together with $SiCl_2$ are its photodissociative products. Whether $SiCl_2$ was formed by photodetachment of H_2 from SiH_2Cl_2 or by two successive photodetachment of H atoms was not determined.

3. Origin of luminescence.

When SiH_2Cl_2 was irradiated with focused CO_2 laser radiation tuned to an off-resonance line, i.e., P(20) of 9.6 μ bond, no emission was observed. However, emission was observed when the CO_2 laser was tuned to resonant lines. Fig. (35) is an oscillogram taken when SiH_2Cl_2 was irradiated with a CO_2 laser

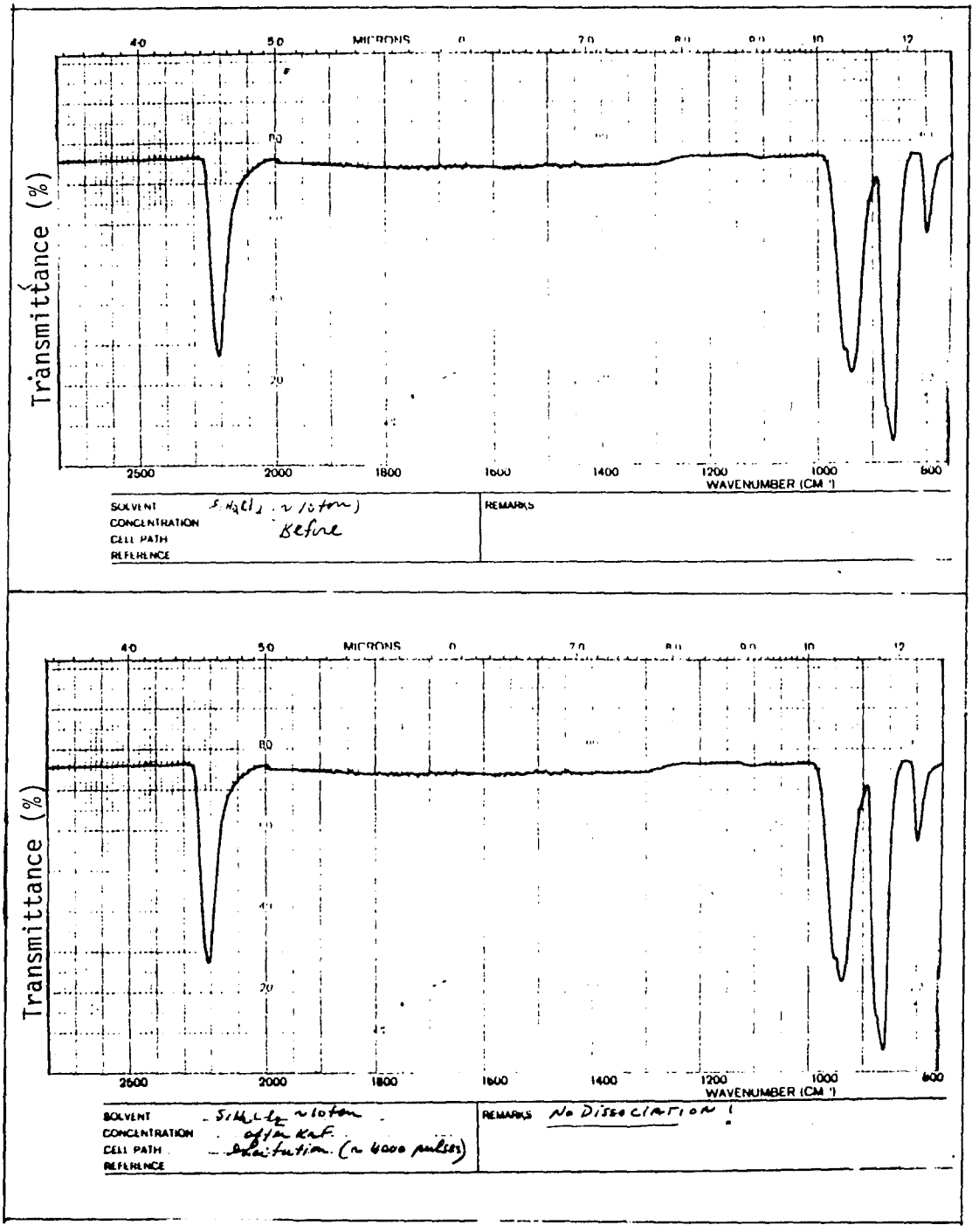

Figure (34) The infrared spectrum of SiH_2Cl_2 (~ 10 torr) before and after it was excited with ~ 4,000 KrF laser pulses. Each pulse has a wavelength of 248 mm and 100 mJ of energy.

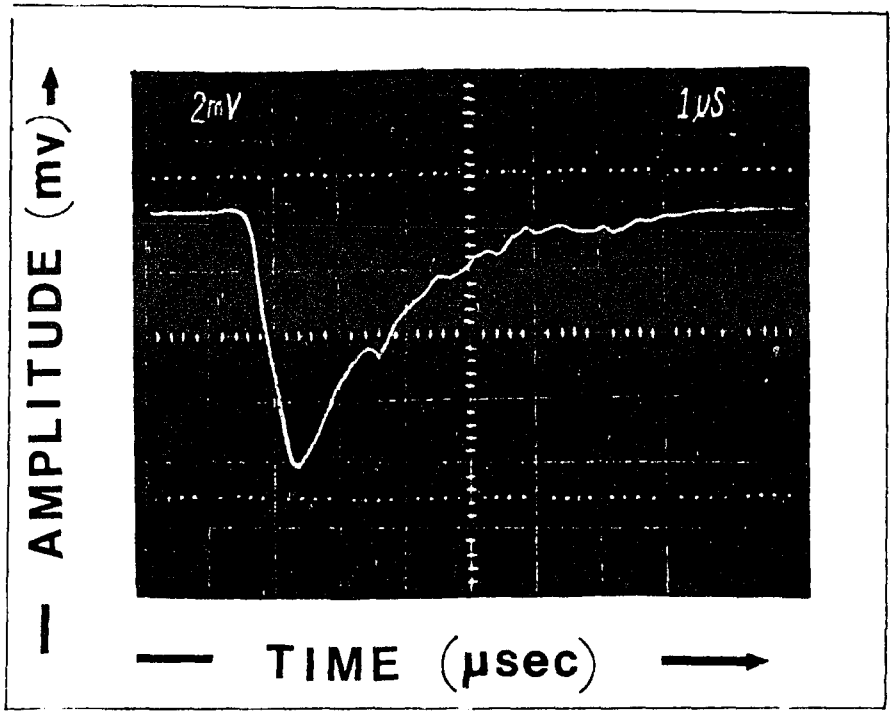

Figure (35) - An oscillogram of the emission following CO_2 laser excitation of SiH_2Cl_2 at a pressure of 60 mtorr, fluence of .6 J and a wavelength of 330 nm.

tuned to P(16) of 10.6 μ at a pressure of 60 mtorr, laser energy of .6 J, and a wavelength of 360 nm.

Presented in Fig. (36) is a spectrum of the emission. This spectrum is assigned to the $SiCl_2$ specie, since it is identical to previously published spectra [45-47]. A plot of the emission amplitude as a function of laser energy at 20 mtorr is shown in Fig. (37). It can be seen that the emission amplitude, in the energy range up to 1.5 J, is linearly dependent on the laser energy and has a threshold of .3 J.

The initial risetime of the luminescence signal, as in the case of $VOCl_3$, is independent of both pressure (< 1 torr) and laser energy (< 1.5 J). The decay time of the luminescence is independent of laser energy (< 1.5 J) and wavelength (38), but is dependent on pressure (39).

Fig. (38) shows a plot of decay times as a function of wavelength at a pressure of 20 mtorr. The decay times, which have a value of 4.0 μsec, are not dependent on wavelength. This suggests that no other specie contributes to the luminescence assigned to $SiCl_2$.

From the Stern-Volmer plot, presented in Figures (39) and (40), a radiative lifetime of 4.6 μsec and quenching rate of 2.6×10^6 $sec^{-1}torr^{-1}$ is extracted.

In short, then, irradiation of SiH_2Cl_2 with a pulsed CO_2 laser tuned to P(16) of the 10.6 μ band yielded

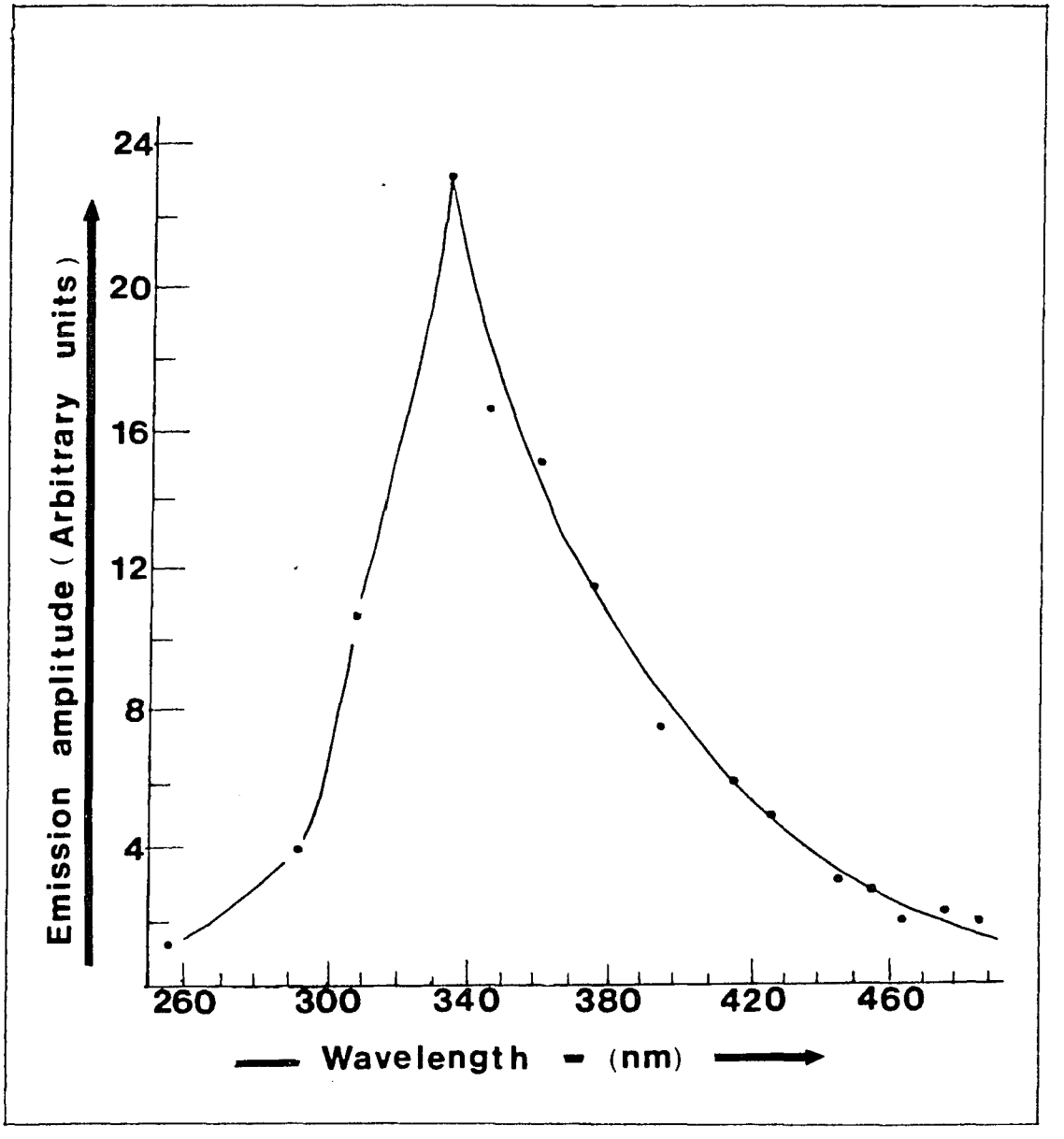

Figure (36) - The emission spectrum following the irradiation of SiH_2Cl_2 by a CO_2 laser tuned to P(16) of the 9.6 μ band. The spectrum was recorded under flow conditions with a cell pressure of 20 mtorr.

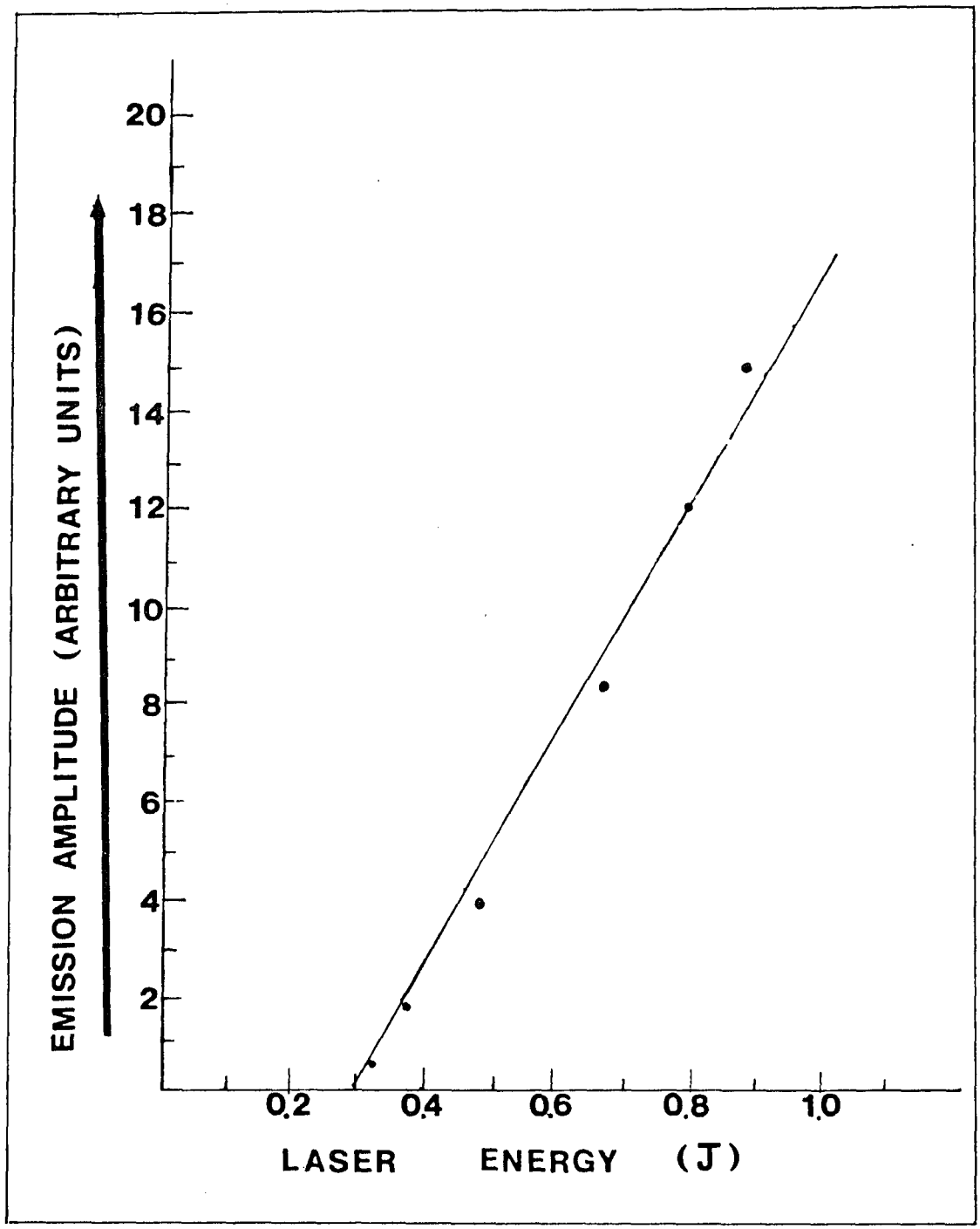

Figure (37) - A plot of emission amplitude as a function of laser energy for SiH_2Cl_2 at a pressure of 20 mtorr and a wavelength of 330 nm.

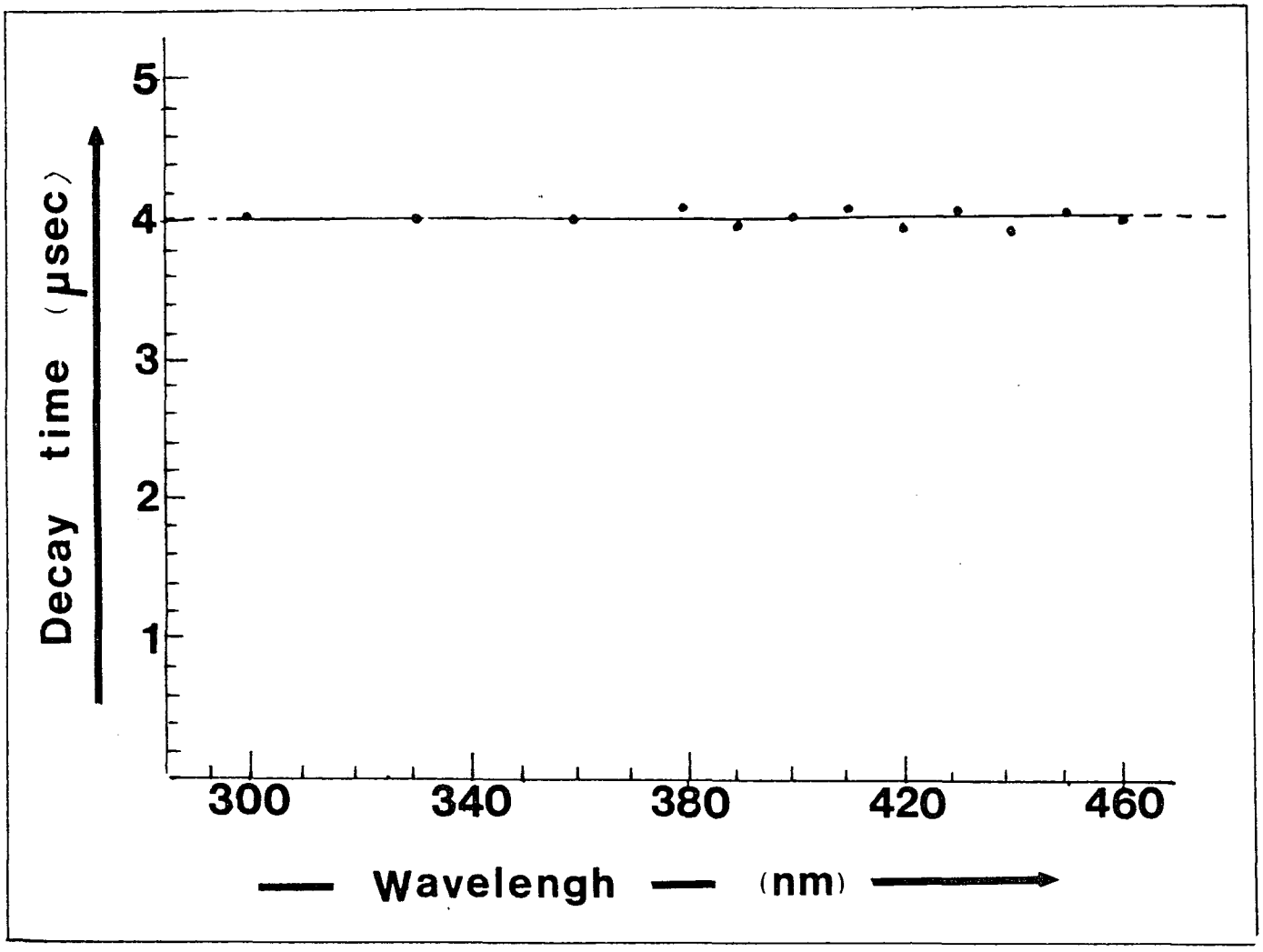

Figure (38) - A plot of emission lifetimes as a function of wavelength at a pressure of 20 mtorr and a laser energy of .5 J.

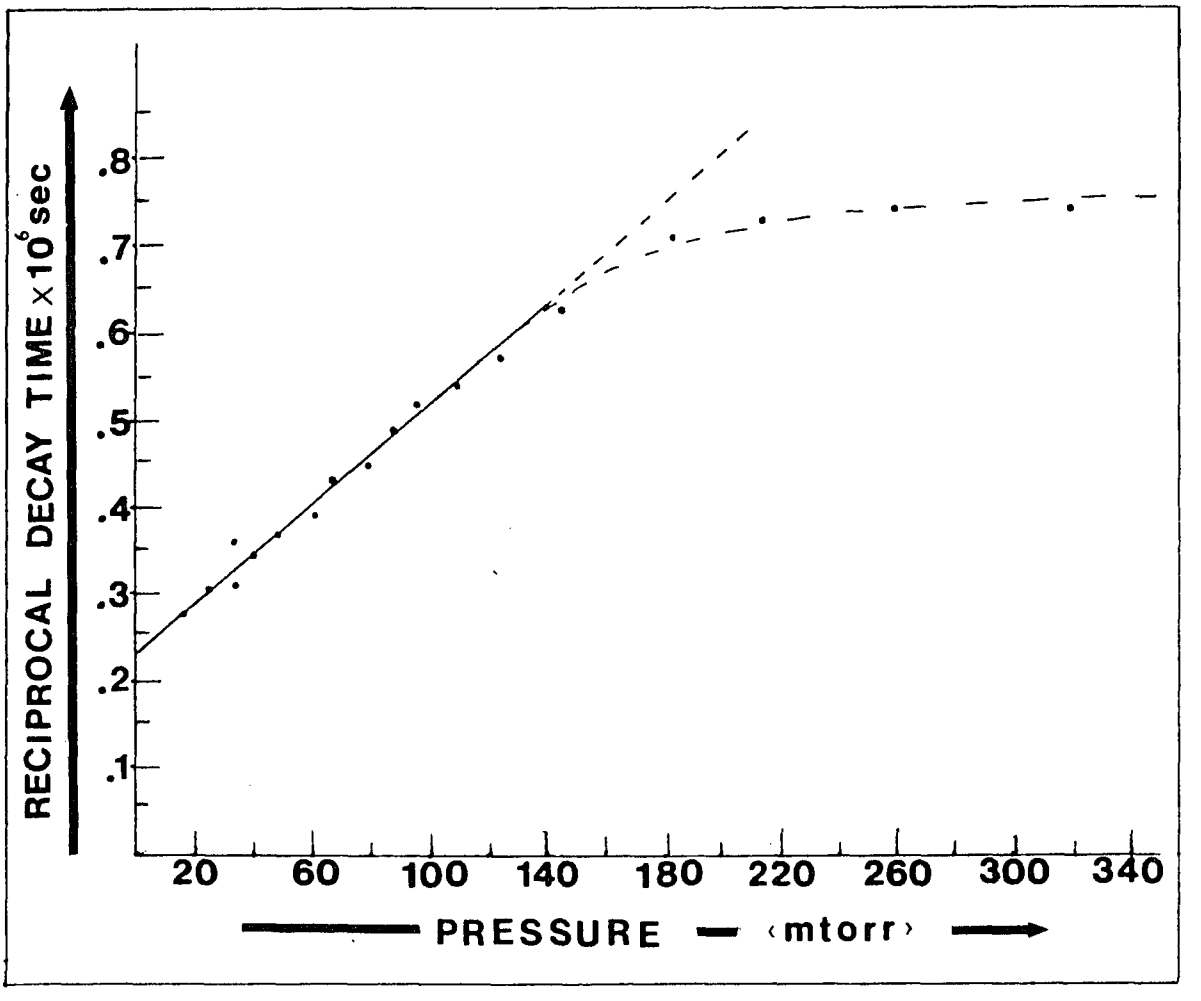

Figure (39) - A Stern-Volmer plot of the 330 nm emission.

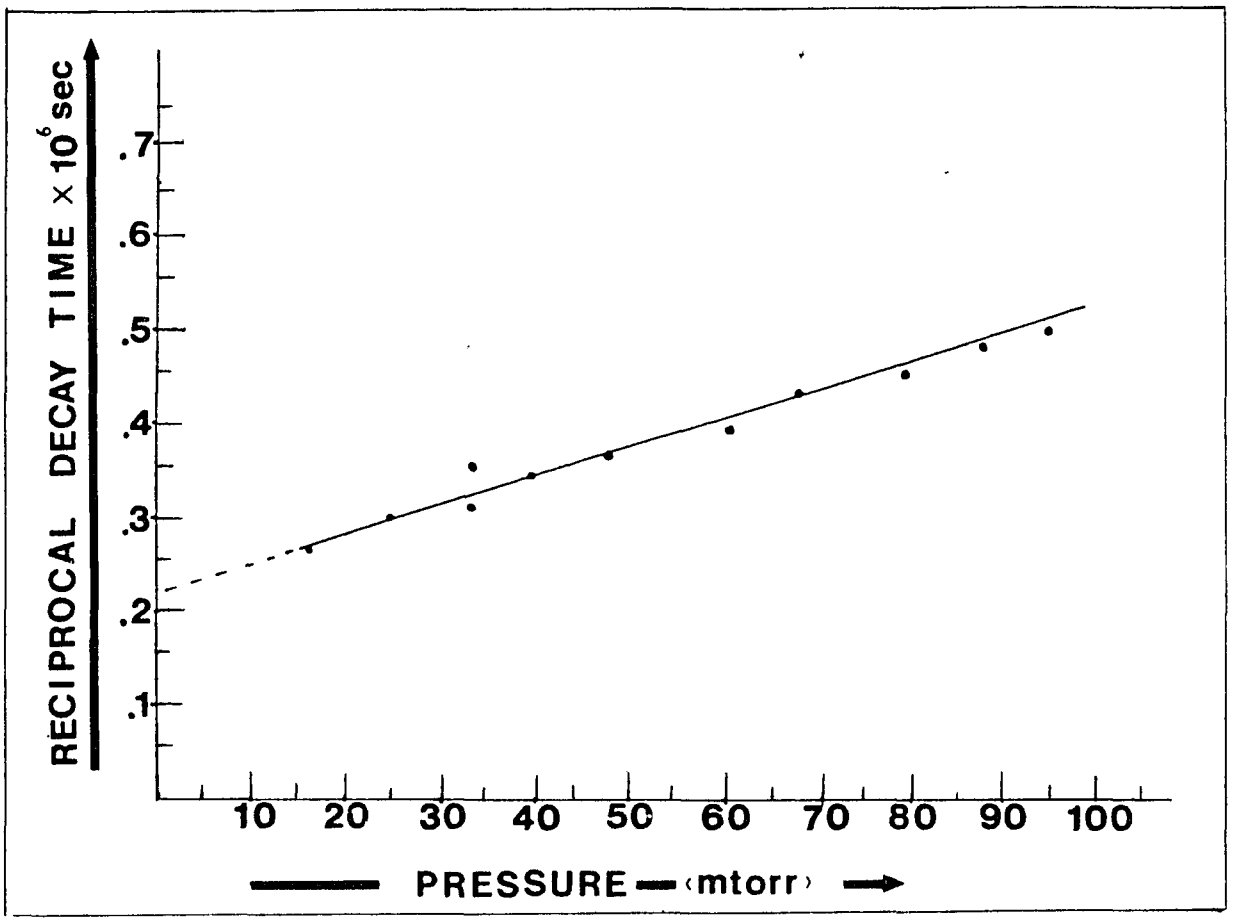

Figure (40) - A Stern-Volmer plot of the 330 nm emiision (expanded scale).

$SiCl_2$ and H_2. $SiCl_2$ is a short-lived specie and may polymerize to $(SiCl_2)_n$. The radiative lifetime and quenching rate of $SiCl_2$ were found to be 4.6 μsec and 2.6×10^6 $sec^{-1}torr^{-1}$ respectively. It was not determined whether $SiCl_2$ was formed by photodetachment of H_2 from SiH_2Cl_2 or by two successive photodetachment of H atoms.

2.5 CONCLUDING REMARKS

The multiphoton dissociation of $VOCl_3$ and SiH_2Cl_2 can be explained, as was SF_6, by the absorption of photons into a region where the molecular states are discrete, a second region where they form a quasi-continuum, and a third where they form a continuum.

The vibrational anharmonicity in the quantum gaps presents an obstacle that $VOCl_3$ and SiH_2Cl_2 must overcome for successful excitation. This vibrational anharmonicity is mostly compensated, as shown in Table (V), by the A.C. Stark shift in the discrete energy region and by the high density of states in the quasicontinuum.

It is the density of states that defines the quasicontinuum, determines whether additional photons will be absorbed by SiH_2Cl_2 and $VOCl_3$, and dominates the theory of intramode energy flow. The density of states of $VOCl_3$ and SiH_2Cl_2, at various vibrational energy, was computed by using the Rice-Marcus approximation method [52], and is presented in Fig. (41). It is evident from

Table V. D. C. Stark Shift, A. C. Stark Shift, and Anharmonic Constants.

MOLECULE	MODE ν_i (cm^{-1})	DIPOLE MOMENT OF ν_i MODE (μ_{10})	ROTATIONAL CONSTANT	ANHARMONICITY CONSTANT	A.C. STARK SHIFT [g] Field ~ 10^6 v/cm	D.C. STARK SHIFT [h] Field ~ 10^6 v/cm	D.C. STARK SHIFT Field ~ 10^5 v/cm
SF_6	ν (965)	~.30 D [a]	.030 cm^{-1}	5.6 cm^{-1} [d]	ΔR = ~ 5 cm^{-1}	$\overline{\Delta\nu}$ ~ 8×10^{-5} cm^{-1}	$\overline{\Delta\nu}$ = ~.08 cm^{-1}
$VOCl_3$	ν(1040)	~.36 D [b]	.058 cm^{-1}	2.0 cm^{-1} [e]	ΔR = ~ 6 cm^{-1}	$\overline{\Delta\nu}$ ~ 2×10^{-4} cm^{-1}	$\overline{\Delta\nu}$ = ~.2 cm^{-1}
SiH_2Cl_2	ν (947)	~.60 D [c]	.467 cm^{-1}	8.5 cm^{-1} [f]	ΔR = ~ 10 cm^{-1}	$\overline{\Delta\nu}$ ~ 2×10^{-3} cm^{-1}	$\overline{\Delta\nu}$ = ~ 2 cm^{-1}

[a] As obtained from reference [15].

[b] The value was obtained by using the following expression:

$$|\langle\mu_{10}\rangle|^2 = \frac{3hc\,(1000)}{8\pi^3 N\nu_{10}} \cdot \int\gamma(\alpha)d\nu \text{ [48]}.$$

The term $\int\gamma(\alpha)d\nu$ is equal to $1/Cl\int \ln(I_o/I)\cdot d\nu$ where $\int \ln(I_o/I)\cdot d\nu$ represents the area of the mode's infrared spectrum (cm^{-1}), C the concentration (mole/ℓ), and ℓ the cell's path length (cm). The symbols h, c, N, and ν_{10} represent Planck's constant (6.63×10^{-27} erg·sec), the speed of light (3.0×10^{10} cm/sec), Avagadro's number (6.02×10^{23} molecules/mole), and the mode's vibration (cm^{-1}). (1000 is used to convert from liters to cm^3) The matrix dipole moment will have units of Debye (D) if the equalities 1 erg = $g\cdot cm^2/sec^2$, 1 esu = $(g^{\frac{1}{2}}cm^{3/2})/sec$. and 1 D = 10^{-18} esu·cm are used. For $VOCl_3$, the area of the spectrum's fundamental mode (1042 cm^{-1}) obtained by weighing a 5X expanded spectrum and converting it to cm^{-1}, was 1075 cm^{-1}. The experiment was conducted at room temperature in a 10-cm cell at a pressure of 6.38 torr (C = mole/ℓ = P/RT).

[c] See footnote (b)

$\int \ln(I_o/I)\cdot d\nu$ = 2338 cm^{-1}, ν_{10} = 947 cm^{-1}, P = 5.51 torr, and ℓ = 10 cm.

[d] As obtained from reference [49].

[e] The value was calculated by using the experimental values of the ν_1, ν_2, and $\nu_1 + \nu_2$ frequencies [50] and assuming that both the ν_1 and ν_2 modes contribute equally to the anharmonicity.

[f] See footnote (e)

The ν_1, ν_5, and $\nu_1 + \nu_5$ vibrations were used [51].

[g] These values were obtained by using equation (2.2) and the following equalities: 10^7 erg = 1 V·Coul, 1 Coul = 3×10^9 esu, and 1 D = 10^{-18} esu·cm, and $\nu = c/\lambda$.

[h] Values obtained by using eq. (2.1).

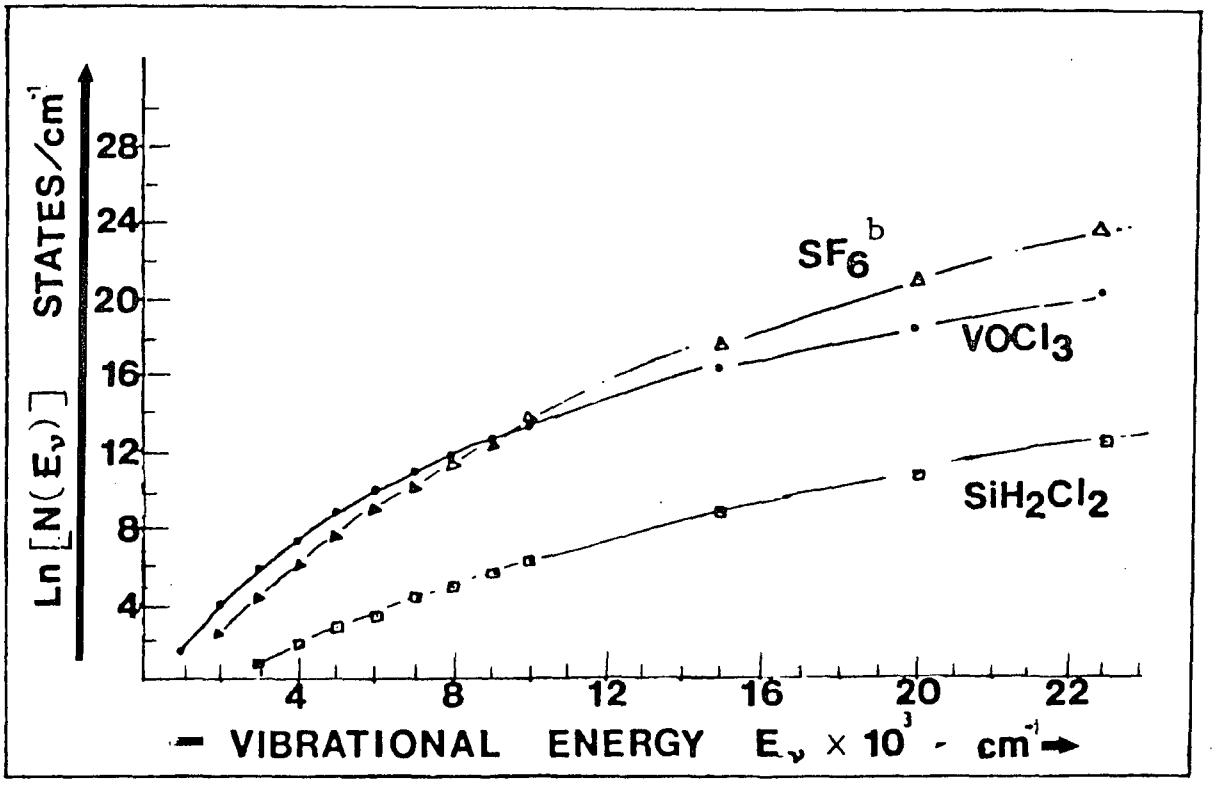

Figure (41) - A plot of the density of states as a function of vibrational energy.[a]

[a] The values where obtained by the Rice-Marcus approximation method. This method gives $N(E_v) = (E_v + E_z)^{s-1}/(s-1)!\prod_{i=1}^{s} h\nu_i$ for the density of vibrational states, $N(E_v)$, at vibrational energy E_v above the ground vibrational energy state. The quantity, E_z, is the zero point vibrational energy and is equal to $\sum_{i=1}^{s} (\frac{1}{2}h\nu_i)$. s is the number of vibrational degrees of freedom, and ν_i is the set of fundamental vibrational frequencies.

[b] The fundamental frequencies of SF_6 were obtained from reference [53] and are listed for comparative purposes. $\nu_1(a_{1g}) = 775\ cm^{-1}$, $\nu_2(e_g) = 644\ cm^{-1}$, $\nu_3(f_{1u}) = 965\ cm^{-1}$, $\nu_4(f_{1u}) = 617\ cm^{-1}$, $\nu_5(f_{2g}) = 524\ cm^{-1}$, $\nu_6(f_{2u}) = 363\ cm^{-1}$.

Fig. (41) that the density of vibrational states increases exponentially with increasing energy. In addition, Fig. (41) reveals that SF_6, which has the most vibrational modes, has the largest density of states at high vibrational energy. At low vibrational energy, the number of low energy fundamentals contribute more to the density of states and, thus, SiH_2Cl_2 which has the greatest number of low energy fundamentals has the lowest density of states.

The onset of the quasicontinuum is different for different molecules and largely depends on the pressure and laser energy conditions. For SF_6, it is widely accepted that the quasicontinuum begins between 4,000-6,000 cm^{-1}. This energy range corresponds to a density of 10^2 - 10^4 states/cm^{-1}. Using this density range, Fig. (41) reveals that the quasicontinuum of $VOCl_3$ and SiH_2Cl_2 begins between 3,000 - 5,000 cm^{-1} and 7,000 - 10,000 cm^{-1}, respectively. This, of course, assumes that the pressure and laser energy conditions are the same for all three molecules.

Once $VOCl_3$ and SiH_2Cl_2 absorb sufficient photons to reach the quasicontinuum, the absorbed energy distributes among other vibrational modes. This intrastate vibrational energy redistribution can be specified by an effective vibrational temperature, T*. T* is then increased by a sequence of one photon absorption processes

until the photodissociation threshold is reached.

In the case of SF_6, one cannot be certain that the bond which ruptured was precisely the one which was excited. In SiH_2Cl_2, the bond which was excited was indeed the bond which ruptured. However, this does not constitute a case of bond selective chemistry since the laws of statistical thermodynamics are not violated. In $VOCl_3$, the bond which was excited (V = O stretch) was the strongest, but the bond which ruptured was again the weakest. These results, as pointed out earlier, are in accordance with the RRKM theory of unimolecular dissociation.

The multiple photon process raises another important question pertaining to laser infrared chemistry. That is, can any molecule with a resonant absorption band dissociate by CO_2 laser excitation? A polyatomic molecule can be dissociated because of the relatively small vibrational anharmonicity in the lower transitions and large density of states in the quasicontinuum. However, small molecules, such as diatomics, have not been found to dissociate by multiphoton excitation. Because these molecules have much greater anharmonicity in the low-lying levels and possess a small number of vibrational degrees of freedom, no quasicontinuum can be reached.

As was mentioned earlier, it is presently not known

whether $SiCl_2$ is formed by the photodetachment of H_2 from SiH_2Cl_2 or by two photodetachments of H atoms. A simultaneous detachment may be explained, as was SF_6 or $VOCl_3$, by Fig. (42a). A sequential detachment, on the other hand, may be explained by one of the following mechanisms.

In the first mechanism, SiH_2Cl_2 absorbs enough photons to reach its dissociation limit where a competition between the up-pumping and dissociation rates occur In this region, absorption of a few more laser photons can continue until levels with very large dissociative widths are reached. The dissociation lifetimes of these levels increases exponentially with excess energy, as predicted by RRKM theory, and dissociation becomes the preferred channel. Indeed, polyatomics similar to SiH_2Cl_2 in size have been found to dissociate with an average excess energy of 4 - 6 laser photons and dissociative lifetimes in the range of 10^{-12}-10^{-9} sec [54]. The vibrationally hot fragment, in this case $SiHCl_2$ since atomic hydrogen can only accept excess energy to its translational degrees of freedom, can then be further excited by the remaining portion of the laser pulse until it dissociates to $SiCl_2$ [Fig. (42b)]. It must be noted that absorption of additional photons by the vibrationally excited fragment can occur if the dissociation of the parent SiH_2Cl_2 molecule leaves the $SiHCl_2$ radical in its quasicontinuum, where frequency

Figure (42) - Multiphoton dissociation of SiH_2Cl_2. (A) A one-step elimination of a hydrogen molecule. (B) A two-step detachment of H atoms by a $SiHCl_2$ intermediate. (C) A hybrid of A and B. Predissociation of SiH_2Cl_2 to $SiHCl_2$ with subsequent dissociation to $SiCl_2$.

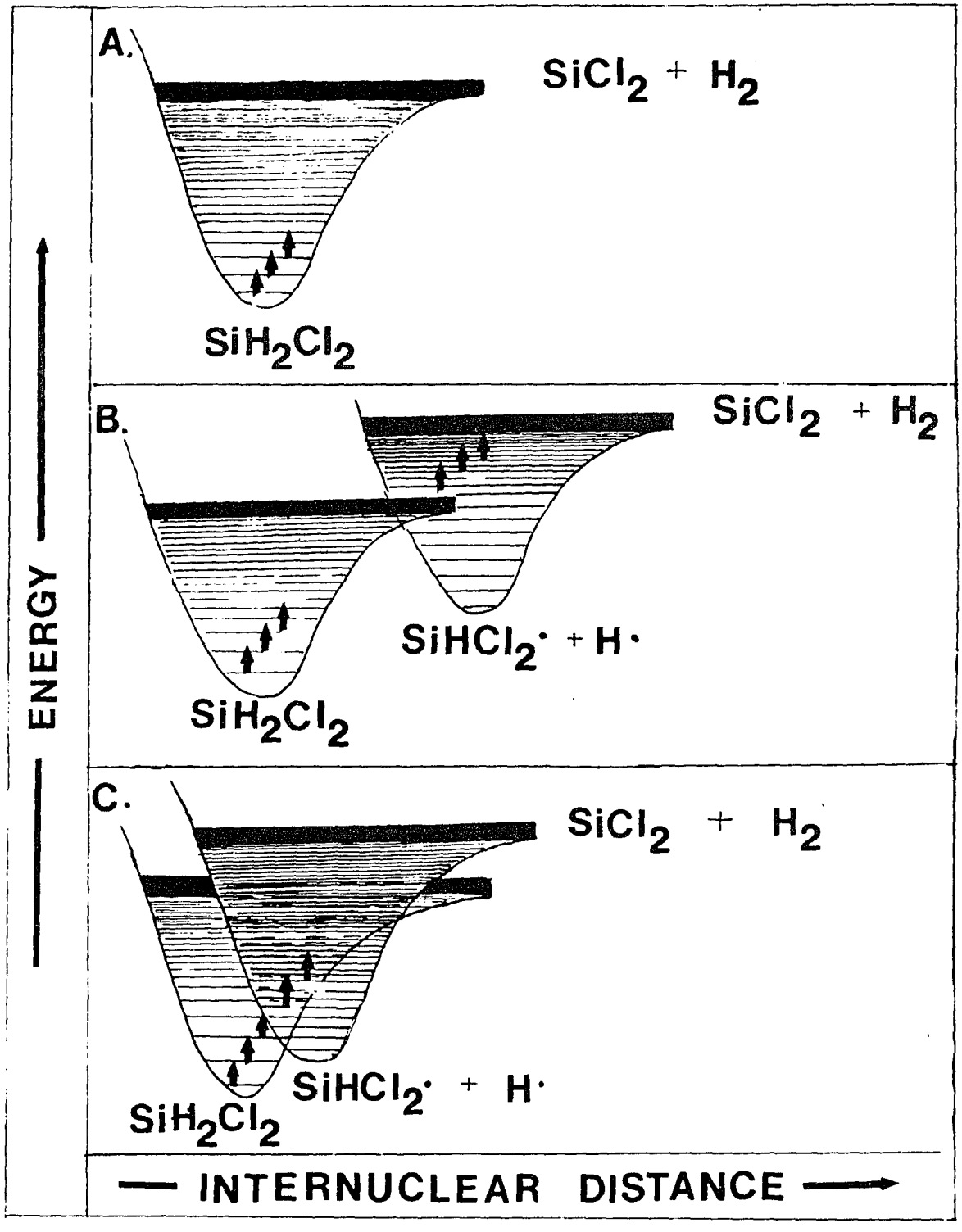
A.
$SiCl_2 + H_2$
SiH_2Cl_2
B.
$SiCl_2 + H_2$
$SiHCl_2\cdot + H\cdot$
SiH_2Cl_2
C.
$SiCl_2 + H_2$
$SiHCl_2\cdot + H\cdot$
SiH_2Cl_2
ENERGY
INTERNUCLEAR DISTANCE

matching is not a requirement for absorption of laser photons. Actually, even $SiHCl_2$ fragments that are not sufficiently hot to attain their vibrational quasicontinuum may absorb additional laser photons. The Si-H stretch present in $SiHCl_2$ retains its frequency of ~ 954 cm^{-1} in such diverse species as $SiHCl_3$ [55] and SiH_2Br_2 [56]. It is then reasonable to assume that this is also the approximate value in $SiHCl_2$ and that, therefore, the resonance condition between the fragment and the laser field can exist even for transitions within the discrete region of the vibrational ladder.

In the second mechanism, shown in Fig. (41c), SiH_2Cl_2 absorbs enough photons to reach its quasicontinuum where a mixing of highly excited vibrational-rotational states in the ground electronic state of SiH_2Cl_2 with $SiHCl_2$ result in crossover and further absorption of photons by $SiHCl_2$ causes it to dissociate to $SiCl_2$. This mechanism is different from the previous one described in that the energy is "tunneled" from one ground state potential surface to another.

The bond strengths of SF_5-F and $VOCl_2$-Cl are estimated as being 90 kcal/mole and 83 kcal/mole respectively. A simple calculation using the above bond strengths together with the energy of one CO_2 laser photon (~ 2.3 kcal/mole), yields approximately 39 and 36 as the number of photons needed to dissociate SF_6 and $VOCl_3$ respectively. The bond strengths of $SiCl_2H$-H and $SiCl_2$-H are estimated as being 93 kcal/mole and 52 kcal/mole respectively. Thus, SiH_2Cl_2 absorbs ~ 63 photons before it dissociates to $SiCl_2$.

The collisionless production of electronically excited fragments by multiphoton is not addressed by statistical theories, such as RRKM, which predict that the dissociation from the ground state potential energy surface typically yields ground state products. Thus, vibrational excitation within the ground state manifold of the parent molecule is not generally expected to yield electronically excited fragments. Nevertheless, this photophysical phenomenon has been observed and an allowance must be made for the possibility of populating a fragment's excited electronic states in a collisionless regime. Using $VOCl_3$ as an example, the following mechanisms are proposed. In the first, $VOCl_3$ is vibrationally excited within its ground electronic state until it reaches its continuum and dissociation to $VOCl_2$ occurs. The $VOCl_2$ fragment is formed, as was

described with the $SiHCl_2$ radical, in its ground state. This is consistent with the general rule that the ground state of a molecule correlates adiabatically with ground state products. $VOCl_2$ can then absorb further photons until an electronically excited state is reached, thus effecting emission.

In the second mechanism, $VOCl_3$, once vibrationally excited by MPE, dissociates along a potential surface which correlates with the electronically excited $VOCl_2$ fragment. $VOCl_2$, in turn, relaxes to its ground state by giving off a visible photon [Fig. (43a)].

In the third mechanism, $VOCl_3$ is vibrationally excited by sufficient photons to reach the fragments' electronic state whose minimum is located below the ground state disssociation limit. A mixing of highly excited vibrational levels in the ground electronic state with levels of the excited state results in crossover (tunneling) and, thus, provide $VOCl_3$ an alternate pathway in lieu of dissociation. $VOCl_3$ is vibrationally excited at one end of the tunnel and the predissociation of $VOCl_3$ to $VOCl_2$ occurs in between. $VOCl_2$, which is electronically excited, emits, as in the previous case, a visible photon and, thus, relaxes to its ground state [Fig. (43b)].

The first mechanism, although applicable to $VOCl_3$, cannot account for the luminescence observed from SiH_2Cl_2 upon MPE. The reasoning is as follows. If the

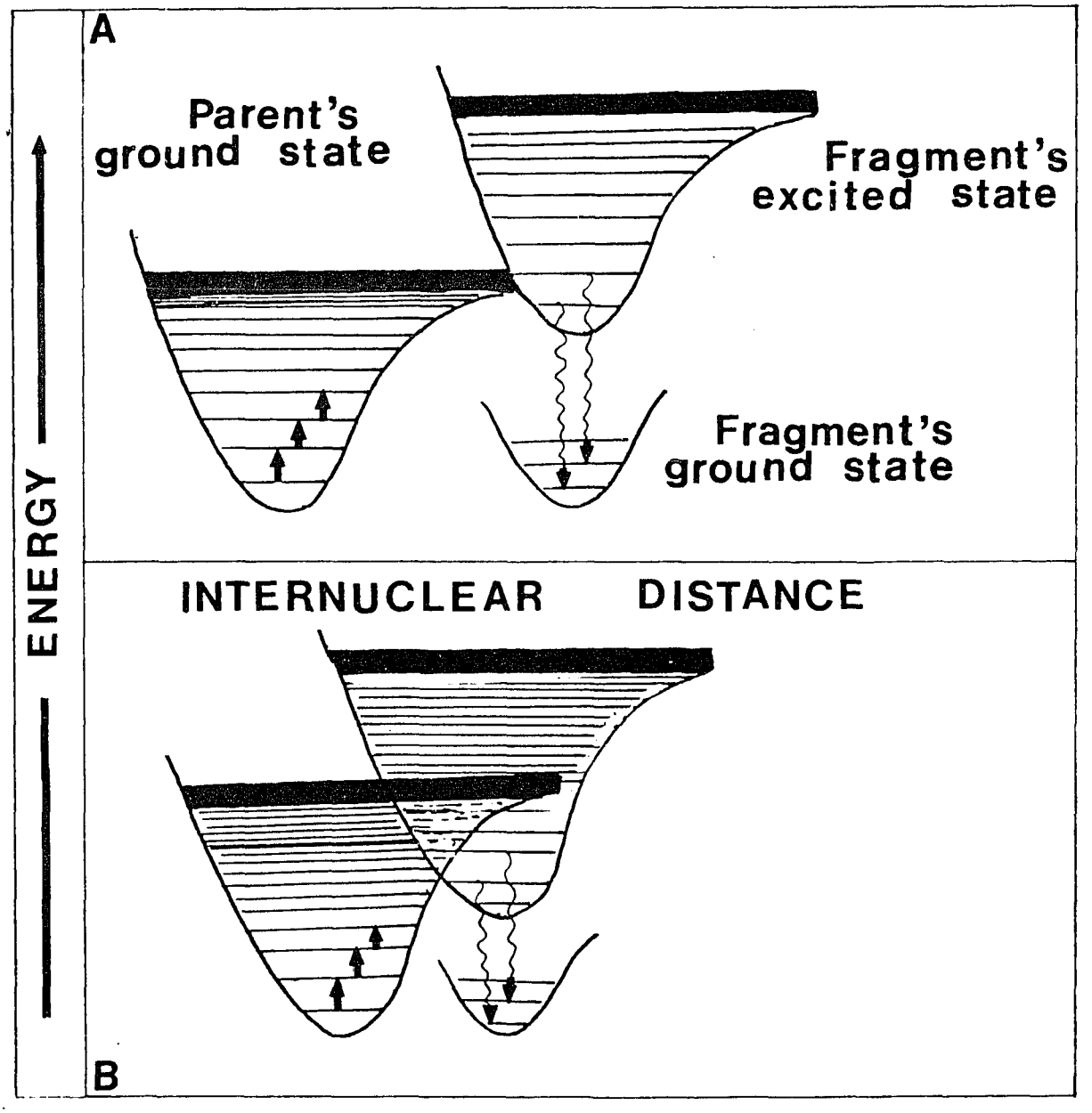

Figure (43) - Fragment luminescence induced by MPD. (A) Ground state dissociation to a fragment's electronic state followed by electronic emission. (B) Predissociation to an electronically excited fragment followed by relaxation to fragment's ground state.

fragment is formed in its ground electronic state, it must absorb additional photons to reach an excited electronic state. This, as was mentioned earlier, can occur if the dissociation of the parent molecule leaves the fragment in the quasicontinuum, where frequency matching is not a requirement for absorption of laser radiation. The other possibility is that the fragment is formed vibrationally cold. In this case, the fragment can only absorb further photons if it retains a stretching mode which is in resonance with the laser radiation. Neither possibility is applicable in the case of $SiCl_2$. First, $SiCl_2$ is a triatomic and thus is not likely to have a qusicontinuum. In fact, a simple calculation using the Marcus-Rice approximation revels that $SiCl_2$ has only "10" states/cm^{-1} even at 30,000 cm^{-1} above its ground vibrational state! Second, its parent molecule was excited via its ν_2 (S-H) bending mode at 954 cm^{-1}. No such frequency or any other within the CO_2 lasing region exists in $SiCl_2$. Therfore, whether $SiCl_2$ is formed in Region (I) or (II) of its ground state, it cannot possibly absorb additional photons to reach an electronic state.

A necessary condition for populating a fragment's excited electronic states by the last two mechanisms is that the fragment's excited state must lie below the ground state of the parent molecule. This is indeed the case in $VOCl_2$ and $SiCl_2$. The $VOCl_2$ luminescence corrsponds to an energy of ~ 62 kcal/mole (460 nm) and

is less than the energy required to rupture the $VOCl_2$-Cl bond. In the case of $SiCl_2$, the luminescence, corresponding to an energy of ~ 83 kcal/mole (337 nm), is also less than the energy required to rupture the ($SiCl_2$-H,H) bonds. This suggests that one of the last two mechanisms may be correct. However, while it is not experimentally clear whether the second or third mechanism predominates, a simple quantum mechanical probability calculation is sufficiently convincing to overwhelmingly favor the second.

In conclusion, then, in view of the lack of any bond selective chemistry occuring in the infrared multiple photon dissociation process, the collisionless production of electronically excited fragments may prove to be one of the most useful applications. This study has provided valuable new information concerning the laser chemistry of $VOCl_3$ and SiH_2Cl_2. In addition, it has provided spectroscopic data of the $VOCl_2$ and $SiCl_2$ radicals which, until now, have been very difficult to generate under clean and well-characterized conditions. Research in this area is, at present, only in its initial stages and much remains to be investigated. In particular, additional experimental data on other molecules and theoretical models addressing intramolecular energy transfer and multiphoton exciation within excited states are still needed.

REFERENCES

1. C. Borde, A. Henry, and L. Henry, Compt. Rend. Academ. Sci. (Paris) B 262, 1389 (1966).

2. V. V. Losev, V. P. Papulovski, V. P. Tischinski, and C. A. Fedina, High Energy Chem. 8, 331 (1969).

3. N. R. Isenor, V. Merchant, R. S. Hallsworth, and M. C. Richardson, Can. J. Phys., 51, 128 (1973).

4. R. V. Ambartzumium, N. V. Chekalin, V. S. Doljikhov, and E. A. Ryabov, Chem. Phys. Lett., 25, 515 (1974).

5. R. V. Ambartzumium and V. S. Letokhov, Chemical and Biochemical Applications of Lasers, edited by C. B. Moore (Academic Press: New York, 1977) Vol. III.

6. V. E. Merchant, Opt. Comm., 25, 259 (1978).

7. G. Yahav and Y. Haas, Chem. Phys., 35, 41 (1978).

8. M. H. Yu, H. Reisler, M. Mangin, and C. Wittig, Chem. Phys. Lett., 62, 439 (1979).

9. M. R. Levy, H. Reisler, M. S. Mangir, and C. Wittig, Opt. Eng., 19, 29 (1980).

10. Z. Karny, A. Cupta, R. N. Zare, S. T. Lin, J. Nieman, and A. M. Ronn, Chem. Phys., 37, 15 (1979).

11. A. A. Makarov, G. N. Makorov, A. A. Puretzkii, and V. V. Tyakht, App. Phys., 23, 391 (1980).

12. G. Walk, R. Weston Jr., and G. Flynn, Chem. Phys., 73, 1949 (1980).

13. P. Kolodner, C. Winterfeld, and E. Yablonovitch, Opt. Comm., 20, 119 (1977).

14. M. J. Coggiola, P. A. Schulz, Y. T. Lee, and Y. R. Shen, Phys. Rev. Lett., 38, 17 (1977).

15. J. P. Aldridge, J. H. Birely, C. D. Cantrell, and D. C. Cartwright, Physics of Quantum Electronics, edited by S. F. Jacobs, M. Sargent III, N. O. Scully, and C. T. Walker (Addison-Wesly: Reading, Mass., 1977) Vol. IV.

16. R. V. Ambartzumian and V. S. Letokhov, Acc. Chem. Res., 10, 61 (1977).

17. N. Bloembergen, Opt. Comm., 15, 416 (1975).

18. J. G. Black, E. Yablanovitch, N. Bloembergen, and S. Mukamel, Phys. Rev. Lett., 38, 1131 (1977).

19. R. V. Ambartzumian, Yu. A. Gorokhov, V. S. Letokhov, G. N. Makarov, A. A. Puretzkii, and N. P. Furzikov, Pis'ma Zh. Eksp. Teor. Fiz. 23, 217 (1976).

20. H. S. Kwok and E. Yablonovitch, Phys. Rev. Lett., 41, 745 (1978).

21. S. T. Lin, S. M. Lee, and A. M. Ronn, Chem. Phys. Lett., 53, 260 (1978).

22. I. R. Levine, Physical Chemistry, edited by D. C. Jackson and M. Gardner (McGraw-Hill: New York, 1978) Chap. 15.

23. H. Braune and S. Knare, Z. Phys. Chem., 331, 297 (1933).

24. S. T. Lin, Ph.D. Dissertation, City University of New York (1978).

25. K. J. Palmer, J. Am. Chem. Soc., 60, 2360 (1938).

26. K. Karakinda, K. Kuchitsu, and C. Matsumura, Chem. Lett., 293 (1972).

27. A. M. Miller and W. White, Spectrochimica Acta, 9, 98 (1957).

28. C. Dlikgraaf, Spectrochimica Acta, 24, 1119 (1965).

29. R. J. Clark and D. M. Rippen, Molecular Physics, 28, 305 (1974).

30. J. E. Eberhardt, D. A. Johnson, R. B. Knott, A. W. Pryor, and A. B. Waugh, Chem. Phys. Lett., 93, 448 (1982).

31. A. C. Briggs and R. J. Kemp, J. Chem. Soc. Dalton Trans., 1223 (1972).

32. A. M. Ronn, Scientific American, 240, #5, 114 (May, 1979).

33. G. Flesh and S. Svec, Inorganic Chemistry, 14, 1817 (1975).

34. J. P. Sung and D. W. Setser, Ber. Bunsenges. Phys. Chem., 83, 1272 (1980).

35. P. C. Mahanti, Proc. Phys. Soc., 47, 433 (1935).

36. R. W. Davis, A. G. Robiette, and M. C. Gerry, J. Mol. Spect., 85, 399 (1981).

37. R. W. Davis and M. C. Gerry, J. Mol. Sepct., 60, 117 (1976).

38. D. H. Christensen and O. F. Nielsen, J. Mol. Spect., 27, 489 (1968).

39. G. C. Causely and B. R. Russell, J. Electron Spectrosc. Relat. Phenom., 8(1), 71 (1976).

40. T. F. Deutsch, J. Chem. Phys., 70, 1187 (1979).

41. A. H. Schwebel, private communication.

42. T. N. Bell, K. A. Perkins, and P. G. Perkins, J. Chem. Soc. Far. Trans., 77, 1779 (1981).

43. P. L. Timms, Inorg. Chem., 7, 387 (1968).

44. D. E. Milligan and D. E. Jacox, J. Chem. Phys., 49, 38 (1968).

45. R. K. Asundi, M. Karim, and R. Samuel, Proc. Phys. Soc. (London) 50, 581 (1938).

46. T. Sedgwick and G. V. Arbach, Proceedings of the 10th Materials Research Symposium on Characterization of High Temperature Vapors and Gases (National Bureau of Standards Special Publication 561, Gaithersburg, Maryland, 1979) pg. 885 and references therein.

47. J. E. Smith and T. O. Sedgwick, Thin Solid Films, 40, 1 (1977).

48. G. M. Barrow, Molecular Spectroscopy (McGraw-Hill, New York: 1962).

49. R. S. McDowell, J. P. Aldridge, and R. F. Holland, J. Phys. Chem., 80, 1203 (1976).

50. F. A. Miller and L. R. Cousins, J. Chem. Phys., 26, 329 (1957).

51. J. A. Hawkins and M. K. Wilson, J. Chem. Phys., 21, 360 (1953).

52. P. J. Robinson and K. A. Holbrook, Unimolecular Reactions (Wiley-Interscience, New York: 1972) Chap. 5.

53. G. H. Hertzberg, Molecular Spectra and Molecular Structure (D. van Nostrand, New York: 1945), Vol. II.

54. (a) M. J. Coggiola, P. A. Schulz, Y. T. Lee, and Y. R. Shen, Phys. Rev. Lett., 38, 17 (1977). (b) P. A. Schulz, Aa. S. Subdø, E. R. Grant, Y. R. Shen, and Y. T. Lee, J. Chem. Phys., 72, 4985 (1980).

55. J. A. Hawkins, S. R. Poto, and M. K. Wilson, J. Chem. Phys., 21, 1122 (1953).

56. J. Bunnel, B. C. Crofford, and T. A. Ford, J. Mol. Structure, 61, 383 (1980).

CHAPTER 3

INFRARED LASER GENERATED VANADIUM OXIDES AND SILICON CONTAINING FILMS BY DIELECTRIC BREAKDOWN

3.1 INTRODUCTION

Reactions carried out by laser induced dielectric breakdown (LIDB) offer unique advantages over those conducted thermally, by an electric discharge, or by multiphoton dissociation (MPD). First, because LIDB reactions are carried out in the absence of cell walls which introduce complicating catalytic effects, they are cleaner with fewer side products than thermal or electric discharge conducted reactions [1-6]. Second, LIDB reactions, unlike MPD, require no resonant condition between an absorption band of the reactant molecule and that of the laser radiation. Thus, LIDB can be applied to any molecule capable of being put into the gaseous state. Third, reactions conducted under LIDB may offer an economic advantage over those conducted by MPD [7]. The reactions involving the latter are most efficient under low pressure and laser energy conditions while those involving LIDB can be conducted under conditions of higher pressure and laser energy. Hence, a greater quantity of products can be produced per laser pulse.

LIDB is easily achieved by focusing the CO_2 laser's radiation into a gaseous sample. A simple explanation of

this process is that electrons, accelerated by the large A.C. electric field of the laser, acquire sufficient energy by colliding with atoms and molecules to start an avalanche of electrons that culminates in a spark of ionized plasma [Fig. (1)]. The plasma formed is short lived, approximately the duration of the laser pulse, and is rich in ionic, neutral, and radical species. The above process is repeated for a number of pulses until the desired reaction is complete.

Dielectric breakdown may, in addition, initiate an explosive chain reaction if the radicals produced by the plasma can further propagate the reaction without the aid of additional laser pulses. This process, appealing in that complete conversion of reactants to products can be achieved by one laser pulse, is known as laser combustion [8]. An example of such an event is captured by a photograph shown in Fig. (2).

With these thoughts in mind, a comparison of the dissociative products of $VOCl_3$ and SiH_2Cl_2, in the neat and in the presence of scavenger gases with resonant and nonresonant radiation, was studied and the results, along with the unique characteristics of each method, presented in the following sections.

3.2 THEORY

The generally accepted model for the mechanism of

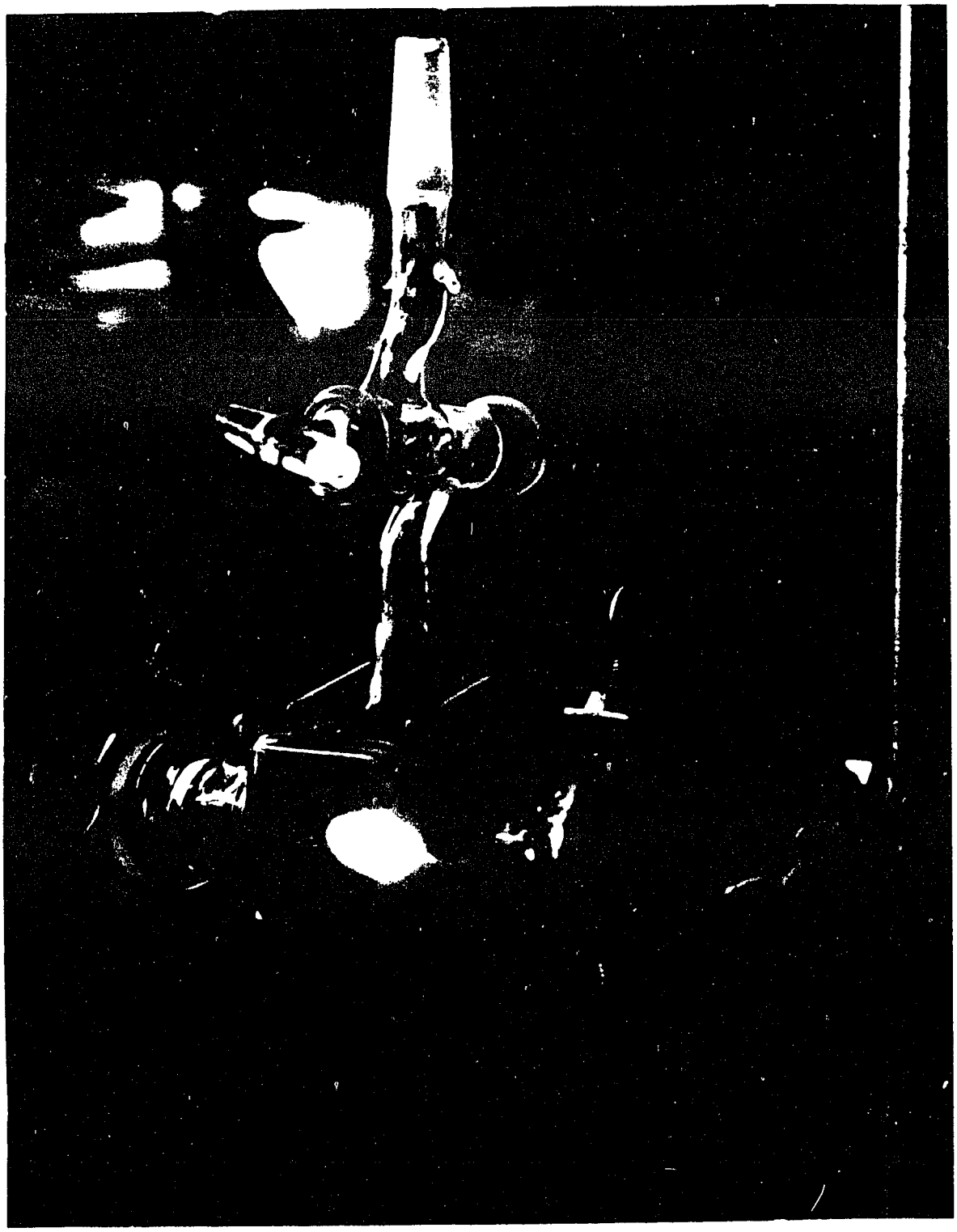

Figure (1) - A photograph of a typical plasma produced by LIDB.

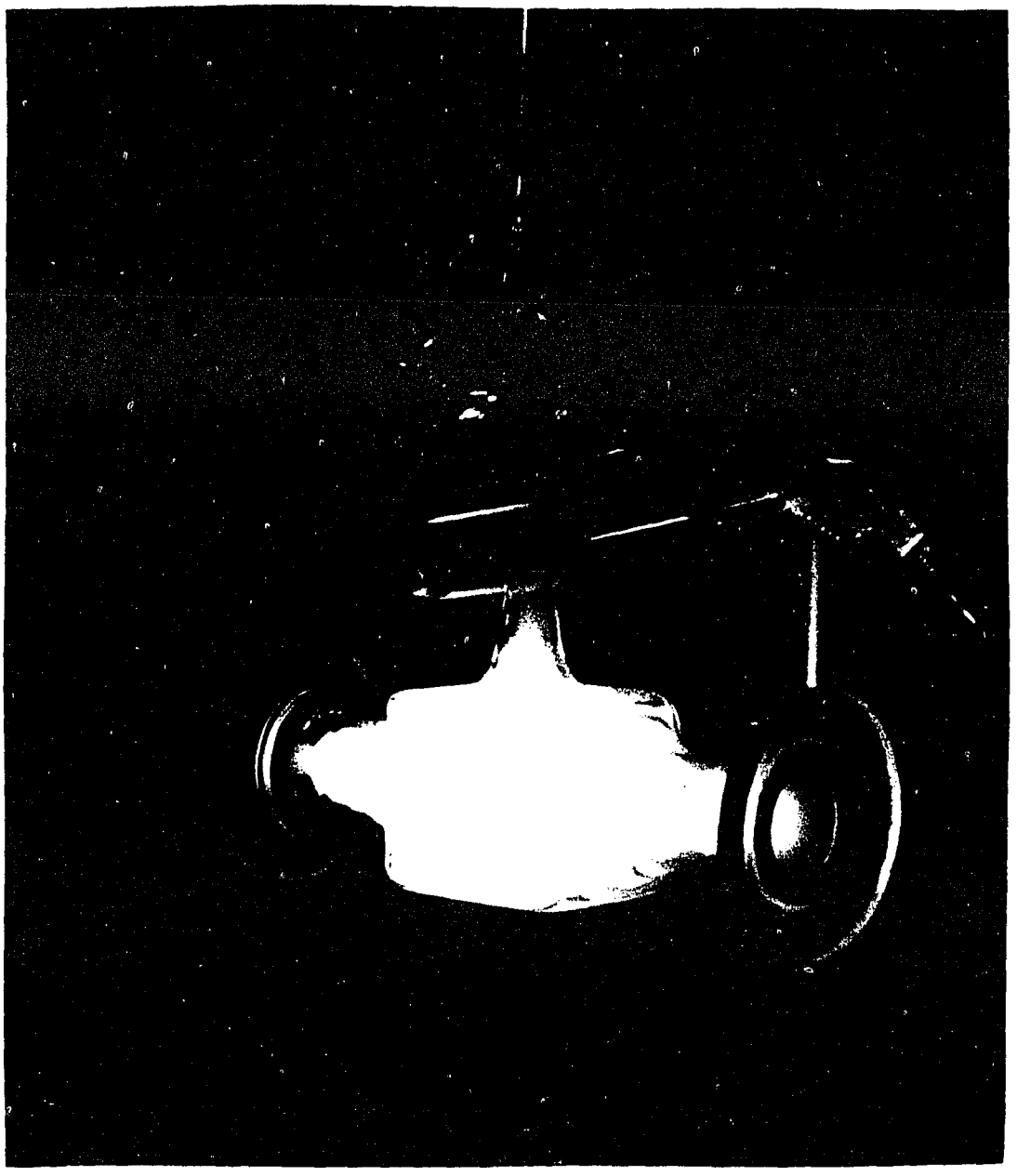

Figure (2) - A photograph capturing an explosive chain reaction induced by LIDE.

CO_2 laser induced dielectric breakdown is the avalanche theory [9]. Electrons, which are accelerated by the large A.C. field of the laser's radiation, acquire energy by colliding with atoms and molecules. Once sufficient energy is acquired, they in turn ionize the atoms and molecules to produce more electrons which repeat the process. In this way, an avalanche or cascade of electrons develops and "breakdown" occurs. The state of breakdown is arbitrarily defined as the ionization of a fraction δ, usually taken as 10^{-3}, of the gas atoms or molecules in the focal region [10]. Once "breakdown" occurs, the ionization growth will continue as long as the irradiation continues. There, then, follows the development of a plasma, a production of highly ionized hot expanding gas, which further absorbs the laser radiation. As the electron and ion concentration increases, electron-ion and ion-ion interactions contribute to the growth mechanism. The gas will remain heated for the duration of the laser pulse which created it, but the extinction process of recombination diffusion, and radiation loss from excited atoms and molecules remove energy from the plasma region and local thermodynamic equilibrium with the surrounding gas is re-established in a time $\geq$ 1 μsec. The reactions that proceed under this plasma condition are thus related to conventional high temperature chemical studies.

A physical picture of the breakdown process can be obtained by considering the interaction of a free electron with the oscillating electromagnetic laser radiation and surrounding gas. A simple formula for the rate of energy gained by a free electron can be formulated and a breakdown threshold intensity deduced.

The velocity of an electron as it interacts with an electric field can be obtained by setting the difference between the force exerted by the field on the electron and the frictional force equal to the rate of change of the electron's momentum. This is expressed mathematically by the following first order differential equation.

$$F_e - F_f = F_a \tag{3.1}$$

or

$$-eE - (mv)\nu_m = m\frac{dv}{dt} \tag{3.2}$$

In the first term, e is the charge of the electron and E, equal to $E_o e^{-i\omega t}$ where ω represents the angular frequency, the electric field associated with the laser radiation. The second term, $(mv)\nu_m$, represents the rate of momentum of the electron due to collisions per second. The symbol, ν_m, which represents the collision frequency for momentum transfer, is equal to τ_m^{-1} where τ_m

represents the average time between collisions. In the third term, m and v are used to represent the electron's mass and velocity respectively.

The solution to equation (3.2) yields the desired result*.

$$v = \frac{-ieE}{m(\omega+i\nu_m)} \tag{3.3}$$

Since the amount of energy the electron gains each time it collides with an atom is equal to its kinetic energy, the rate of gain of energy from the electric field during the laser pulse is expressed as

$$\frac{d\varepsilon}{dt} = (\tfrac{1}{2}m|v|^2)\nu_m \tag{3.4}$$

Substituting equation (3.3) into the above equation results in

---

* Rearranging equation (3.2) yields $dv/dt + \nu_m v = -eE/m$ where $E = E_o e^{-i\omega t}$. Letting $a = \nu_m$, $b = -eE_o/m$, and $c = -i\omega$, one obtains $dv/dt + av = be^{ct}$ or $v' + p(t)v = q(t)$ where $p(t)$ and $q(t)$ were substituted for a and be^{ct}, respectively. An integrating factor which is independent of v and of the form $I(t,v) = e^{\int p(t)dt} = e^{\int a dt} = e^{at}$ is used as a multiplicative factor to solve the first order differential equation. Hence, $e^{at}v' + ave^{at} = be^{ct}e^{at}$ or $(d/dt)(e^{at}v) = be^{(a+c)t}$. Integrating yields $ve^{at} = [be^{(a+c)t}/a+c] + K$ and by resubstituting for a, b, and c, one obtains $v = (-eE_o/m)(e^{-i\omega t})/\nu_m - i\omega + K/e^{\nu_m t}$. Since the collisional frequency (ν_m) is large at high pressures and laser field intensity, the second term approaches zero and one is thus left with $v = -ieE/(\omega+i\nu_m)m$, after multiplying by (i/i) and resubstituting E for $E_o e^{-i\omega t}$.

$$\frac{d\varepsilon}{dt} = \frac{e^2 E \nu_m}{2m(\nu_m^2+\omega^2)} = \frac{n(t)e^2E^2\nu_m}{2m(\omega^2+\nu_m^2)} \qquad (3.5)$$

where n(t) is included since, at any time, t, during the laser pulse, n(t) electrons absorb the energy. The above expression gives a picture for the inverse frequency dependence on the absorption as well as the role of collisions.

One can now deduce a simple formula for the breakdown threshold intensity by equating the rate at which the electrons absorb energy from the field to the rate at which they expend it in ionization. The rate of energy absorption in ionization is

$$(\frac{d\varepsilon}{dt}) = I_p \frac{dn}{dt} \qquad (3.6)$$

where I_p represents the ionization potential of the gas and dn/dt, equal to the ionization collision frequency (ν_i) times the electron concentration (n), the rate of generation of electrons. Thus, equating expression (3.5) to (3.6), integrating, and using Poynting's theorem

yields an expression for the breakdown threshold intensity*

$$I = \frac{2mc\varepsilon I_p(\omega^2+\nu_m^2)\ \ln\ (\frac{n_f(\tau)}{n_o})}{e^2\nu_m\tau} \qquad (3.7)$$

Here, I represents the laser power density (W/m^2), c the speed of light (m/sec), ε the free space permittivity ($coul^2/nt\cdot m^2$), $n_f(\tau)$ the final electron density (m^{-3}), and τ the duration of the laser pulse (sec). The symbols m, I_p, ω, e, and ν_m, which were previously defined, have units of kg, Joules, sec^{-1}, coul, and sec^{-1} respectively.

The angular frequency of the CO_2 laser radiation, which is much larger than the electron atom collision frequency at a pressure less than 1 atm [10], is directly proportional to the pressure. Using this approximation and setting $n_f(\tau)/n$ equal to 10^{19}, as the condition for breakdown [11], yields

$$I \simeq \frac{m\omega^2 I_p}{e^2\tau P} \qquad (3.8)$$

---

* Substituting equation (3.5) for dn/dt in equation (3.6) yields $n(t)e^2E^2\nu_m/2m(\omega^2+\nu_m^2) = I_p(dn/dt)$ or, after rearranging it, $dn/n(t) = [e^2\nu_mE^2/2m(\omega^2+\nu_m^2)I_p]dt$. Integrating the last equation in the time of the laser pulse, τ, yields $\ln n\Big|_0^\tau = e^2\nu_mE^2t/2m(\omega^2+\nu_m^2)I_p\Big|_0^\tau$. Substituting in the limits of integration yields $\ln [n_f(\tau)/n_o] = e^2\nu_mE^2\tau/2m(\omega^2+\nu_m^2)I_p$ or $E^2 = 2m(\omega^2+\nu_m^2)I_p\ \ln [n(\tau)/n_o]/e^2\nu_m\tau$. Using Poynting's theorem, $I = \varepsilon cE^2$, one obtains $I = 2m\varepsilon c(\omega^2+\nu_m^2)I_p\ \ln [n_f(\tau)/n_o]/e^2\nu_m\tau$. If one uses the following relationships, 1 J = N·m and 1 W = kgm^2/sec^3, I will have units of (W/m^2).

where the letter, P, represents the pressure.

It can be seen from the above expression that the breakdown threshold intensity is dependent on the nature of the gas, characterized by its ionization potential, pressure, and laser radiation, characterized by its frequency and flash duration. In addition to ionization potential, threshold pressure conditions are linked to the molecular properties of the gas, such as polarization and dipole moment [11].

The assumptions made in the above treatment of dielectric breakdown are as follows: First, a classical treatment was used. In the classical treatment, the electrons acquire energy by colliding with atoms whereas, in a quantum mechanical treatment, they acquire energy by inverse bremsstrahlung absorption [12]. The classical treatment holds whenever the photon energy is much less than the total free energy which is approximately equal to the ionization of the gas [12]. For a CO_2 laser, $h\nu \simeq 1.8$ e.v. and I_p for a gas, say $VOCl_3$, is $\simeq 12$ e.v. [13]. However, the quantum mechanical model would be more suitable for breakdown radiation approaching the UV portion of the electromagnetic spectrum or for breakdown studies of gases with low ionization potential. Second, the magnetic field effects, also produced by the laser's electromagnetic radiation, were ignored since the electron velocities

didn't approach the velocity of light. Third, in equation (3.6), the rate of electron generation, recombination, diffusion, and radiative loss processes were neglected. Fourth, but not least, the avalanche theory presumes the existence of initial electrons which are accelerated by the electromagnetic field. The initial electrons may be accounted for by either naturally occuring electrons as a result of cosmic rays, ~ 10^1 - 10^2 electrons/cm^3, low ionization impurity atoms in the sample, low ionization impurities on the cell's entrance window, or a combination thereof [14].

3.3 EXPERIMENTAL

The laser apparatus, equipment, and compounds used were the same as those described in the experimental section of Chapter Two. In addition, in order to facilitate collection of large samples of microparticles, specially designed 500-ml and 1000-ml spherical pyrex cells, to which a 35-ml removable glass finger was attached by means of an O-ring joint, were used. The gas pressure ranged from .5 - 100 torr and was calibrated by either a M.K.S. baratron or a Wallace Tiernan Gauge (0 - 100 torr). The accuracy of the Wallace Tiernan Gauge was ±.2 torr.

In the case of $VOCl_3$, it was necessary to heat the cell in order to obtain a vapor pressure exceeding that

of room temperature. The cell was resistively heated to a known temperature by means of a variac and the pressure calculated by using the following expression.

$$\ln P \approx 2.08 \ln T - \frac{2.78 \times 10^3}{T} \qquad (3.9)$$

The above expression, $\ln P \sim a \ln T - b/T$ [15], is a version of the Clausius-Clapeyron equation where P, in units of torr, represents the pressure and T, the temperature, is expressed in units of Kelvin. The letters, a and b, are constants whose values were solved for by using the experimental points (273 K, 4.4 torr) and (298 K, 12.4 torr).

Infrared analysis of samples, both prior and after laser irradiation, was carried out using various infrared spectrophotometers (see Section 2.3). In addition, scanning electron microscopy (SEM) and x-ray diffraction (XRD) helped determine particle size, composition, and tendency of agglomeration. These analysis were performed at the Research Center of the International Nickel Corporation (INCO).

3.4 RESULTS AND DISCUSSION

Table (I) summarizes the dielectric breakdown study of $VOCl_3$ and SiH_2Cl_2. As is evident from Table (I), dielectric breakdown of $VOCl_3$ is consistent with the high

Table I. Dielectric breakdown of $VOCl_3$ and SiH_2Cl_2 in the neat and with scavenger gases.

REACTANTS	TYPICAL PRESSURE (Torr)	TYPICAL LASER ENERGY (J)	MAJOR PRODUCTS FORMED
A. $VOCl_3$			
$VOCl_3$	5	1.0	VO / Cl_2
$VOCl_3$ / Ar	5/20	1.0	VO / Cl_2
$VOCl_3$ / Cl_2	5/20	1.0	NONE
$VOCl_3$ / H_2	5/20	1.0	V_2O_3 / HCl / H_2O
$VOCl_3$ / O_2	5/20	1.0	V_2O_5 / Cl_2
B. $SiCl_2H_2$			
$SiCl_2H_2$	5	1.0	$(SiCl_2)_x$ H_2
$SiCl_2H_2$ / Ar	5/20	1.0	$(SiCl_2)_x$ H_2
$SiCl_2H_2$ / Cl_2	5/20		$SiCl_4$ HCl
$SiCl_2H_2$ / H_2	5/20	1.0	amorphous Si HCl

pressure and laser energy MPD studies in that VO + Cl_2 are the initial photodissociative products but, then, any further dissociation cannot be achieved because VO recombines with Cl_2 to yield $VOCl_3$. Also, as in MPD, addition of argon to $VOCl_3$ inhibits the recombination of VO and Cl_2 while addition of Cl_2 inhibits the dissociation of $VOCl_3$. Hence, the production of large quantities of VO particles via LIDB is fruitless. However, when H_2 or O_2 was added to $VOCl_3$ and dielectric breakdown performed, the reactions were driven to completion and yielded V_2O_3 and V_2O_5 respectively. Whereas dielectric breakdown of SiH_2Cl_2 in the neat and with argon resulted, as in MPD, in the formation of H_2 and $(SiCl_2)_x$ polymer, in the case of SiH_2Cl_2 and Cl_2, it was not necessary to induce a chemical reaction. The reactants, upon mixing, were spontaneously converted to $SiCl_4$ and HCl. Lastly, dielectric breakdown on mixtures of SiH_2Cl_2 and H_2 resulted in the formation of HCl and an amorphous silicon-containing film having a small concentration of chlorine. The latter results are encouraging regarding its possible use for solar cells. Ovshinsky and co-workers [16,17] have reported on the fabrication of solar cells based on silicon-containing films with small concentration of fluorine. They claim that any univalent species, such as Cl, F, or H, would be ideal for use in amorphous silicon solar cells.

The pattern in the above cases is that the reactions, conducted under plasma conditions, are thermodynamically controlled and thus similar to high temperature reactions. A mechanism for the above reactions can be illustrated by the following scheme.

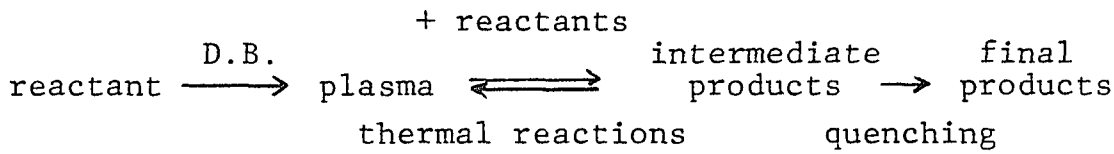

The first phase is the formation of the plasma during the laser pulse. Then, the plasma plays a role as a heat source to induce the thermal reaction. Finally, the products are quenched by collisions with environmental molecules.

The plasma itself, when observed, is composed of a small dense inner core surrounded by a less dense region. Spectroscopic investigations have shown the inner core to be composed of ionic species while the outer core by free radicals [18-19]. The fact that ions have shorter lifetimes than radicals strongly suggest that most of the chemistry is carried out in the less dense region by free radicals.

The plasma, which is rich in free radicals in its outer sphere, may further propagate the reaction without

the aid of additional laser pulses. Such an event, a branched chain explosion, has indeed been found to be the case when dielectric breakdown on different $VOCl_3/H_2/O_2$ mixtures was performed. The reactants, in one laser pulse, were completely converted to different vanadium oxide particulates. The results, presented in Table (II), reveal that V_2O_5 was always formed when the H_2/O_2 ratio was less or equal to two. When the H_2/O_2 ratio was increased, reduction of $VOCl_3$ to compounds which have vanadium oxidation numbers less than five took place.

Although the reactions are thought to proceed by free radical mechanisms, the pathways leading to product formation are presently not well understood. However, the results can be mostly explained by Table (III), which lists the set of possible products, along with the oxidation state of vanadium, which can be formed from different $VOCl_3/H_2/O_2$ mixtures by using different H_2/O_2 concentrations. The only discrepancy between Table (II) and Table (III) is that VO is not formed, as predicted by the first equation in Table (III), at a H_2 to O_2 ratio equal to five. It was anticipated that larger H_2/O_2 ratios would eventually lead to the formation of VO. However, under such conditions, only dielectric breakdown without combustion could be induced. An explanation of this result is that, in order to have an explosion, a sufficient concentration of free radicals must be formed to initiate the chain reaction.

Table II. Laser induced combusion of different $VOCl_3/H_2/O_2$ mixtures.

PRESSURE Torr $VOCl_3$	H_2	O_2	H_2/O_2 RATIO	MAJOR PRODUCT
20	20	40	1 : 2	V_2O_5
20	20	20	1 : 1	V_2O_5
20	40	20	2 : 1	V_2O_5
20	50	20	2.5 : 1	V_2O_5 / VO_2
20	35	10	3.5 1	V_2O_3 / VOCl / $VOCl_2$
20	40	10	4 : 1	V_2O_3 / VOCl
20	42	10	4.2 : 1	V_2O_3 / VOCl
20	40	10	5 : 1	V_2O_3
15	30	5	6 : 1	Breakdown
15	45	7	~ 6.4 : 1	Breakdown
10	50	5	10 : 1	Breakdown

Table III. (A) Reactions involving different $VOCl_3/H_2/O_2$ concentrations leading to different product formation.

(B) Products formed by using different H_2/O_2 ratios in the above reactions (A).

A.

$2VOCl_3$	+ $5H_2$	+ O_2	⟶	$2VO$	+	$6HCl$	+	$2H_2O$
$2VOCl_3$	+ $4H_2$	+ O_2	⟶	V_2O_3	+	$6HCl$	+	H_2O
$2VOCl_3$	+ $4H_2$	+ O_2	⟶	$2VOCl$	+	$4HCl$	+	$2H_2O$
$2VOCl_3$	+ $3H_2$	+ O_2	⟶	$2VOCl_2$	+	$2HCl$	+	$2H_2O$
$2VOCl_3$	+ $5H_2$	+ $2O_2$	⟶	$2VO_2$	+	$6HCl$	+	$2H_2O$
$2VOCl_3$	+ $4H_2$	+ $2O_2$	⟶	V_2O_5	+	$6HCl$	+	H_2O

B.

PRODUCT	OXIDATION STATE OF VANADIUM	MOLES			H_2/O_2 RATIO
		$VOCl_3$	H_2	O_2	
VO	+2	2	5	1	5 : 1
V_2O_3	+3	2	4	1	4 : 1
VOCl	+3	2	4	1	4 : 1
$VOCl_2$	+4	2	3	1	3 : 1
VO_2	+4	2	5	2	2.5 : 1
V_2O_5	+5	2	4	2	2 : 1

However, an increased pressure also produces other radicals, ions, or neutral atoms which may hinder the combustion process rather than help it. VO was instead produced in a chain reaction when mixtures of $VOCl_3/H_2/Cl_2$, with typical pressures of 10/20/20 torr respectively, were irradiated via dielectric breakdown.

The above reactions occur in one laser pulse and utlize a mere 5×10^{19} photons (1 J/pulse) costing approximately $.02 [7]. The production of V_2O_5, for example, is calculated to cost $3.70/gram*. In the present market, the price of V_2O_5 ranges from $.84/gram (purity > 90%) to $4.30/gram (purity > 99.98%) [20]. This example illustrates the notion that laser chemistry can become an economically competitive method for producing fine chemicals.

The sizes of the particulates produced by LIDB vary depending on the compound produced and conditions used, i.e. pressure, focusing lens, energy of laser

---

* This value is obtained by using equation (6) of Table III, assuming a 100% yield of V_2O_5 (.1 g for each 5×10^{-4} mole), and using prices of $.25 for $VOCl_3$ (20 torr, 1 ℓ), calculated from the price listed in the alpha/inorganic handbook (1981), and $.12 for H_2 and O_2 (40 torr H_2, 20 torr O_2, 1 ℓ), calculated from a listed price in the 1981 Matheson handbook.

pulse, etc. Fig. (3) shows an SEM photograph of V_2O_5 particles collected over an aluminum oxide support. The size of the V_2O_5 particles are ~ 1 μ.

V_xO_y particles are powerful catalysts used for many organic and inorganic reactions, an example is the use of V_2O_5 in the oxidation of SO_2 to SO_3. This reaction is of particular importance since SO_2, produced mainly from the burning of coal, is a major contributor to air pollution. Hence, using V_2O_5 as a catalyst to oxidize SO_2 to SO_3 before it is let into the atmosphere, and then treating SO_3 with water to produce sulfuric acid, is one route which can lead to cleaner air.

3.5 CONCLUSION

Dielectric breakdown and laser combustion methods were used to produce various vanadium oxides and silicon-containing films from $VOCl_3$ and SiH_2Cl_2. The photo-decomposition reactions proceed via the lowest energetic channel and thus form the most thermodynamically stable products, as in the case of multiphoton dissociation. The products are finely divided particles of very large surface area and high purity. Both dielectric breakdown and laser combustion are amenable to large scale productions and can be shown to be economically competitive with other fine particle decomposition processes.

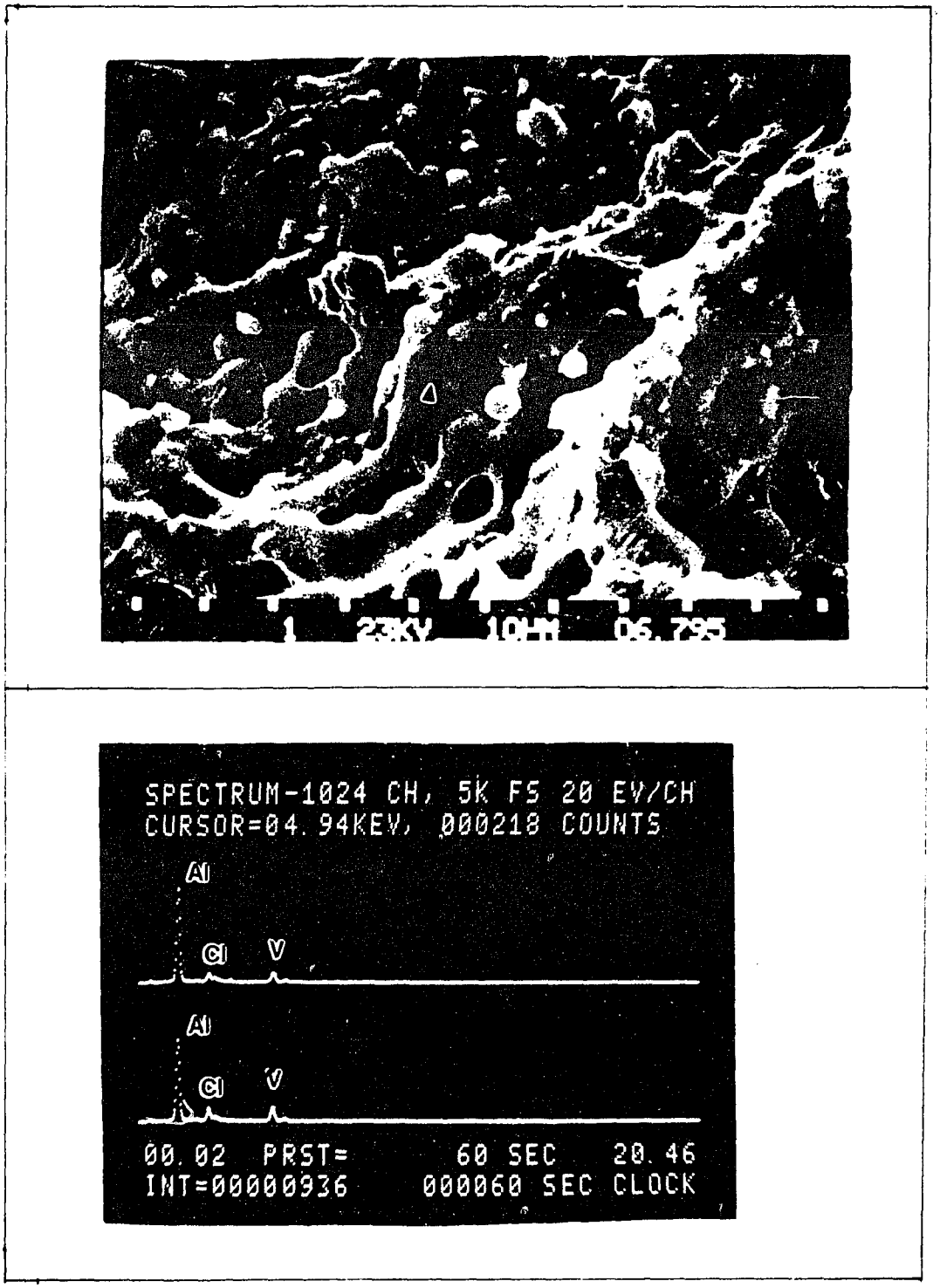

Figure (3) - SEM photograph of V_2O_5 particulates collected over an aluminum oxide support.

REFERENCES

1. A. M. Ronn, Scientific American, 240, #5, 114 (May, 1979).

2. S. T. Lin and A. M. Ronn, Phys. Lett., 56, 414 (1978).

3. A. M. Ronn, U. S. Patent #4,230,546 (1980).

4. Y. Langsam and A. M. Ronn, Chem. Phys., 54, 277 (1981).

5. C. W. Draper, Metall. Trans., 11A, 349 (1980).

6. S. D. Allen, Proc. Soc. Photo-opt. Instrum. Eng., 198 (1980).

7. A. M. Ronn, Applications of Lasers to Chemical Problems, edited by T. R. Evans (Wiely: New York, 1982) Vol. XVII, Chapter 4.

8. A. M. Ronn, U. S. Patent #4,343,687 (1982).

9. J. P. Wright, Proc. Phys. Soc., 84, 41 (1964).

10. C. G. Morgan, Electrical Breakdown of Gases, edited by J. M. Meek and J. D. Graggs (Wiley-Interscience: New York, 1978) Chapter 9.

11. S. T. Lin, Ph.D. Dissertation, City University of New York, (1978).

12. Y. B. Zel'dovich and Yu. P. Paizer, Sov. Phys. JETP, 20, 772 (1965).

13. P. Burroughs, S. Evans, A. Hammett, A. F. Orchard, and N. V. Richardson, J. Chem. Soc. Faraday Trans., 70, 1895 (1974).

14. R. G. Evans and P. C. Thonemann, Phys. Lett., 38A, 398 (1971).

15. K. Denbigh, The Principles of Chemical Equilibrium, 3rd ed. (Cambridge Univ. Press: England, 1971).

16. S. R. Ovshinsky, Patent Cooperation Treaty Appl. 7,900,724 (cl. H01L45/00), Oct. 4, 1979, U. S. appl. 884,664, Mar. 8, 1978.

17. A. Madan and S. R. Ovshinsky, Nature (London) 276, 5682 (1978).

18. Y. Langsam, Ph.D. Dissertation, Polytechnic Institute of New York, (1979).

19. A. H. Schwebel, Ph.D. Dissertation, City University of New York, (1982).

20. Alfa Catalog (1981).